ENTERGY OPERATIONS

Engineering Report

For

The Evaluation of BWR Control Rod Drive Mounting Flange

Cap Screw

APPLICABLE SITES

ANO Unit 1: ☐	GGNS: X	W-3: ☐
ANO Unit 2: ☐	RBS: X	ECH: ☐

Safety Related: X Yes

No

Prepared by: J. S. Brihmadesam Date: 6/8/98
Responsible Engineer

Prepared by: Brian C. Gray Date: 6/8/98
B. C. Gray
Responsible Engineer

Reviewed by: K. R. Rao Date: 6/22/98
Reviewer

Reviewed by: Lee R. Howell Jr. Date: 6/9/98
L. R. Howell
Reviewer APP. 2 Sec. XI
APP. 3

Reviewed by: J R Hamilton Date: 6-23-98
J. R. Hamilton
Manager, Engineering Programs
Central Design Engineering

Approved by: J R Hamilton Date: 9-1-98
J. R. Hamilton
Responsible CDE Manager
(for multiple site reports only)

Blank Page

Table of Contents

List of Figures

List of Appendices

Appendix No.	Appendix Title	No. of Pages
1	Stress Analysis	39
2	Fracture Mechanics Evaluation of Flaws in Bolts	56
3	Bolted Joint Calculations: CRD Cap Screw Evaluation	7
4	Mechanical Testing and Evaluation of Circumferentially Notched CRD Capscrew Material	22

Record of Revision

Revision Number	Reason for Revision
01	Added Appendix 4, & modified report to incorporate results from Appendix 4

1.0 INTRODUCTION

Nondestructive examination (NDE), metallurgical and analytical evaluation of control rod drive (CRD) mounting flange cap screws were initiated in response to the requirements of references 1 and 2. Past evaluations of the CRD cap screws for Grand Gulf Nuclear Station (GGNS) and River Bend Nuclear Station (RBS) are documented as follows:

GGNS :- References 3,4 and 21
RBS :- References 16 and 17

In reference 3 stress analysis and fracture mechanics evaluations were used to develop an inspection scope expansion criterion. This criterion was based on metallurgical evaluation of flaws found in the CRD cap screws at GGNS. In reference 15 the CRD cap screws from RBS were examined by metallurgical techniques and the findings were found to be in agreement with those in reference 3.

The purpose of this engineering report is to evaluate the scope expansion criterion with respect to the relevant engineering requirements provided in the applicable sections of the ASME Boiler and Pressure Vessel Code, Section XI. These requirements are obtained from reference 5 for GGNS and reference 6 for RBS.

The scope of the evaluation performed in preparation of this engineering report encompassed the following:

1) Determination of appropriate material property to establish a conservative lower bound toughness value.
2) Stress analysis to define a conservative upper bound stress distribution for the head-to-shank fillet region of the CRD cap screw based on preload.
3) Structural evaluation to establish a maximum full circumference flaw depth without exceeding the allowable ASME stress limits. ($3 \times S_m$).
4) Evaluation of the bolted joint connection to establish a maximum full circumference flaw depth that would preclude joint separation under postulated internal pressure load.
5) Fracture mechanics evaluation to conservatively determine the flaw depth that would meet the lower bound threshold toughness for the material in the environment for the CRD cap screw.
6) To compare the flaw depth determined above, (items 3, 4 & 5), with the inspection scope expansion criterion presented in reference 3.

2.0 BACKGROUND

CRD cap screws have been inspected at GGNS and RBS in accordance with the requirements contained in references 1 and 2. Cap screws that were found to show any degradation were replaced following the recommendations in references 1 and 2. The inspections at GGNS and RBS have shown that the degradation was predominantly located at the head-to-shank fillet region and occasionally in the shank region removed from the fillet region. In all the inspections conducted to date there has not been a single indication of a flaw in the thread root region. Metallurgical evaluations of the degradation show that the flaw to have a pit type morphology (references 3, 4 &17).

The indications on the cap screws at GGNS, that were found during the Spring 1992 inspection, were metallurgically evaluated (reference 3). The findings from the metallurgical evaluation and the guidance provided in reference 2 led to the development of an inspection scope expansion criterion. This criterion was presented as a recommendation in reference 3. The basis for the criterion was developed by determining the stress distribution in the head-to shank fillet region using finite element analysis (FEA) and the use of fracture mechanics model for a circumferentially notched bar under tensile stress. The limiting flaw depth was based on the applied stress intensity factor ($K_{Iapp.}$) for a given flaw depth to be less than the threshold toughness. A conservative upper bound $K_{Iapp.}$, (by virtue of the circumferentially notched model with high surface stress used for the tensile stress), and a lower value for threshold toughness ensured that the criterion based on flaw depth was conservative.

In order to implement the scope expansion criterion, in a time efficient manner, an Eddy Current test technique was developed and qualified (reference 7). This technique was utilized in the Fall 1996 CRD cap screw inspection at GGNS. The Eddy Current based sizing of the flaws was compared to the metallographically determined depths for selected CRD cap screws. Results of the evaluation (reference 4) showed that the Eddy Current based sizing was conservative ($Depth_{eddy\ current} > Depth_{met.}$).

At RBS the inspection of CRD cap screws conducted in January 1996 showed pitting in the head-to-shank fillet region on some cap screws. The depth of the pits were found to be lower than the depth provided in reference 2 and were in the range of the GGNS results documented in references 3 and 4.

3.0 EVALUATION SCOPE

The scope of this engineering report, based on the documented findings and the need to establish compliance with the established engineering requirements of references 1, 2, 5 and 6, are as follows:

1) Establishment of lower bound material property, for use in fracture mechanics analysis in accordance with the requirements of section XI of the applicable ASME code (references 5 & 6), based on cap screw mechanical properties and established correlation available in published literature.
2) Detailed stress analysis to establish an upper bound stress distribution and proper Linearization of the stress profile in the head-to-shank fillet region. The resulting stress components and linearized profiles are for use in the fracture mechanics evaluation.
3) Review of bolted joint connection to ascertain prevailing (residual) preload.
4) Determination of a limiting full circumference flaw/notch depth which would result in bolt stress within ASME allowable limit of $3 \times S_m$.
5) An evaluation of the bolted connection, using bolting structural formulations, to determine potential for joint separation under postulated internal pressure load.
6) Review and evaluation of postulated flaws by various fracture mechanics solutions available in published literature.
7) Comparisons with the results from metallurgical evaluations from references 3 and 4 as applicable.
8) Comparison of the results from the present evaluation with the inspection scope expansion criterion provided in reference 3.
9) Mechanical testing and notch analysis of CRD Capscrew material to verify the results obtained from analytical evaluation.

4.0 Details of Evaluation:

ASME Code Requirements and Material Properties:

In order to ensure that the damage found in the cap screws were dispositioned in an appropriate manner, guidance provided in paragraph IWB-3600 of Section XI from references 5 and 6 were considered. A review of this paragraph in both referenced editions and addenda showed the contents to be similar. The requirements that need to be satisfied are:

a) Acceptability of flaw size based on fracture mechanics analyses; and,
b) Meeting the primary stress limits of NB-3000 assuming a local area reduction of the primary pressure retaining member

Based on the evaluations performed to satisfy the above requirements an acceptable flaw size, which is the lower of the flaw sizes developed by the analyses in accordance with "a" or "b' above.

Primary stress determination is based on assuming a full circumference flaw located in the shank of the CRD cap screw. When evaluating flaws in bolts it must be recognized that it is not technically correct to calculate, much less address, net section average stresses. Because the very presence of the flaw causes the re-distribution of stresses, there by creating a combined tension plus bending load. This aspect has been appropriately articulated in reference 28. The discussion states in part, the following:

> *"Paragraph NB-3230 includes methods for establishing design conditions, determining the average stress, maximum stress or maximum stress intensity, and the method for designing to avoid fatigue failure. The number and cross-sectional area of bolts for a given application are determined using Appendix E of Section III of the ASME Code. Appendix E describes in detail the method for determining the minimum number and cross-sectional area of bolts for gasketed joints based on the design of the gasketed joint, the system operating pressure and temperature, and the characteristics of the gasket material. Appendix E also allows the use of the methods given in Appendix A-6000, "Discontinuity Stresses", if the methods given in Appendix E are inadequate. The stresses calculated using Appendix E or A must satisfy the requirements for maximum stress or maximum stress intensity and fatigue stress in Sections NB-3230.*
>
> *Paragraph NB-3232 states that the service stresses in bolts may be higher than the stresses in Table I-1.3. The maximum average cross-sectional stress may be as much as twice the stress given in Table I-1.3. The maximum stress at the periphery of the bolt may be as much as three times the stress given in Table I-1.3 as long as the fatigue stresses are not exceeded. These stresses arise from the direct tension and bending, neglecting stress concentrations."*

4.0 Details of Evaluation (Continued)

Therefore, the criterion to evaluate the stress limits, at the location of the flaw, are the combined tension plus bending stresses limits. This criterion, simply stated, will ensure that the bolt will not fail by an over-load condition, which is also the primary intent of IWB-3610 (b). Attempting to postulate the flaw as reduction of the bolt shank's cross-section over its entire length will undoubtedly increase average stresses, but as is shown later it will reduce the bolt stiffness which in turn will result in the joint having to sustain additional stresses. Since the primary interest of IWB-3610 (b) is to preclude failure by primary stress overload, the appropriate criterion is the maximum stresses due to direct tension and bending. This location of interest is where groove type pitting was observed (reference 3). The prevailing stresses at the flaw location are based on the results of the finite element analysis performed for the head-to-shank transition region. Applying this stress in the shank region is conservative.

In reference 8 it was shown that the prevailing preload on the bolt was always lower than the initial preload at installation. Data from references 8 and 9 showing the reduction in magnitude owing to various causes, as follows:

Immediate relaxation after final installation: - 5% to 10% reduction (Ref. 8)
Elastic Interaction (embedment etc.) relaxation: - 12% to 18% reduction (Ref. 8)
Gasketed joint relaxation (depends on gasket material): - 10% to 50% (Ref. 8)
Long term (1000 hr.) stress relaxation at 550° F: - 20% (Ref. 9)

A total reduction factor of 0.632 was computed by taking the average values stated in reference 8 and ignoring the relaxation due to gaskets, (formulation used in computing the reduction factor is provided in Appendix 3). Thus the prevailing preload and hence the stress in the bolt would be 63.2% of the initially installed value. Ignoring the reduction for gasketed joints and using the average values for the other reduction factors provides a lower bound estimate of reduction factor. Using the reduction factor and the installation preload of 30.0 kip (reference 3) results in a prevailing preload of 18.97 kip. The material allowable stress intensity at 550° F was obtained from reference 13 as 29.5 ksi. The primary stress limit for bolting provided in NB-3232.2 from the same year and addenda as in references 5 and 6 is stated as follows :

$$P_m + P_b \leq 3 \times S_m$$

The approach presented in IWB-3612 is to determine an acceptable K_{Iapp} for the postulated flaw such that the inequality criteria are satisfied. The criteria provided in IWB-3612 are as follows:

1) $K_{Iapp} < K_{Ia} / \sqrt{10}$ ---------- for Normal and Upset conditions;

and,

2) $K_{Iapp} < K_{Ia} / \sqrt{2}$ ---------- for Faulted and Emergency conditions.

4.0 Details of Evaluation (Continued)

where K_{Ia} is defined as the available fracture toughness based on crack arrest.
and, K_{Ic} is defined as the available fracture toughness based on fracture initiation.

The first criterion, based on arrest toughness, is derived from dynamic fracture mechanics principles (reference 10). The arrest toughness is the lower bound toughness at the point of arrest of a rapidly propagating crack. The fracture arrest toughness in structural (carbon and low alloy) steels is an inherent manifestation of the effect of imposed loading rate on the materials flow strength property (reference 10). In high strength alloy steels, such as the cap screw material, the strain rate sensitivity of fracture toughness is very low (reference 11). The effect of strain rate (loading rate) (reference 11) on fracture toughness, is quantified by an absolute temperature shift between the static and dynamic toughness values for the ductile to brittle transition temperature. The measured temperature shift for various steels, from medium to very high strength, as a function of strength is shown in figure 4.53 of reference 11. Data from this figure was used to reconstruct figure 1 in this report. Typical reactor pressure vessel steels that have yield strength in the range from 60 to 70 ksi show a temperature shift of 110°F to 130°F. CRD cap screw material, which belongs to the low alloy quenched and tempered (LAQT) classification of steel, posses yield strength in the range from 120 to 130 ksi. For this class of steels the temperature shift is in the range from 20°F to 35°F. The larger temperature shift is indicative of significant sensitivity of fracture toughness to loading rate. Conversely smaller temperature shifts indicate insensitivity of fracture toughness to loading rate. The effect of higher loading rate on rate sensitive materials is manifested by a measurable drop in fracture toughness. Therefore for a material which is not rate sensitive, like the cap screw material, the fracture toughness is not affected by the loading rate. CRD cap screw material,(LAQT steel), at GGNS possessed an yield strength of 120 ksi (reference 3) and at RBS 110 ksi (reference 16 & 17). At these levels of yield strengths the effect of loading rate on fracture toughness is expected to be very small to negligible. In addition, from reference 10 (page 15) for bolting material, the following statement is made:

> *"The applicable toughness property value for bolts should be the static fracture toughness value K_{Ic}. Dynamic loading would not be expected to occur in bolting. Also, these higher strength steels generally exhibit very little influence of loading rate on fracture toughness."*

Therefore the toughness property applicable to the CRD cap screw material is K_{Ic}, hence for the evaluation of flaws the second criterion of IWB-3612 is applicable. The degradation of CRD cap screws was found to be corrosion induced pitting (references 3, 4, 16 & 17). Thus the fracture toughness parameter to account for the corrosion mechanism would be K_{Iscc} (stress corrosion cracking). The value for K_{Iscc} for the CRD cap screw material, based on the yield strength (references 3, 16 & 17), was determined from figure 11B-2 of reference 12 as 130 ksi $\sqrt{in}$. The evaluation criterion for the CRD cap screw can be re-written as follows:

4.0 Details of Evaluation (Continued)

$$K_{Iapp} < K_{Iscc} / \sqrt{2} \quad (K_{Ic} \text{ replaced by } K_{Iscc})$$

With K_{Iscc} value of 130 ksi $\sqrt{in}$. the criterion reduces to:

$$K_{Iapp} < 91.92 \text{ ksi}\sqrt{in}.$$

In addition to using the CRD cap screw material yield strength to determine K_{Iscc}, the Charpy absorbed energy was used to determine the value for K_{Ic} for the material. The Charpy and tensile data obtained from references 3, 16 and 17, for the cap screws, show:

Charpy Absorbed Energy (lowest) = 68 ft-lbs.
Yield Strength = 110.0 ksi

The Charpy-K_{Ic} correlation of reference 11 (equation 6.1) was used along with the values provided above to estimate the K_{Ic}. The value was determined to be 185 ksi$\sqrt{in}$. This value is higher than the value for K_{Iscc} obtained from reference 12. Thus the lower bound value would provide conservative results (smaller allowable flaw depth).

In order to use the guidance provided in article IWB-3612 from references 5 and 6, it is necessary to address the requirements of article IWB-3610-(b). This requirement necessitates satisfying the primary stress limits of the applicable articles in subsection NB-3000. A review of the relevant articles, pertaining to bolts, shows that the stress limit requirements are for bolt regions removed from discontinuities. However, the stress analysis performed for this report, described in the following section, does model the fillet radius. Thus the requirements for the primary stress limits, are discussed in the stress analysis section.

Stress Analysis:

General Considerations:

The observed corrosion damage on the CRD cap screws were found in two distinct regions, namely: head-to-shank fillet and the shank region. In the head-to-shank fillet region the state of stress is expected to be complex owing to the constraint imposed by the cap screw head. Where as in the shank region, removed from the fillet, the stresses are expected to be uniform. Therefore for the head-to-shank fillet region detailed finite element analysis (FEA) was performed. For the shank region the tensile stress, due to preload, were obtained from reference 3. Details of the FEA and subsequent stress analysis are provided in Appendix 1 and summarized below.

4.0 Details of Evaluation (Continued)

Finite Element Analysis:

FEA of the head-to-shank fillet region was performed using a two dimensional axi-symmetric model. Details of the model and the results are presented in Appendix 1. Two models using different fillet radii, 0.05 inch and 0.075 inch based on reference 22, were developed. Both models utilized a very fine mesh refinement to model the fillet region. The FEA model is shown in figure 2. A linear elastic analysis was performed. The applied load equal to the tension developed in the shank with an applied preload of 30.0 kip (reference 3) was applied at the shank end. The bolt head was fixed along the bottom edge to prevent movement in any direction. The effect of fillet radii differences in the stress distribution obtained were insignificant. The stress distribution obtained from the FEA analysis showed a sharp gradient in the head-to-shank fillet region. In the shank region, removed from the fillet, the stresses were uniform. In the head-to-shank region the stress distribution (Von Mises stress) had to be linearized so that the effective distribution could be used as input to the fracture mechanics model.

Linearization of Stresses:

The FEA stress distribution in the fillet region showed high surface stresses (peak) that rapidly decayed within one element width. Since the analysis was linear elastic, the surface stresses were higher than the material's yield strength. The previous FEA analysis (reference 3) used a coarser mesh thereby precluding the construction of a detailed stress profile in this region. Hence, Linearization of the stresses in this region was not performed. Therefore, unrealistically high stresses were used as input to the fracture mechanics analysis.

In this evaluation a stress profile, along a radial-axial plane from the surface towards the center of the cap screw, was developed. This stress profile was input to two Linearization algorithms as follows:

1) Linearization in accordance with Appendix "A" of Section XI; ASME B&PV Code {references 5 & 6) to obtain the components P_m and P_b.
2) Linearized profile based on strain energy density.

Details for these algorithms are provided in Appendix 1. Figure 3 shows the FEA stress profile and the linearized profiles obtained from the two algorithms.

The Linearization technique, in accordance with Appendix "A" of references 5 and 6, results in decomposition of the applied stresses into tension (membrane) and bending components. These are defined as P_m (tension) and P_b (bending). The values for P_m and P_b were utilized for fracture mechanics evaluation which is presented in a later section. The Linearization of the applied stress profile, using strain energy density algorithm, was necessitated for fracture mechanics formulations where the stress term did not separately account for tension and bending. Therefore by developing a reasonable stress profile other fracture mechanics solutions, in which only tensile stresses are considered, could be evaluated and compared.

4.0 Details of Evaluation (Continued)

Structural Evaluation of Bolted Joint:

The values for the component stresses were utilized to demonstrate that the requirements of IWB-3610-(b) of references 5 and 6 are satisfied both in the as installed and degraded conditions. The requirement for bolting application implies that the maximum stress limits of Section III, article NB-3232.2 (for the same year and addenda as references 5 & 6) are met. However the requirements stated in NB-3232.2 are for maximum stress intensity neglecting stress concentration. For the CRD cap screws, evaluated in this report, the values for P_m and P_b account for the stress concentration caused by the fillet. The results presented in Appendix 1 show that the combined ($P_m + P_b$) stress value to be 69.78 ksi. This value is compared to the allowable value permitted by NB-3232.2 as follows:

$(P_m + P_b) < 3 \times S_m$ --------- for static loading.
and
$(P_m + P_b) < 2.7 \times S_m$ --------- for fatigue loading.

The material allowable stress intensity (S_m) values were obtained from Section III, Appendix I (same year and addenda as reference 5 & 6) for the CRD cap screw material and were found to be 29.5 ksi at a temperature of 550°F. The calculated value for the combined stresses is found to be less than the more restrictive $2.7 \times S_m$. Thus the requirements of IWB-3612-(b) are satisfied for the as installed CRD cap screws.

Fatigue of bolts in a bolted joint is dependent on the joint configuration, initial preload and the magnitude of the external load experienced by the bolt. Information obtained from reference 8 shows the following:

1) *The magnitude of the mean load on the bolt depends on the preload in the bolt.*
2) *The magnitude of the load excursion (ΔF_B) depends on:*
   a) *The magnitude of external tension load;*
   b) *The bolt-to- joint stiffness ratio (K_B/K_J); and,*
   c) *Whether or not the external tension load exceeds the critical load required to separate the joint.*

Elsewhere in this section and in the discussion section the bolted joint analysis presented show that the CRD bolted joint based on prevailing preload has a high critical load required to cause joint separation. The prevailing preload is also relatively high and that the stiffness of the joint is considerably higher than the CRD cap screw. The considerably higher joint stiffness, compared to the CRD cap screw, ensures that only a small fraction of the applied alternating load will be experienced by the cap screw. The relatively high preload and therefore the high value of critical load required to cause joint separation will provide added assurance that the bolt is not subject to alternating loads. Together these aspects and properties, developed for the bolted joint representing the CRD cap screw, provide adequate assurance that fatigue is not a cause for concern for the degraded cap screw within the limits determined in this report.

4.0 Details of Evaluation (Continued)

For CRD cap screws that have been in service for a number of years, the structural performance required to satisfy the requirements of IWB 3610-(b) can be stated as follows:

a) Demonstrate that the ASME Code allowable stress ($3 \times S_m$) is not exceeded for a cap screw having a full circumference flaw of a certain depth and subjected to a combined load of residual preload plus anticipated internal pressure.
b) Demonstrate that the residual preload on the cap screw having a full circumference flaw of a certain depth will sustain postulated internal pressure without joint separation.

In order to satisfy the requirements stated above a three step process was adopted. a brief description of the process is provided below. The details of the numerical analysis performed to determine the allowable flaw depth based on the structural requirements delineated above is provided in Appendix 3. In the discussion below only the basic formulations are provided since the detailed equations are presented in Appendix 3 as a Mathcad work sheet.

The first step to satisfy the requirements of "a" and 'b" above necessitates the determination of an allowable flaw size (depth) subjected to the estimated preload that would preclude tensile failure of the bolt (i.e. exceed $3 \times S_m$). The primary stress used is the residual value of the combined stresses from Appendix 1. The combined stress in the head-to-shank transition was determined to be 69.78 ksi based on an installation preload of 30.0 kip. As shown earlier the residual preload is expected to be reduced to 63.2% of the installation value over a period of time (operation of 1000 hours). This residual value remains on the bolted connection. The allowable full circumference flaw size, for the residual preload, can be determined by the following relationship:

$$d_n = \{D_{sh} - [\sqrt{((69.78 \times 0.632)/(3 \times S_m))} \times D_{sh}]\}/2$$

where:

d_n = depth of flaw (inch)
D_{sh} = Diameter of cap screw shank (inch), and
S_m = Allowable ASME stress (ksi)

Substituting the appropriate value the depth of a full circumference flaw is determined to be 0.120 inch.

In the second step the joint integrity based on a full circumference flaw which is 0.120 inch deep was determined and the details of the calculation are provided in Appendix 3. This evaluation uses the bolted joint analysis scheme presented in reference 8. Three CRD cap screw geometry's and one joint configuration were used in the evaluation. The joint stiffness was computed using the configuration of the assembly from references 26 and 27 and the formulations from reference 8. The joint stiffness from reference 8 is given as:

4.0 Details of Evaluation (Continued)

$$K_J = E \times A_C/T$$

where;

K_J = Joint Stiffness (kip/in)
E = modulus of Elasticity (ksi)
A_C = Area of the Equivalent Cylinder comprising the Joint (inch^2) and,
T = thickness of the Joint or Grip length of Bolt (inch)

The stiffness for the CRD cap screw was computed for three different conditions, namely; 1) an undegraded nominal cap screw, 2) a degraded cap screw with a reduction in the shank diameter by the depth of the full circumferential flaw over the entire length, and 3) a notch in the middle of the shank with the depth of 0.12[illegible]h and width of 0.05 inch. The first degraded condition would provide the lowest bolt stiffness and the second degraded condition would provide the stiffness of the bolt commensurate with the conservatively assumed flaw description. The formulations used in computing the bolt stiffness were obtained from reference 8 and the three geometry's used are presented as case 1 through 3 in Appendix 3. The basic form of the bolt stiffness equation (reference 8) is:

$$K_B = 1/\{[L_{be}/(E \times A_B)] + [L_{se}/(E \times A_S)]\}$$

where:

K_B = Stiffness of the cap screw (kip/in)
L_{be} = Effective length of Bolt body (inch)
A_B = Cross-sectional area of the shank (inch^2)
L_{se} = Effective length of Threads (inch), and
A_S = Cross-sectional area in the thread region (inch^2)

In order to determine the joint separation equation 12.11 of reference 8 was used. The critical external force (load) required for joint separation, on a per bolt basis, given a residual preload in the joint is given as:

$$L_{xcrit} = F_P \times (1 + K_B/K_J)$$

where:

L_{xcrit} = External force required for joint separation (kip)
F_P = Residual preload in the bolt (kip)

The joint separation force was calculated for the three bolt geometry's described above. The lowest joint separation force was used to determine joint integrity. The imposed external force was calculated using the accident internal pressure in the CRD housing from reference 25. The maximum internal pressure for the CRD housing was given as 5,872 psi. This pressure acts on the CRD cover plate which is connected to the flange by the CRD cap screw. The area of the plate exposed to the pressure was computed from the

4.0 Details of Evaluation (Continued)

CRD housing internal diameter obtained from reference 27. Thus the total force on the entire bolted joint was determined. The number of CRD cap screws in the connection was eight (reference 27). Thus the external force per CRD cap screw joint could be determined. This value of the external force (L_X) was compared with the critical external force required to cause joint separation (L_{xcrit}). The lowest value of the critical joint separation force was used for this comparison. The details of these computations are provided in Appendix 3

In the third step the computed joint force due to the internal pressure of 5,872 psi was used to calculate the additional bolt load using the relationship from reference 8, which is given as:

$$\Delta F_B = \{K_B/(K_B + K_J)\} \times L_X$$

where:

ΔF_B = Additional load on the cap screw (kip)
L_X = External force per bolt caused by internal pressure (kip)

The additional bolt load was added to the residual preload and then ratioed to the residual preload. This ratio was used to adjust, upward, the residual combined stress in the bolt. Based on the revised bolt stresses a new allowable flaw depth was computed. Since the bolt stress was revised upward (increased), it was not necessary to recalculate the joint integrity because a lower bolt stiffness used to establish joint integrity.

Fracture Mechanics Analysis:

General Considerations:

Stress Intensity Factor (SIF) formulations from available literature were reviewed and used in the current evaluation. The fracture mechanics evaluation for the CRD cap screw were divided into three regions , to account for the different stress profiles in these regions, as follows:

1) Thread Root
2) Shank
3) Head-to-Shank Fillet

The metallurgical evaluations of the CRD cap screws at GGNS and RBS (references 3, 4 & 15) clearly demonstrate that the corrosion induced flaws were predominantly located in the head-to-shank fillet region. There were a few groove type pitting flaws located in the mid-shank region. There were no flaws found in the thread root region of the CRD cap screws. Hence the fracture mechanics evaluation of the thread root region was performed and presented here for the sake of completeness.

4.0 Details of Evaluation (Continued)

The magnitude and type of stress used in the various fracture mechanics formulations, by the cap screw region of evaluation, were obtained as follows:

1) Thread Root :- Tension stress due to bolt preload from reference 3.
2) Shank :- Tension stress due to bolt preload from reference 3.
3) Head-to-Shank Fillet :- FEA and stress linearization presented in previous section.

The nomenclature for the applied SIF, used in this report, is subscripted with the initials of the author(s) of the formulation. In this manner the data files in Appendix 2 could be used to develop combination plots for comparison. For the applied stress terms the nomenclature is as follows:

Stress Type	Appendix 2	Literature & Report
Uniform Tension	S_0	σ, σ_t σ_0
Membrane	P_m	σ_t
Bending	P_b	σ_b
Peak Surface	S_{peak}	Used to define the variable stress
Nominal	S_{nom}	profile using the strain energy density

In Appendix 2 for each solution the terms utilized in the solution are defined and where the linearized profile was used the linearization scheme has been presented. The solutions described in the following sections follow the solution numbers of Appendix 2. All formulations were solved iteratively, for various flaw depths, using Mathcad 7 professional version. Appendix 2 provides all the Mathcad files and evaluated data.

Stress Intensity Factor Formulations (See Appendix 2 for details):

SOLUTION IA through IC:

Formulations provided in reference 18 were based on an evaluation of other available solutions and experimental data The authors of this reference developed an empirical correlation to fit all the available data in the literature at that time. The final solution was developed to accommodate the differences in the behavior of K_I for two different crack profiles, namely: a circular crack front and a straight crack front. The cases considered were for a single crack in a round bar. The empirical equation developed facilitated a smooth transition between the K_I behavior for the two crack profiles. The effect of the thread root was incorporated using an exponential term in the equation for tensile stresses. However for the bending stress this effect, the exponential term was not incorporated owing to lack of sufficient experimental data (reference 18). The equation for K_I was:

4.0 Details of Evaluation (Continued)

For Tension (membrane) stress:

$$K_I = \sigma\sqrt{\pi a}\,(2.043e^{-31.73x} + 0.6507 + 0.5367x + 3.0469x^2 - 19.504x^3 + 45.647x^4) \quad -- (1)$$

Where; x = a/D , and a = flaw depth, D = nominal bolt diameter.

Likewise for bending stress:

$$K_I = \sigma_b\sqrt{\pi a}\,(0.6301 + 0.03488x - 3.3365x^2 + 13.406x^3 - 6.0421x^4) \quad -- (2)$$

As mentioned earlier, the exponential term is not used in equation 2. In order to utilize equation 1 in the shank region, following the recommendation of reference 18, the exponential term was ignored. In the head-to-shank transition region where bending stresses dominate at the surface, equations 1 and 2 are superimposed (added) to obtain the total stress intensity factor. The equations used in the present evaluation for the three regions of the cap screw were combined as follows:

Thread Root Region	: Equation 1
Shank Region	: Equation 1 without the exponential term
Head-to-Shank Fillet Region	: Equation 1 w/o exponential term + Equation 2

Details of the solution for the CRD cap screws are provided in Appendix 2 as solution numbers IA through IC.

SOLUTION II

This formulation, from reference 19, follows from the solution developed in reference 18. The general form of the stress intensity factor equation retains the same form as in equation 1 but the coefficients were modified based on the author's empirical evaluation of additional data. The equation was developed only for tension (membrane) loading and is provided below:

$$K_I = \sigma\sqrt{\pi a}\,(2.437e^{-36.5x} + 0.5154 + 0.4251x + 2.4134x^2 - 15.4491x^3 + 36.157x^4) \quad -- (3)$$

A comparison of equations 3 and 1 shows that the behavior of K_I with respect to the normalized crack depth would be similar. In Appendix 2 the solution provided is for the thread root region only since the other regions were evaluated by the solution presented in the preceding section. Details of the solution are provided in Appendix 2 solution II.

4.0 Details of Evaluation (Continued)

SOLUTION III A & IIIB and SOLUTION IV

The stress intensity factor solutions were obtained from reference 20. These solutions were for part circumferential circular fronted cracks and were empirically developed based on experimental data and analytical results from finite element analysis. In these solutions the tension and bending loads were explicitly considered. The stress intensity factor solution provided (reference 20) were:

$$K_I = \sqrt{\pi a}\ \{\sigma_0 F_0(\lambda) + \sigma_b F_b(\lambda)\} \quad \text{--------(4)}$$

with:

$$F_0(\lambda) = g(\lambda)\ [\ 0.752 + 2.02\lambda + 0.37(1 - \sin(\pi\lambda/2)^3\ ] \quad \text{---- (5)}$$

$$F_b(\lambda) = g(\lambda)\ [\ 0.923 + 0.199(1 - \sin(\pi\lambda/2)^4\ ] \quad \text{---- (6)}$$

$$g(\lambda) = 0.92\ (2/\pi)\ \{\sqrt{[\tan(\pi\lambda/2)/(\pi\lambda/2)]}\ /\ \cos(\pi\lambda/2)\} \quad \text{------ (7)}$$

where: λ = a/D and a= crack depth, D= nominal bolt diameter.

In the head-to-shank transition region, the stress profile obtained from linearization of the finite element analysis results provided the tension and bending stresses explicitly (Appendix 1). The applied stress intensity factor results for this region is provided in Appendix 2 as solution IIIA.

For the shank region, where the uniform tension stress dominates, equation 4 was modified to eliminate the bending term, since the bending stress is negligibly small. The resulting values for the stress intensity factors are provided in Appendix 2, solution IIIB.

In order to evaluate the significance of the rapidly decaying surface stresses at the head-to-shank transition region the tensile stress term in equation 4 was defined as a linear variable dependent on the normalized crack depth. The decaying stress was forced to reach the value of the uniform tension stress at a depth determined from the stress profiles (strain energy density) developed from the finite element analysis. The final formulation used in determining the stress intensity factor and the results for the applied stress intensity factors are provided in Appendix 2 solution IV.

SOLUTION VA &VB

The formulation used in modeling the crack are a combination of the tension and bending solutions for straight fronted cracks provided in reference 18. The equations utilized (reference 18), are as follows:

$$K_I = \sigma_t\sqrt{\pi a}\ (0.926 - 1.771x + 26.421x^2 - 78.481x^3 + 87.911x^4\ ) + \sigma_b\sqrt{\pi a}\ (1.04 - 3.64x + 16.86x^2 - 32.596x^3 + 28.41x^4\ ) \quad \text{------- (8)}$$

4.0 Details of Evaluation (Continued)

In the solution of equation 8, the tension stress (σ_t) is the nominal membrane stress removed from the discontinuity (S_{nom}) where the stress profile attains an asymptotic value. The bending stress (σ_b) is defined as a linearly varying function of crack depth and the stress profile was developed using the strain energy density principle (Appendix 1). The details of adapting the stress profile to determine the bending stress is provided in Appendix 2, solution VA. Solution VA was developed for the head-to-shank transition region and the details of the applied stress intensity factor determination as a function of crack depth is provided in Appendix 2, solution VA.

The straight fronted crack solution of reference 18 was used to develop the applied stress intensity factor in the shank region of the bolt. In this evaluation the tension (membrane) stress used was the tensile stress developed in the shank region due to bolt preload. The applied stress intensity factor equation is the same as the tension portion of equation 8, and is as follows:

$$K_I = \sigma_t\sqrt{\pi a}\,(0.926 - 1.771x + 26.421x^2 - 78.481x^3 + 87.911x^4) \quad \text{--- (9)}$$

The details of the evaluation for this equation as it applies to the CRD cap screw is provided in Appendix 2, solution VB.

SOLUTION VIA & B

The solutions developed for analysis use the circumferentially notched bar geometry described in reference 21. For this geometry the crack is simulated as a full circumferential crack. The solution provided in reference 21 is for tension loading and hence for the head-to-shank transition region a linearized stress profile, developed using the strain energy density principle (Appendix 1), was used to determine the net section tension stress (σ_{net}). The stress intensity factor solution for this geometry, from reference 21, is given as:

$$K_I = \sigma_{net}\sqrt{\pi D}\ f(d/D) \quad \text{---(10)}$$

with: $\sigma_{net} = \sigma/(d/D)^2$ ---(11)

where:

σ = nominal tension stress in bar (ksi)
d = reduced diameter at the notch (in)
D = nominal diameter of bar (in)
f(d/D) = influence function, table 5 of reference 19.

In order to utilize the influence function {f(d/D)} in a parametric form, data from table 5 of reference 21 was curve fitted with a ninth order polynomial with (d/D) as an independent variable. This would permit determination of the influence function at various crack depths in a continuous manner. The resulting polynomial was tested against the values

4.0 Details of Evaluation (Continued)

in table 5 of reference 21 and good agreement was achieved. The polynomial developed is provided in Appendix 2, solution VIA.

The applied stress intensity factor in the head-to-shank transition region was evaluated using two variations of equation 10 above. In the first formulation the tension stress was the linearized peak surface stress (strain energy density principle), and the influence function was taken at its maximum value of 0.24 from table 5 of reference 21. This solution is identical to the solution utilized in reference 3. This solution is provided in Appendix 2, as solution VIA-I (constant stress). The second formulation the stress term of equation 11 was defined as a linear variable of crack depth. The linear stress profile was determined from the finite element stress contours and linearized using the strain energy density principle (Appendix 1). Additionally the influence function was defined by the polynomial function described earlier. The applied stress intensity factor determination is provided in Appendix 2 as solution VIA-II.

For the shank region the stress term was set equal to the nominal tension stress developed in the shank due to bolt preload, and the influence function was defined by the polynomial function. The applied stress intensity factor determination is provided in Appendix 2 as solution VIB.

SOLUTION VII

The development of toughness requirements for bolting materials, reference 10, were based on the following findings:

1) The stress intensity factor for notched cylindrical bars when tested in bending showed a rapid rise with increasing crack depth. This was attributed to the assumption that the notched region on the compressive side could not sustain compression;
2) The observation that tight cracks could sustain compressive loads; and,
3) The single edge notched geometry (SEN) was considered to be more applicable for bending loads.

Thus in reference 10, the stress intensity factor determination to support fracture toughness requirements were based on superposition of the tension solution from notched cylindrical bar testing and the bending solution from the single edge notched specimen. Hence the combined (superposition) solution accounted for both the effects; tension plus bending.

In a similar manner, the tension solution from reference 21 could be combined with the bending solution of reference 20. In reference 18 a straight crack front profile solution was used and in reference 20 a solution for a circular crack front profile was developed. It was demonstrated in reference 18, that the stress intensity factor for a straight crack front was always higher than that for a circular crack front for lower crack depths. At larger crack depths the results for the two crack front profiles converged. This aspect suggests that a bounding solution can be obtained by using the stress intensity factor solution

4.0 Details of Evaluation (Continued)

for a straight crack front profile for bending loads. Thus in this solution the tension solution for a circumferentially notched cylindrical bar (reference 21) was superimposed on the straight crack front solution in bending (reference 18). The resulting formulation can be represented in the following equation:

$$K_I = \sigma_t/(d/D)^2 \sqrt{\pi D}\ f(d/D) + \sigma_b\sqrt{\pi a}\,(1.04 - 3.64x + 16.86x^2 - 32.596x^3 + 28.41x^4) \quad -- (12)$$

The variables in the above equation have been previously defined. This combined solution follows the logic utilized in reference 10, which was the bases document for establishing the fracture toughness requirements presented in Section III of the ASME Boiler and Pressure Vessel code. The tension stress (σ_t) was taken as the membrane stress component (P_m) determined by the profile linearization (Appendix 1), in accordance with Appendix "A" of references 5 and 6. The influence function was the polynomial equation described earlier. The bending stress is the bending stress (σ_b) was taken as the bending stress component (P_b) from the linearization mentioned above. This solution was developed for the head-to-shank transition region only. The details of the evaluation are presented in Appendix 2, as solution VII.

SOLUTION VIII

This solution is applicable in the head-to-shank transition. The stress intensity factor solutions were obtained from reference 24. The solutions were developed for a full circumference notch in a cylindrical bar subject to bending and tension. The applied stress intensity solutions are as follows:

$$K_{It} = \sigma_t \sqrt{\pi a}\,\{0.5\,x^{-1.5}\,(1 + 0.5x + 0.374x^2 - 0.363x^3 + 0.731x^4)\} \text{ (tension)} \quad -- (13)$$

and,

$$K_{Ib} = \sigma_b \sqrt{\pi a}\,\{0.375\,x^{-2.5}\,(1 + 0.5x + 0.375x^2 + 0.3125x^3 + 0.2734x^4 + 0.537x^5)\} \text{ (bending)} \quad -- (14)$$

where $x = (D-2a)/D$; a = flaw depth and D= diameter of shank.

The above equations were combined to produce the solution for the head-to-shank transition. Details of the equations and results are presented in Appendix 2, solution VIII.

Mechanical Testing:

Mechanical testing of CRD capscrew material was performed to:

1) Determine mechanical properties to establish equivalency with the CRD capscrew material.
2) Obtain load-strain trace for applied loads equivalent to the CRD capscrew preload at operating temperature.
3) Evaluate the load-strain traces to determine the effect of notch depth, and to

4.0 Details of Evaluation (Continued)

establish the instability load and strain.

4) Elastic-plastic notch analysis, using Neuber's rule, to determine the limiting load for net section yielding.
5) Comparison of results from testing and the notch analysis with the limiting flaw depth determined by analysis.

The purpose of the testing is to provide experimental verification for the analytically determined flaw limits. The determination of net section yield load and strain would provide the basis for the verification.

Appendix 4 provides the details of the mechanical testing and the notch analysis performed.

5.0 Discussion:

Review of Field Inspection Data {GGNS & RBS}

A review of the data contained in references 3, 4, 16, 17 and 23 show the following:

Site/Year	Number of CRD Cap Screws		Number Confirmed		Max. Depth
	Inspected	w/Ind. (visual)	LP Test	Other Method	(mils)
GGNS/1992	176	17	17(10.23%)	-	42.0
GGNS/1996	208	78	55(15.4%)	32[1]	46.0
RBS/1992	400	53	49(12.25%)	-	-
RBS/1996	24	9	3(12.5%)	2[2]	58.0

Notes: 1) Eddy Current Test.
2) Stereo Microscopy (after cleaning).

In summary the information reviewed and the field results presented above show the following:

1) The percentage of cap screws with verified indications were between 10% to 15.5% of the number inspected, considering a large variation in sample size.
2) The maximum measured depth (metallographically determined), show depths between 42 to 58 mils. The measured difference at GGNS between 1992 and 1996, covering two cycles of operation, is 4.0 mils.
3) The morphology of the flaws, determined by metallography, at both GGNS and RBS were similar. Pitting was the predominant flaw type with occasional cracks at prior austenite grain boundary. These grain boundary cracks were limited to a grain diameter (reference 3). In all the metallurgical evaluations performed (references 3, 4 and 17), no overwhelming evidence of stress corrosion cracking was found.
4) The Eddy Current test method for determining the flaw depth was demonstrated to provide a conservative (upper bound) estimate (reference 4).

In order to provide a perspective of the flaws found on the CRD cap screws at GGNS, one of the cap screws removed in 1992 was photographed with the aid of a stereo microscope.. Figure 4 presents the photographs from the head-to-shank transition region. These photographs were taken at three azimuthal locations. From these photographs it is evident that the flaws in this region are short, basically elongated pits. In some instances there appears to be a linear flaw joining the adjacent pits. The typical flaws observed on CRD cap screws, in the head-to-shank transition region, are discontinuous elongated pits around the

5.0 Discussion (Continued):

circumference and are confined to the fillet radius. Therefore, a full circumferential notch assumption at this location is conservative.

Stress Corrosion Cracking Threshold

The ASME Section XI allowable, established for this report, was based on the K_{ISCC} value obtained from reference 12 at 130 ksi$\sqrt{in}$. This data was shown to be representative of the behavior of low alloy quenched and tempered steels in a water or humid air environment. Two sets of data presented in reference 24 for K_{ISCC} show ; that the water/humid air environment data to be agreement with the data from reference 12 and the data for aqueous chlorides/sea water show lower K_{ISCC} values. In reference 24 the NRC lower bound curve was also presented for comparison. The NRC lower bound curve appears to be an absolute lower bound to all data. Thus the values for K_{ISCC} are significantly lower at the yield strength level of interest. It should be emphasized that the environment of interest is not as aggressive as the aqueous chlorides and the yield strength levels are well below the levels at which stress corrosion cracking is a cause for concern. Therefore the aqueous chloride data and the NRC lower bound data can be considered as affirmation for the factor of safety provided in the ASME Section XI article IWB-3612. Hence the threshold value for K_{ISCC} , which is applicable to the environment for the CRD cap screws, is 130 ksi$\sqrt{in}$.

Stress Analysis

The shape of the stress profiles obtained from the finite element analysis are in agreement with the stress distributions presented in reference 8. The use of validated stress profile based linearization technique provides a comprehensive method to evaluate the load carrying capability of the CRD cap screw. Conservative assumption of a full circumference notch to represent the observed pitting damage would provide a lower bound degradation depth that would preclude tensile failure of the cap screw and preclude joint separation. The structural evaluation of the cap screw (see Appendix 3) using upper bound degradation showed that joint separation is precluded. The calculated external load (L_X), caused by a maximum internal pressure of 5,872 psi, was 13.909 kip. and the joint separation load required for the residual preload (L_{xcrit}) was 20.615 kip. Therefore under the worst combination of degradation and maximum internal pressure joint separation will not occur since $L_X < L_{xcrit}$. The evaluation of bolt strength showed that a flaw of 0.107 inch would not cause the bolt to exceed the ASME allowable value of $3S_m$ for the combined load of residual preload plus the external load from maximum internal pressure. Therefore for a full circumferential flaw with a depth of 0.107 inch the evaluations presented in Appendix 3 demonstrate:

1) No joint separation, under the maximum internal pressure load, would occur; and,
2) The cap screw will not fail by overload under the combined loads from residual preload and maximum internal pressure.

5.0 Discussion (Continued):

Fracture Mechanics Evaluation:

The fracture mechanics evaluations presented in Appendix 2 were performed to evaluate the assumed flaws in three separate regions. These regions were analyzed separately owing to the distribution of stresses in these regions. The finite element analysis was only performed for the head-to-shank transition region because the steep stress gradients necessitated the decomposition of stress into tension and bending components for use in fracture mechanics formulations. For the shank region where uniform tension prevails, straight forward fracture mechanics formulations were available. In the thread root region, recent empirical formulations had become available which used the nominal tension in the shank as the prevailing stress. The discussion, presented below, provides a synopsis of the application of the fracture mechanics solution as it was applied to the CRD cap screw in the three regions. For each of these regions the depth of degradation (flaw depth) of 0.150 inch was used to compare the applied stress intensity factor with the allowable (ASME Section XI IWB 3612 criterion) stress intensity factor.

Head-to-Shank Transition

The results of the finite element analysis show the stresses in this region to be highly non-linear. For the fracture mechanics analysis two approaches to accommodate the non-linear stress profile were used. The two approaches, depending on the particular stress intensity factor formulation, have been described earlier in this report. The results from the various fracture mechanics formulations were compared with the allowable ASME limit (Section XI, IWB 3612) of 91.92 ksi$\sqrt{in}$. This comparison is graphically presented in figure 5. In the previous evaluation (reference 3) a flaw depth limit, based on a full circumferential notch, was set at 0.150 inches (150 mils). The table below provides the pertinent results from the current fracture mechanics evaluations at a flaw depth of 0.150 inches.

Appendix 2	Crack Type & Profile		K_I @ 0.150"	Applied Stress Form
Solution #	Type	Profile	ksi$\sqrt{in}$	
IB	Single	Circular	32.5	$P_m + P_b$
IIIA	Single	Circular	32.5	$P_m + P_b$
IV	Single	Circular	26.88	Profile, Note 1
VA	Single	Straight	32.0	Profile, Note 1
VIA-I	Full Circumference	Notch	85.0	Surface Peak Stress from linearized profile in note 1
VIA-II	Full Circumference	Notch	48.0	Profile, Note 1
VII	Full Circum. & Single	Notch & Straight	50.0	$P_m + P_b$
VIII	Full Circumference	Notch	81.64	$P_m + P_b$

Note 1: Linearized profile using strain energy density principle.

5.0 Discussion (Continued):

The fracture mechanics results presented above lead to two observations, which are:

1) The single crack model prod'ces a lower applied stress intensity than that for a full circumferential notch; and,
2) For a full circumferential notch, the method of applying the stress profile, whether decomposed values ($P_m + P_b$) or a linearized profile, does not affect the applied stress intensity value in a significant way.

The case for a full circumferential notch subjected to an applied stress equal to the peak stress (solution VIA-I) is not a realistic analogue, rather a very conservative upper bound. This case was evaluated because the flaw depth limits for the inspection scope expansion in reference 3 used such a model. As can be seen from figure 5, the applied stress intensity at the depth of interest (0.150 inch) is below the allowable value for all cases evaluated. The results from all the fracture mechanics solutions clearly demonstrate that the flaw depth limit for scope expansion, established in reference 3, was rational based on fracture mechanics results. At this flaw depth some margin to the allowable ASME limit of Section XI IWB 3612 (references 5 and 6) exists. Solution VIII which used a full circumference notch subjected to a combined tension plus bending stress yielded high applied stress intensity values. Those values were very close to the results from Solution VIA-1. These very high values can be explained by the discussions provided in reference 10, which indicates that the full circumference notch is expected to yield a high stress intensity factor when analytically determined. The reasoning (reference 10) provided, suggests that analytically the notched bar in bending cannot support a compressive load on the opposite side and this leads to the unrealistically high stress intensity. Therefore, in reference 10 a superposition of two flaw models, similar to solution VII was developed to establish fracture toughness requirements for bolting. The rapid decay of stress in this region, as shown by finite element analysis, from a peak at the free surface to below the nominal value in the shank region occurs within 0.03 inch. Thus, in accordance with Appendix "A" of reference 5 and 6 it is appropriate to linearize the stresses in this region. When the results of the linearized stresses, stress components, are used as applied stress in determination of the applied stress intensity, then a realistic but conservative value is obtained. From figure 5 it is observed that for flaw depths below 0.130 inch solution VIA-II provides a more conservative value. At flaw depths above this value solution VII provides a more conservative value. This point is academic, since at the flaw depth of interest solution VII provides a conservative value for applied stress intensity. At the flaw depth of interest (0.150 inch) the calculated applied stress intensity is shown to be below the allowable ASME limit.

Shank Region

In the shank region, removed from discontinuities, the stress distribution due to bolt preload is very uniform at an applied stress of 56.5 ksi. For this

5.0 Discussion (Continued):

region the available stress intensity factor solutions were evaluated using a uniform tensile stress of 56.5 ksi. The crack front profiles evaluated were: straight front crack, circular front crack, and a full circumference notch. Details of the evaluation are provided in Appendix 2. Figure 6 presents the results for the applied stress intensity factor as a function of flaw depth for this region. The table below presents a summary of applied stress intensity factors at a flaw depth of 0.150 inch, which was the flaw depth recommended for scope expansion criterion in reference 3.

Appendix 2	Crack Type & Profile		K_I @ 0.15"	Applied Stress Form
Solution #	Type	Profile	ksi√in	
IC	Single	Circular	30.34	Uniform Tension (56.5 ksi)
IIIB	Single	Circular	30.19	Uniform Tension (56.5 ksi)
VB	Single	Straight	42.79	Uniform Tension (56.5 ksi)
VIBE	Full Circumference	Notch	53.77	Uniform Tension (56.5 ksi)

From figure 5 it is observed that the full circumference notch produced the highest applied stress intensity, followed by the single straight front crack profile. At the crack depth of interest (0.150 inch), the above table shows that the highest applied stress intensity is 53.77 ksi√in. This value of applied stress intensity is considerably below the allowable applied stress intensity, in accordance with ASME limits in IWB 3612 (references 5 and 6), of 91.92 ksi√in. Thus the flaw depth prescribed for scope expansion is shown to be conservative with a margin of 1.71 with respect to the allowable value.

Thread Root Region

In the CRD cap screws inspected to date there has been no evidence of flaws in this region based on detailed visual inspection of about six hundred (600) cap screws. However, for the sake of completeness fracture mechanics analysis for this region was performed. The applied stress was taken as the nominal tension in the shank due to bolt preload and the value was 56.5 ksi. Two applied stress intensity factor solutions were found in the literature for thread root region (references 18 and 19). Both solutions were evaluated and the details of the analysis are provided in Appendix 2. The results of these evaluations are summarized in figure 7. From figure 7 it is evident that the applied stress intensity at a flaw depth of 0.245 inch is below the applied stress intensity for the other two regions at the limiting flaw depth of 0.150 inch. In this region the flaw depth is considered to be the sum of thread depth plus the flaw depth. For the CRD cap screw the thread depth is approximately 0.09375 inch. The fracture mechanics presented in Appendix 2 shows that the flaw depth for the scope expansion criterion of 0.15 inch (reference 3) is conservative for this region. This is substantiated by the fact that for a flaw depth of 0.150 inch the additional depth of the thread of 0.09375 would result in a total depth of 0.24375 inch. The applied stress intensity at this total flaw depth is 45.87 ksi√in. This value of applied stress intensity is sufficiently

5.0 Discussion (Continued):

below the allowable value of 91.92 ksi√in. The margin to the allowable value is 2.00. Additionally the specification for the CRD cap screws (reference 22) indicates that the threads were formed by rolling rather than by machining. The threads formed by rolling would have a compressive residual stress at the thread root. Therefore the likelihood of developing stress corrosion cracks in this region is very low given the high threshold stress intensity (K_{ISCC}) and the existence of compressive stresses at the thread root.

Mechanical Testing :

The scope, testing details and results from the mechanical testing and notch analysis are provided in Appendix 4. The mechanical testing consisted of ensuring that the materials used for notched tension testing had equivalent material properties and that the shank diameter of the bolts was equivalent to that of the CRD capscrews. The results from the tests to establish material's mechanical properties demonstrate that the procured bolts were equivalent to the material used to manufacture the CRD capscrews. The tension test data was also used to determine the Ramberg-Osgood coefficients. The determined coefficients from the test data compared favorably with data from published literature for similar materials. The Ramberg-Osgood material model enables incorporation of work hardening behavior in the notch analysis.

The load-strain behavior of both the un-notched and the notched specimens were very similar. The measured specimen strain (nominal strain) for all specimens tested, (one CRD capscrew removed from service at GGNS, two un-notched procured bolts and two specimens for each notch depth of 100, 125 and 150 mils), up to a maximum load of 36.0 kips were nearly the same. Results from a linear regression of the strain and notch depth data, including un-notched data, showed that the notch depth did not affect the nominal strain up to the max load of 36.0 kips and notch depth of 150 mils. The load-strain behavior was linear elastic as indicated by a linear load-strain trace and clear absence of residual strain upon complete unloading of the specimen. The load where net section yielding occured, discernable by a departure from linearity on the load-strain trace, was well above the maximum expected preload for the CRD capscrew.

The notch analysis performed showed that at the maximum applied load of 36.0 kips net-section yielding was precluded as the notch strains remained well below the crtitical strain required for net-section yielding. The results presented in Appendix 4 clearly demonstrate that, for the limiting flaw depth and anticipated CRD cap screw loads, net-section yielding does not occur.

6.0 Conclusions:

The results of the analyses presented support the following conclusions:

1) The structural analysis of the CRD cap screws and CRD flanged joint produced a a maximum degradation depth of 0.107 inch, based on a full circumference flaw.
2) The fracture mechanics evaluation showed that at a degradation depth of 0.150 inch, stress corrosion crack initiation is not likely.
3) The scope expansion criterion of reference 3 was based on fracture mechanics evaluation and did not consider the potential for failure by overload of the net section. Therefore, the scope expansion or screening criterion is revised (lowered) from 0.150 inch (reference 3) to 0.107 inch based on the evaluations presented in this report.
4) The fracture mechanics evaluation also supports the observed flaw morphology, that no evidence of stress corrosion cracking were found. This conclusion is based on the results showing the applied stress intensity at all locations of the CRD cap screw to be significantly below the K_{ISCC} value.
5) The flaw depth measured by Eddy Current testing provides an upper bound value. The upper bound estimate of flaw depth coupled with the conservative threshold depth set for scope expansion criterion provides good assurance against premature failure of CRD cap screws.
6) The measured flaw growth of 4.0 mils over two cycles of operation indicates that there is no evidence of an active stress corrosion cracking mechanism. A comparison of the results from the metallurgical evaluations of the 1992 and 1996 GGNS reports, provides additional support to the results obtained from the fracture mechanics evaluations.
7) Based on the maximum flaw depth and the observed growth rate for degradation the scope expansion criterion, in terms future operating cycles, can be conservatively defined as:

Present Depth (inch) + 0.008 x(number of cycles to next inspection) ≤ 0.107

8) Mechanical testing and notch analysis confirm the analytically determined results, for the limiting flaw depth subjected to anticipated loading, that net section yielding is precluded.

7.0 References:

1) GE RICSIL 483, Revision 1
2) GE RICSIL 483, Revision 2
3) Grand Gulf Nuclear Station Engineering Report, GGNS-92-0033, Revision 0. 1992.
4) Entergy Operations Engineering Report, EP-98-001-00. 1998
5) ASME Boiler and Pressure Vessel Code, Section XI 1977 Edition including Winter 1979 addenda. {for GGNS}
6) ASME Boiler and Pressure Vessel Code, Section XI 1980 Edition including Winter 1981 addenda. {for RBS}
7) "Eddy Current Feasibility Study for Depth Sizing Flaws in Carbon Steel Type-4140 Cap Screws"; EPRI NDE Center. 1996
8) "An Introduction to the Design and Behavior of Bolted Joints"; John H. Bickford; Third Edition, Marcel Dekker Inc. 1997.
9) "Specification for Bolting for Flanges and Pressure Containing Purposes"; British Standard 4882-73; BSI, UK
10) "PVRC Recommendations on Toughness Requirements for Ferritic Materials"; WRC Bulletin 175, 1972.
11) "Fracture and Fatigue Control in Structures - Application of Fracture Mechanics"; Rolfe and Barsom, Prentice-Hall Inc. 1977.
12) "Degradation and Failure of Bolting in Nuclear Power Plants"; Volume 2. EPRI NP-5769, Electric Power Research Institute, 1988.
13) ASME Boiler and Pressure Vessel Code, Section II Part D, 1992 Edition.
14) NISA II/DISPLAY III Users Manual, Version 6.0
15) Mechanics of Materials; Second Edition, F. P. Beer and E. R. Johnson, Jr.; McGraw Hill Inc. 1992.
16) River Bend Nuclear Station, RBS CR 92-0410
17) River Bend Nuclear Station, RBS CR 96-0310
18) "Review and Synthesis of Stress Intensity Factor Solutions Applicable to Cracks in Bolts"; L. A. James and W. J. Mills; Engineering Fracture Mechanics, Volume 30, Number 5; 1988
19) " Behavior of Fatigue Cracks in a Tension Bolt"; Alan Liu; ASTM STP-1236.
20) "Growth Behavior of Surface Cracks in the Circumferential Plane of Solid and Hollow Cylinders"; R. G. Forman and V. Shivakumar; ASTM STP 905
21) "Stress Analysis of Cracks"; Paul C. Paris and George C. Sih; ASTM STP 381
22) GE Drawing Number 117C4515 Revision C; "Cap Screws"
23) GGNS CR 1996-0342-00
24) "Requirements and Guidelines for evaluating Component Support Materials under Unresolved Safety Issue A-12", EPRI NP-3528, June 1994; Electric Power Research Institute, Palo alto, CA.
25) GE Report DCA22A4912 Revision 0; Jan. 11, 1983.

7.0 References (continued):

26) GE Drawing number 149A4291, Revision 2. (washer dimensions)
27) GE Drawing number 922D124, Revision 3. (CRD Nozzle and Flange)
28) " The Regulatory Approach to Fastner Integrity in the Nuclear Industry"; Davis, J. A. and Johnson, R. E.; ASTM STP-1236.

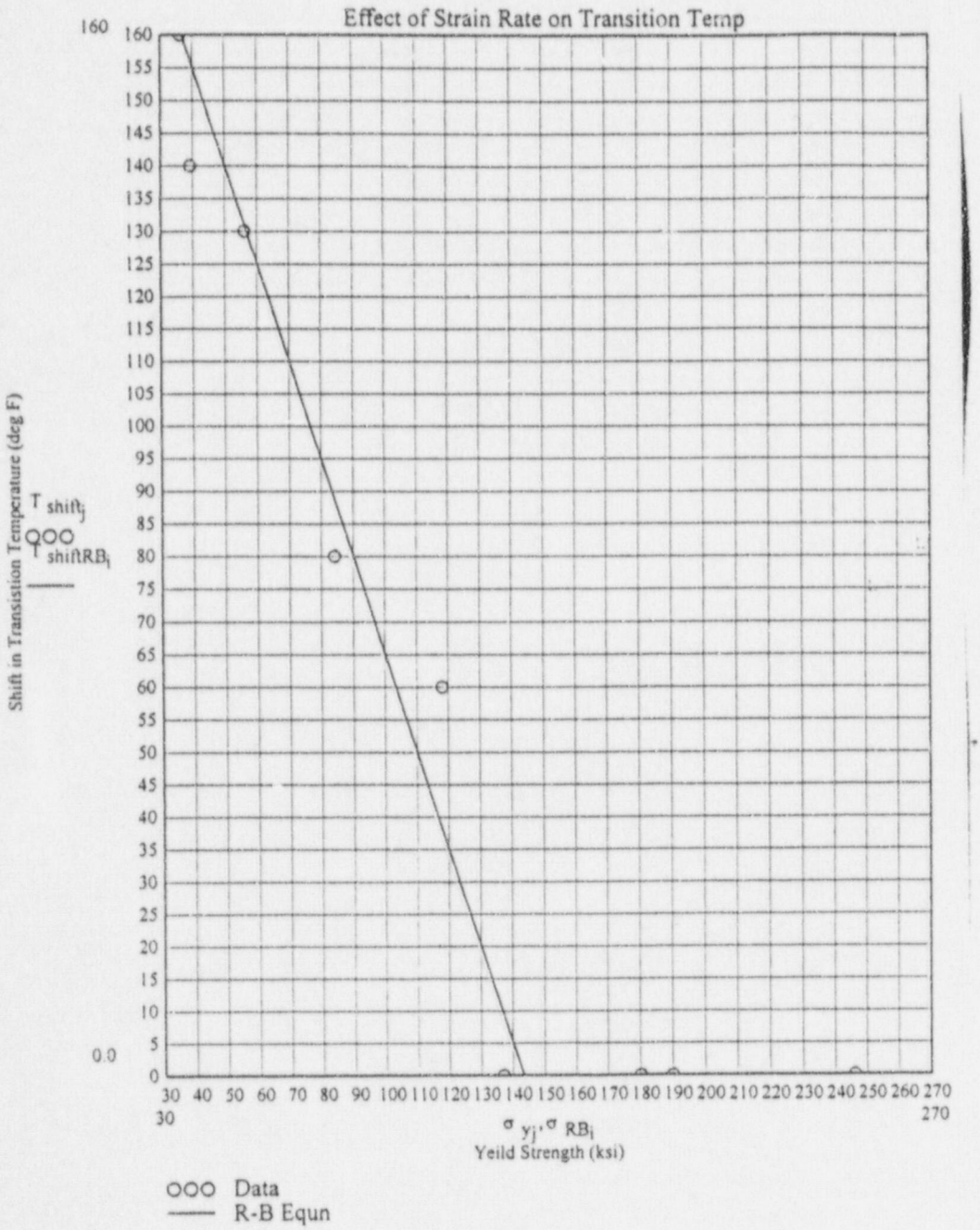

Figure 1: Temperature Shift vs. Yield Strength of Steels {Reference 11}

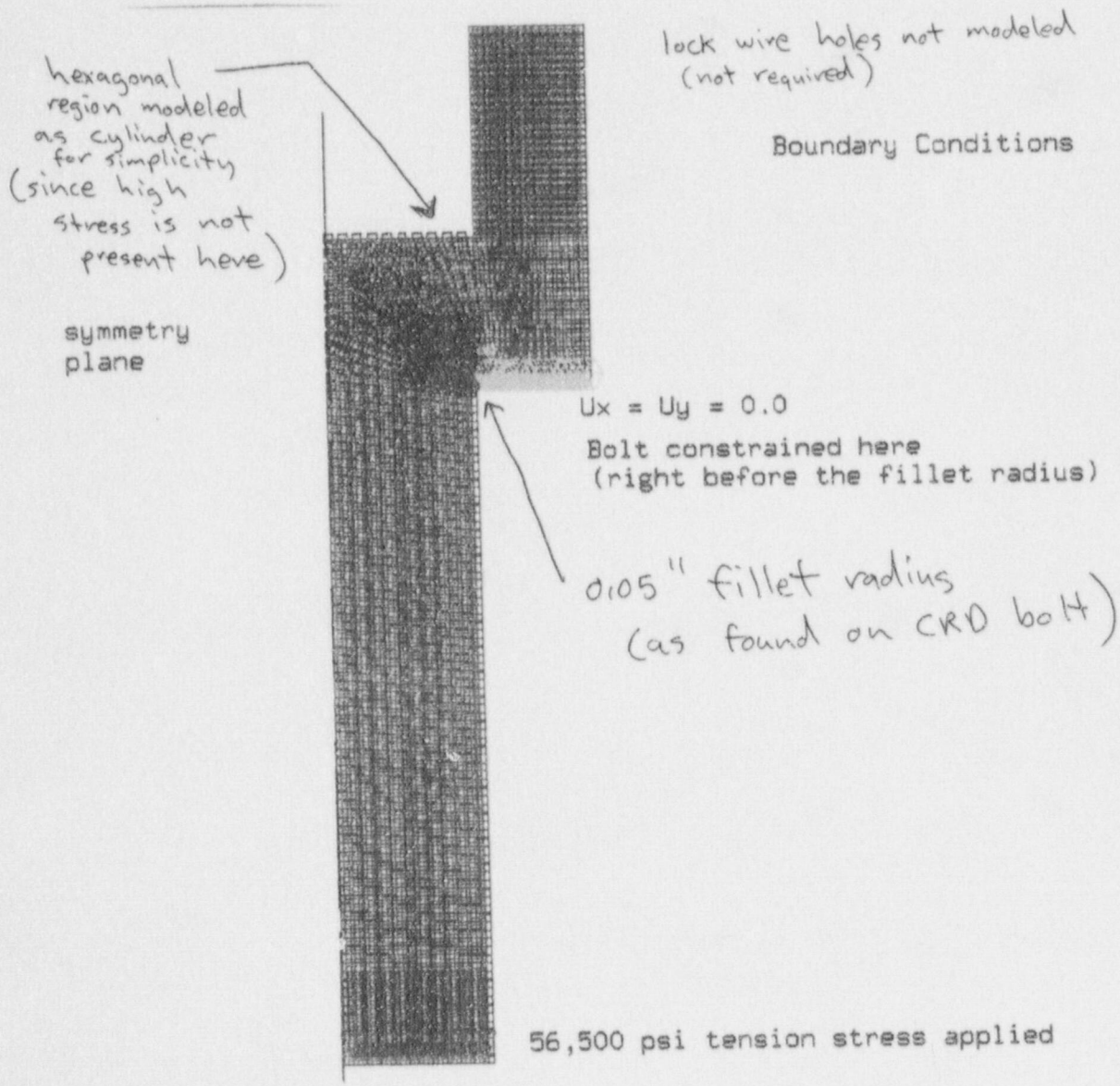

Figure 2: Finite Element Model of CRD Cap Screw {Head-to-Shank Transition}

Graph 1-1: Stress Profile Through the Bolt: Curve Fit of Stress Data

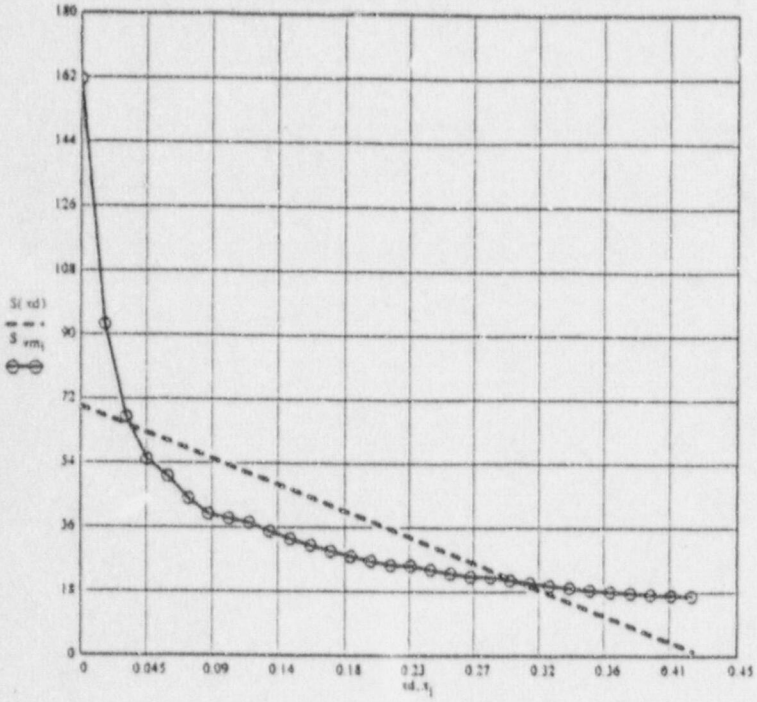

Graph 1-2: Strain Energy Linearization at 0.25 in. from Fillet

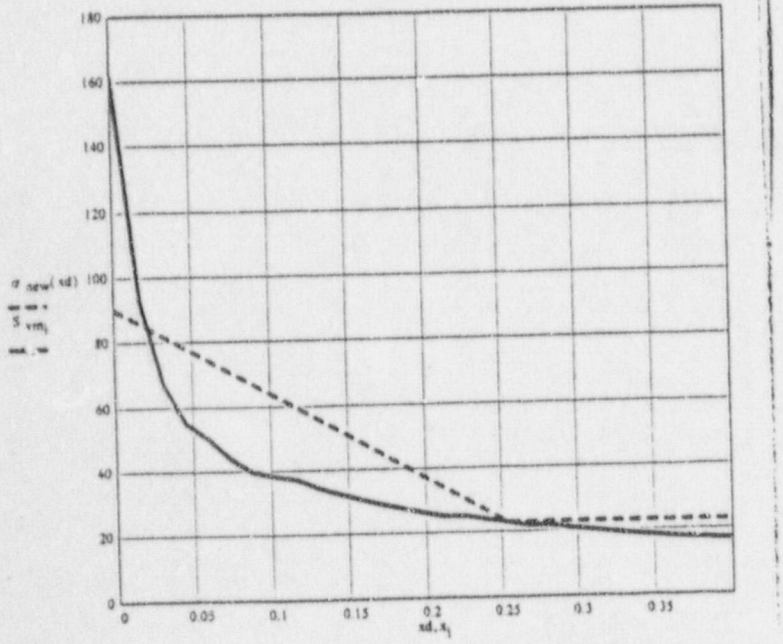

Figure 3: Linearization of Stress Profile

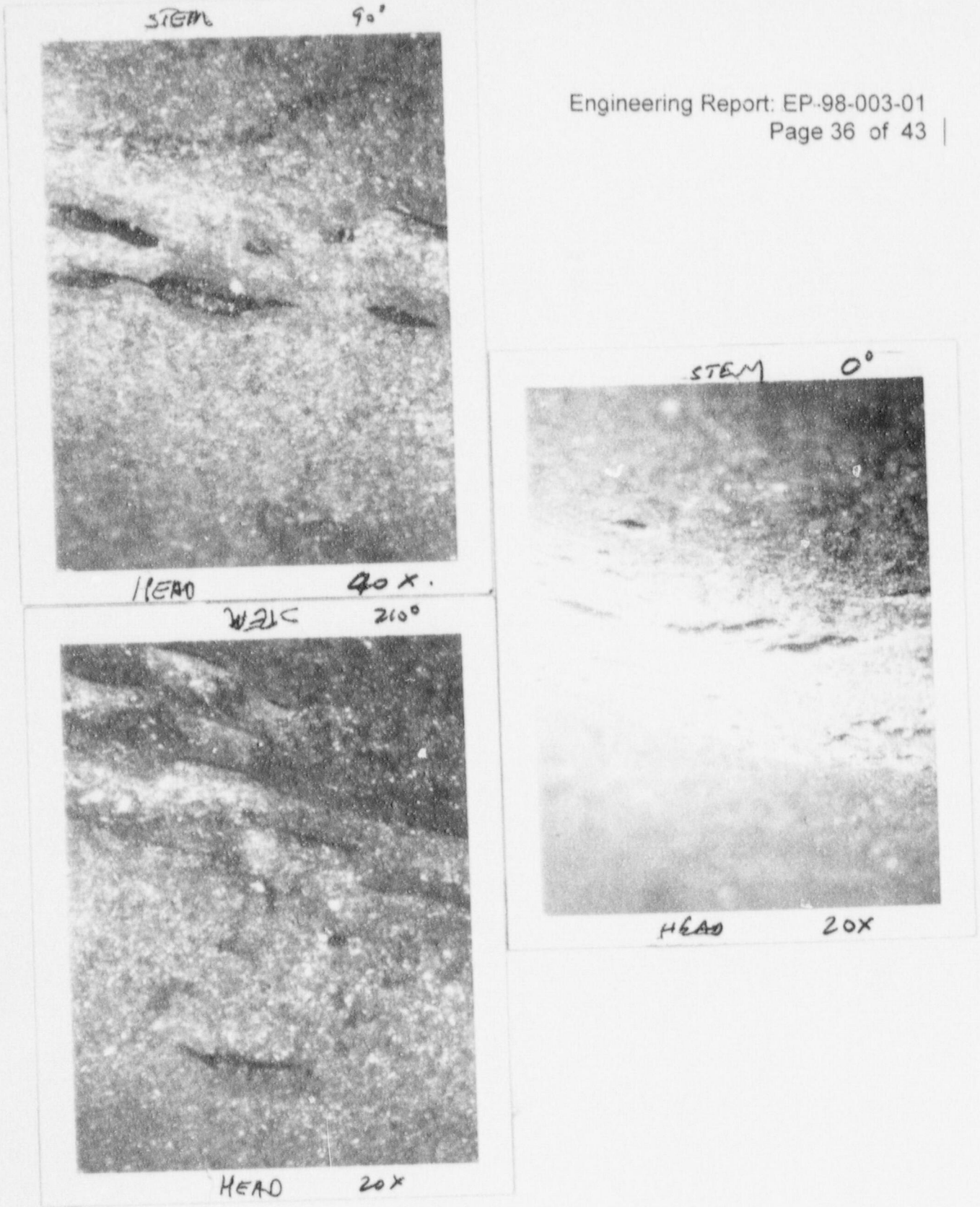

Figure 4: Stereo Microscope Photographs of Flaws in CRD Cap Screw

Graphical Comparisor. of Results from "K" solutions for Head to Shank Region

Note : Paris-Sih correlation is for a Full Circumferential Crack (360 degrees) whereas the other correlations are for Part-Circumferential Cracks.

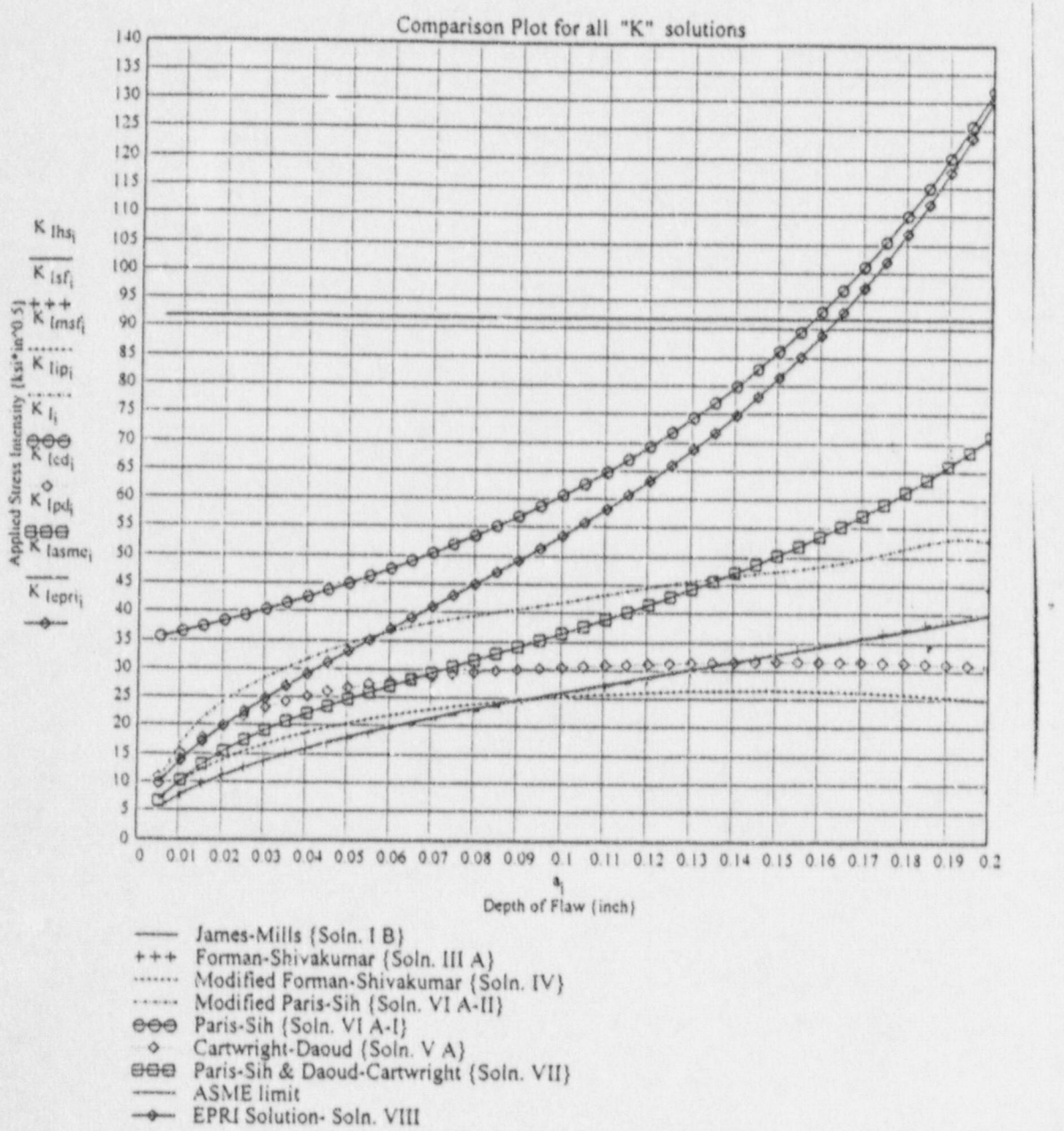

Figure 5: Applied Stress Intensity Results for Head-to Shank Transition Region

Note : Paris-Sih correlation is for a Full Circumferential Crack (360 degrees) whereas the other correlations are for Part-Circumferential Cracks.

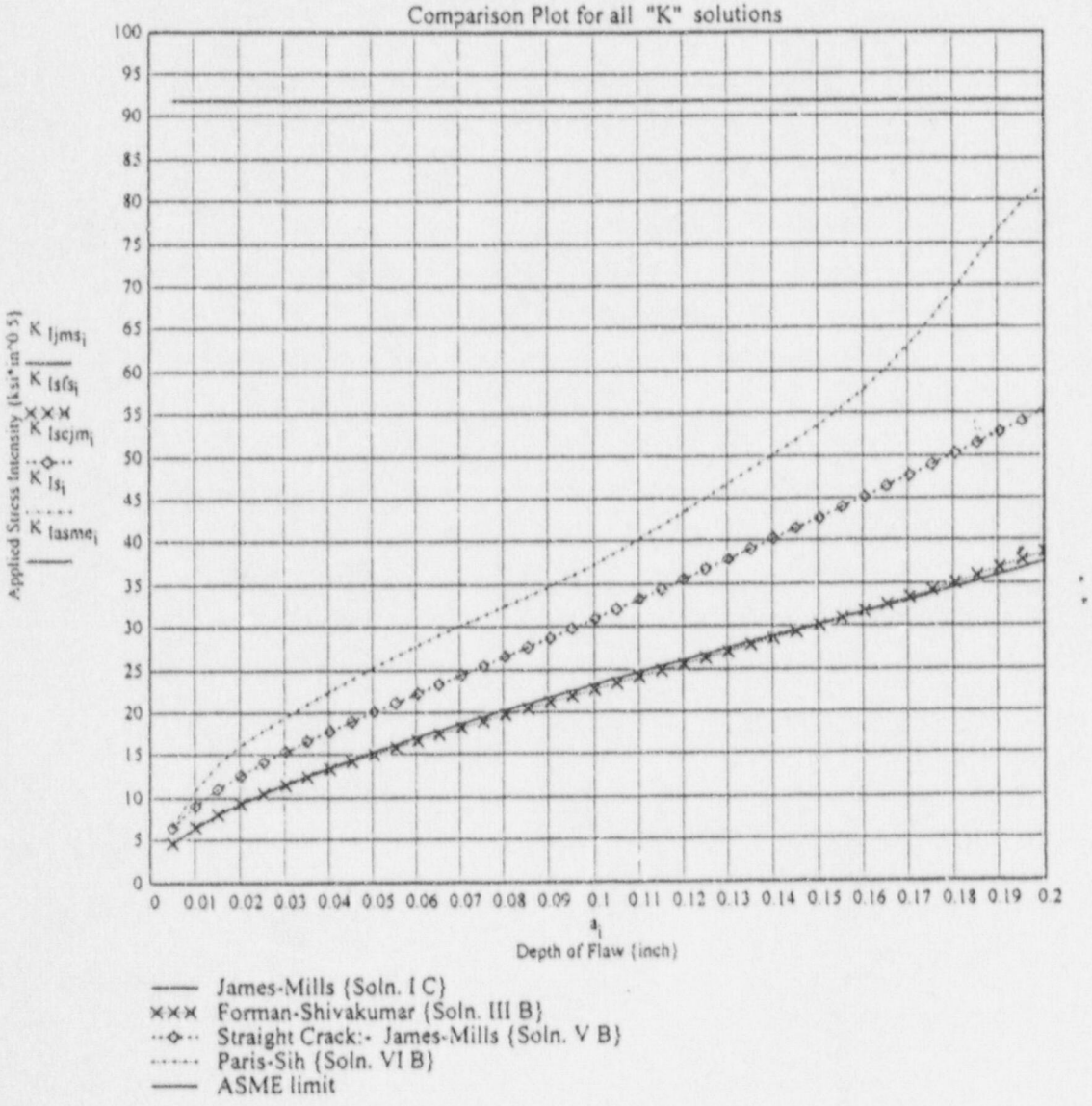

Figure 6: Applied Stress Intensity Results for Shank Region

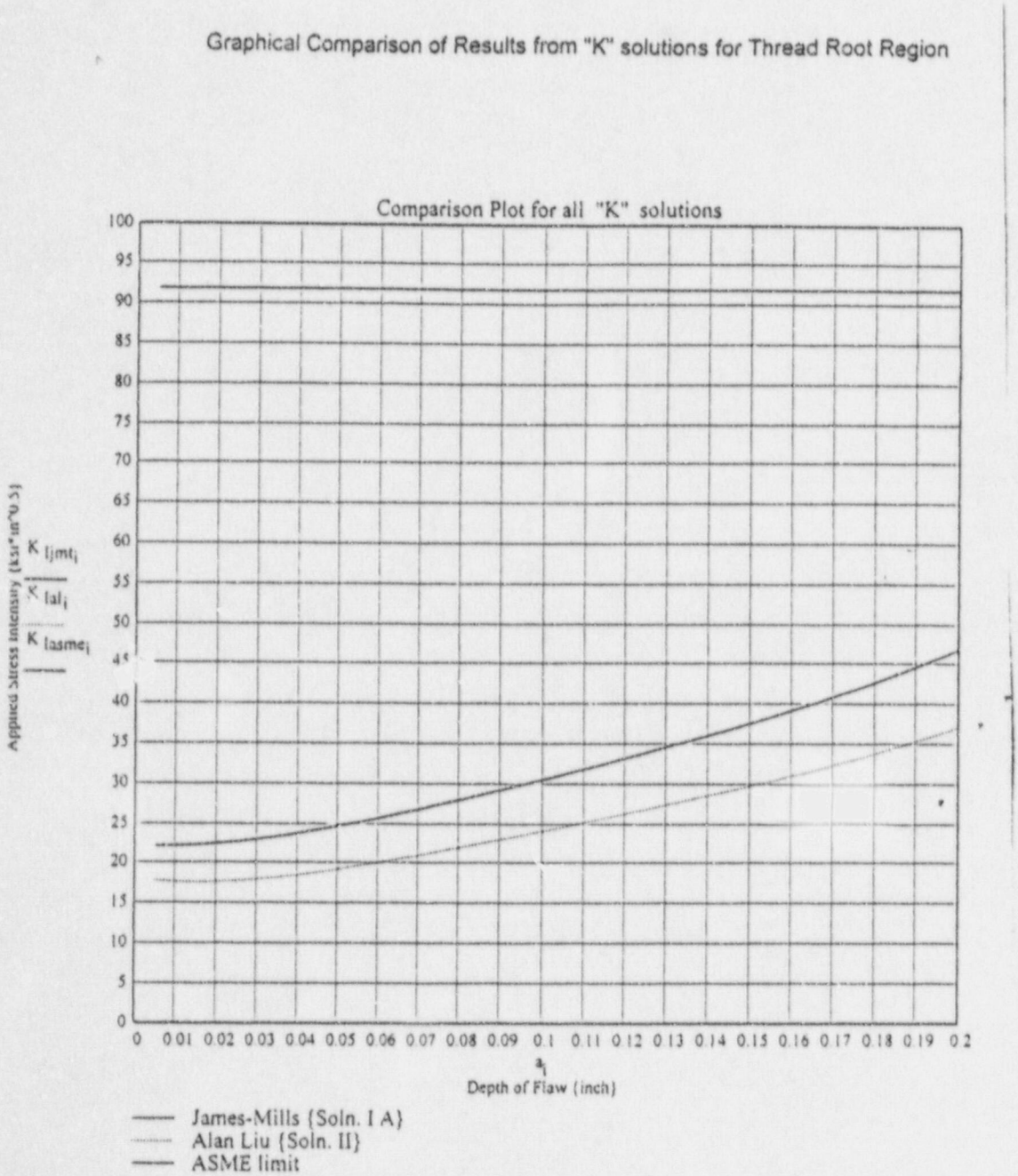

Figure 7: Applied Stress Intensity Results for Thread Root Region

Appendix 1

Finite Element Analysis of CRD Cap Screw

Appendix 2

Fracture Mechanics Evaluation of Flaws in Bolts

Appendix 1: Finite Element Analysis of GGNS CRD Bolt

1.0 Finite Element Model Data

1.1 Geometry: Two CRD bolts were modeled: one with a 0.05" fillet radius (model *bo5a.nis*), which exists on the actual CRD bolt, and one with a 0.075" fillet radius (*bo75.nis*) to show the effects of a slightly larger fillet on the through-thickness stress profile. The dimensions on the half cross section of the bolt are given in Figures 1 (for the 0.05" fillet) and 2 (for the 0.075" fillet). The dimensions were taken from hand measurements on an actual CRD bolt. A 2" segment of the bolt shank has been modeled. The lock wire holes and hexagonal head were not modeled, to preserve the simplicity and refinement of the finite element mesh; this was justifiable, since the high stress concentrations correspond to regions near the fillet radius and not on the upper head portion of the bolts.

1.2 FEA Model: The CRD Bolt was modeled as a 2-D axisymmetric model (shown in Figures 3 and 4) using the NISA II/Display III finite element program. The model consists of nodes and elements (NKTP=3, NORDR=1) representing the right-hand side of a 2-D cross section of the bolt. The axisymmetric model interprets the cross section as a full 360° bolt. Axisymmetric elements were used to allow greater refinement of the mesh around the fillet at the shank-to-head region. As mentioned in Section 1.1, the hexagonal bore in the bolt head was modeled as a cylinder in the axisymmetric model for simplicity and because stresses in this portion of the bolt are relatively low.

1.3 Material Properties: The CRD bolt is made of SA-193 Gr. B7 (4140) steel, with a modulus of elasticity of 30×10^6 psi. Poisson's ratio was taken as 0.3. The material yield strength from ASME B&PV Code Section II, Part D, 1992 Edition (ref. 11), S_y = 105 ksi and the ultimate strength, S_u = 125 ksi. The design stress intensity, S_m = 29.5 ksi (at 550°F).

1.4 Applied Loads: A tension stress of 56,500 psi was applied to the end of the bolt shank (as shown in Figures 2 and 3). This stress represents the preload on the bolt.

1.5 Boundary Conditions: Fixity boundary conditions in both the x- and y-directions ($u_x = u_y = 0.0$) were applied along the bottom of the bolt head, from the edge of the head to just before the onset of the fillet radius.

2.0 Stress Analysis of CRD Bolt from FEA Results

The CRD bolt was analyzed for stresses in the fillet region caused by tension due to preload and bending due to the constraint of the bolt head. The membrane (P_m) and

Appendix 1: Finite Element Analysis of GGNS CRD Bolt (cont.)

bending (P_b) components of the sectional stress are needed in the fracture mechanics correlations.

2.1 Linearization of Stresses

The most critical failure plane for the bolt is a horizontal plane extending from the peak stress location on the surface of the fillet through the thickness of the bolt. This plane is denoted in Attachment 1, Figures 1-3 and 1-4 (*bo5a.nis*) and in Attachment 2, Figures 2-3 and 2-4 (*bo75.nis*), as Plane A-A. It is constructed by drawing a horizontal line from the peak stress node through the bolt cross section. The distance from the reference (peak stress) node to each node (or nodes) along the horizontal plane, closest to the line, is measured. The von Mises stress at these nodes is then plotted against the distance along the plane to give the through-thickness stress profile, as given in Graph 1-1 in Attachment 1 (*bo5a.nis*) and Graph 2-1 in Attachment 2 (*bo75.nis*). Since the bolt material is a very ductile material, stresses obtained using the von Mises theory of failure most accurately predicts the state of stress along the horizontal Plane A-A. Thus, these stresses are used in the linearization procedure, with minimal loss of accuracy over using all the component stresses.

The stress profile begins to go linear as the distance through the bolt increases, an effect of bending (due to constraint of the bolt head) on the applied preload. To resolve the stress profile into separate bending and tension components of stress, the entire profile was linearized using basic principles of mechanics of materials.

To determine the average membrane (or tensile) stress, P_m, across Plane A-A, the trapezoidal method of numerical integration was used to calculate the area under the stress profile using the von Mises stress values at the given points through the thickness. The average stress is determined by

$$P_m = S_{vm,avg} = \frac{1}{t}\sum_{i=1}^{n-1}\frac{1}{2}\cdot\left(S_{vm_i} + S_{vm_{i+1}}\right)\cdot\left(x_{i+1} - x_i\right) \qquad \text{Eqn. (2-1)}$$

where, $S_{vm,avg}$ is the average (von Mises) stress, t is the thickness to the midplane (for an axisymmetric model), and S_{vm} and x are the n-data points taken from the finite element model for von Mises stress and nodal distance, respectively (whether *bo5a.nis* or *bo75.nis*).

Appendix 1: Finite Element Analysis of GGNS CRD Bolt (cont.)

The total membrane plus bending stress, P_m+P_b, is found by performing a linear curve fit on the through-thickness stress profile. The y-intercept of the resulting line will fall below the peak stress value of the bolt and represent the total membrane plus bending stress for the bolt along Plane A-A. The bending stress component, P_b, is found by subtracting P_m in Eqn. (2-1) from the total membrane plus bending stress found using the linear regression technique.

Attachments 1 (for the 0.05" fillet) and 2 (for the 0.075" fillet) give detailed Mathcad calculations of the P_m and P_b values, as well as graphically show the linearization of the stress profile.

2.2 Use of Membrane and Bending Stresses in K_I Solutions

The bending component of stress is caused by the constraint of the CRD bolt head. When performing calculations to determine the stress intensity factors (K_I) for the bolt, several correlations require a separate stress value for both tension and bending. For Plane A-A which extends from the location of peak stress in the fillet radius of the bolt to the mid-plane of the bolt (due to axisymmetry), the membrane stress is less than the applied tensile stress in the shank of the bolt. The membrane plus bending stress, however, is greater than the applied tensile stress. The use of P_m and P_b in K_I correlations includes the effects of the stress concentration by the fillet on the sectional properties of the bolt.

2.3 Results of FEA and Stress Analysis

The membrane and bending stresses obtained from the finite element analyses and subsequent stress analyses of the CRD bolts with a 0.05" fillet radius and a 0.075" fillet radius, along the Plane A-A, are as follows:

FEA Model	**Stress Component (units in ksi)**		
	Membrane, P_m	Bending, P_b	Total, P_m+P_b
0.05" bolt	34.212	35.564	69.776
0.075" bolt	33.502	36.055	69.557

2.4 Strain Energy Approximation to Bolt Stress Profile

An additional stress linearization technique was used to determine a piece-wise linear approximation to the stress profile based on a linear regression, followed by a constant loading across the bolt at Plane A-A. This approximation was justified based the stress profile becoming approximately linear at a distance

Appendix 1: Finite Element Analysis of GGNS CRD Bolt (cont.)

through the bolt (along Plane A-A) of 0.25 inches. Graphs 1-2 (Att. 1) and 2-2 (Att. 2) show the point of linearization, around 0.25 inches. To create an approximation to the stress profile, the concept of equivalent strain energy density was used. With this technique, the area under the stress profile (calculated using numerical integration), divided by the thickness of the bolt at Plane A-A, is equal to the strain energy density (strain energy per unit volume) of the bolt at this location,. The equation for strain energy density, therefore, is a modified form of Eqn. 10.4 from ref. 13:

$$\sigma\varepsilon = \sum_{i=1}^{n-1}\left(\frac{1}{2}\cdot\left(S_{vm_{i+1}} + S_{vm_i}\right)\cdot\frac{\left(x_{i+1} - x_i\right)}{t}\right) \qquad \text{Eqn. (2-2)}$$

where, $\sigma\varepsilon$ is the strain density per unit volume (units of **in.·lb./in^3**), S_{vm} is the von Mises stress, x is the distance along Plane A-A, and t is the thickness of the bolt at Plane A-A (half the total thickness due to axisymmetry. All other dimensions cancel since the only different dimension terms are the thickness, t, and the distance, x across the horizontal cut plane. Eqn. (2-2) is identical to Eqn. (2-1) for average stress, except that it applies to the strain energy density and is used differently.

The strain energy density derived from Eqn. (2-2) is then assumed to be concentrated within the first 0.25 inches along Plane A-A; that is, the entire stress in the bolt head-to-shank region is considered to linearly regress from an initial value to the stress at a distance approximately 0.25 inches from the surface of the fillet. This is due to the behavior of the stress profile at this point. At a distance of approximately 0.25 inches from the surface, the stress profile begins to flatten out and remain linear, with only a very small slope, which is attributed the reduction of bending in this region. For use in fracture mechanics correlations, the stress is then assumed to be constant and equal to the value at 0.25 inches from the surface; however, the strain energy will be considered concentrated only in the first 0.25 inches from the surface.

The equation for this formulation is as follows:

$$\sigma\varepsilon \cdot t = \frac{1}{2}\left(\sigma_o + \sigma_{0.25}\right)d \qquad \text{Eqn. (2-3)}$$

where, σ_o is the y-intercept (reference) stress after linearization, $\sigma_{0.25}$ is the stress at approximately 0.25 inches into the bolt from the surface of the fillet, and d is the nodal distance of approximately 0.25 inches (slightly larger, since an actual point was taken from the FEA model). All other parameters are the

Appendix 1: Finite Element Analysis of GGNS CRD Bolt (cont.)

same as in Eqn. (2-2). This formula is derived from the equation for the area under a trapezoid; the trapezoid, as shown in Graphs 1-2 (Att. 1) and 2-2 (Att. 2) has the two heights as stresses (σ_0 and $\sigma_{0.25}$) and the horizontal width as the distance, *d*.

This method is considered conservative, since an actual linear regression of the stress across the bolt section would reduce the value of the y-intercept stress, σ_0, and allow the strain energy to be released through the entire bolt section and not just within a distance of 0.25 inches from the surface.

The stress $\sigma_{0.25}$ is found in the FEA output at a point closest to 0.25 inches from the fillet surface. From the model *bo5a.nis*, the point on Plane A-A closest to 0.25 inches from the surface of the fillet occurs between nodes 2493 and 2462, with d = **0.252811 in**. The stress at this point is $\sigma_{0.25}$ = **23.125 ksi**. From the model *bo75.nis*, the point on Plane A-A closest to 0.25 inches from the surface of the fillet occurs between nodes 1749 and 1750, with d = **0.24837** in. The stress at this point is $\sigma_{0.25}$ = **23.408 ksi**.

Since the strain energy density, the bolt thickness at Plane A-A, and the stress at the predetermined distance of 0.25 inches, $\sigma_{0.25}$, are known, the only term that is not known is the reference stress, σ_0. Solving for this quantity using Eqn. (2-3), the reference stress is σ_0 = **90.229 ksi** (for model *bo5a.nis*) and σ_0 = **90.636 ksi** (for model *bo75.nis*). Mathcad calculations for the strain-energy approximation are given in Attachments 1 and 2. The regression line using the strain energy approximation is shown in Attachment 1, Graph 1-2 (for *bo5a.nis*), and Attachment 2, Graph 2-2 (for *bo75.nis*).

The stress values using the strain-energy methods are used in the fracture mechanics correlations in Appendix 2 to solve for $\mathbf{K_I}$.

Figure 1: Dimensions of Half Cross-Section of GGNS CRD Bolt with 0.05" Fillet Radius

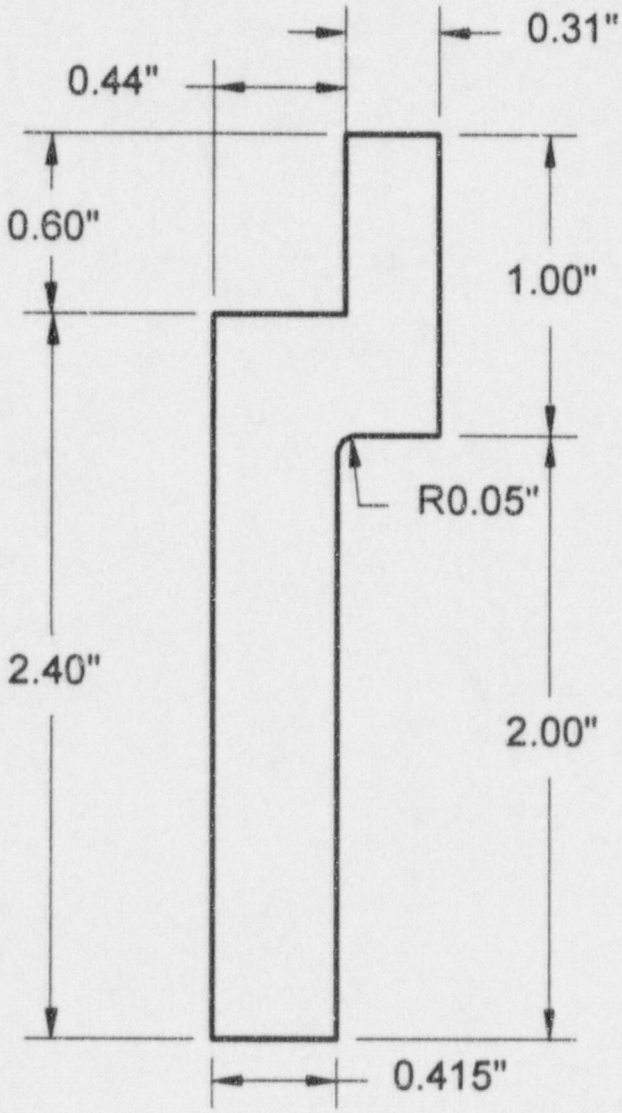

Figure 2: Dimensions of Half Cross-Section of GGNS CRD Bolt with 0.075" Fillet Radius

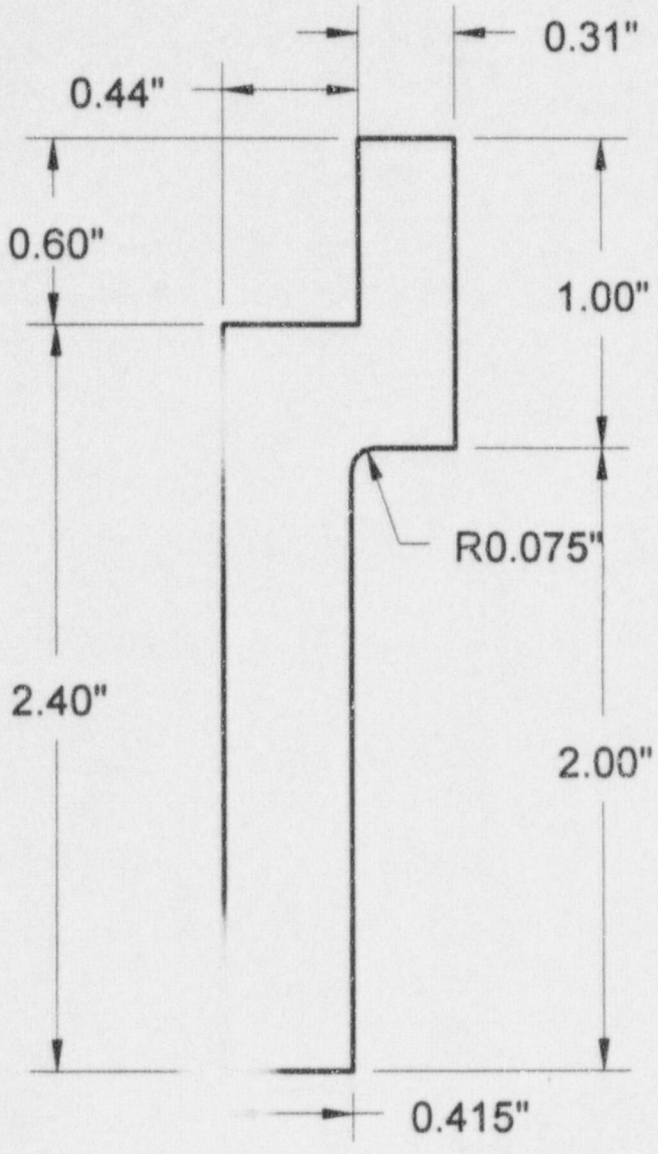

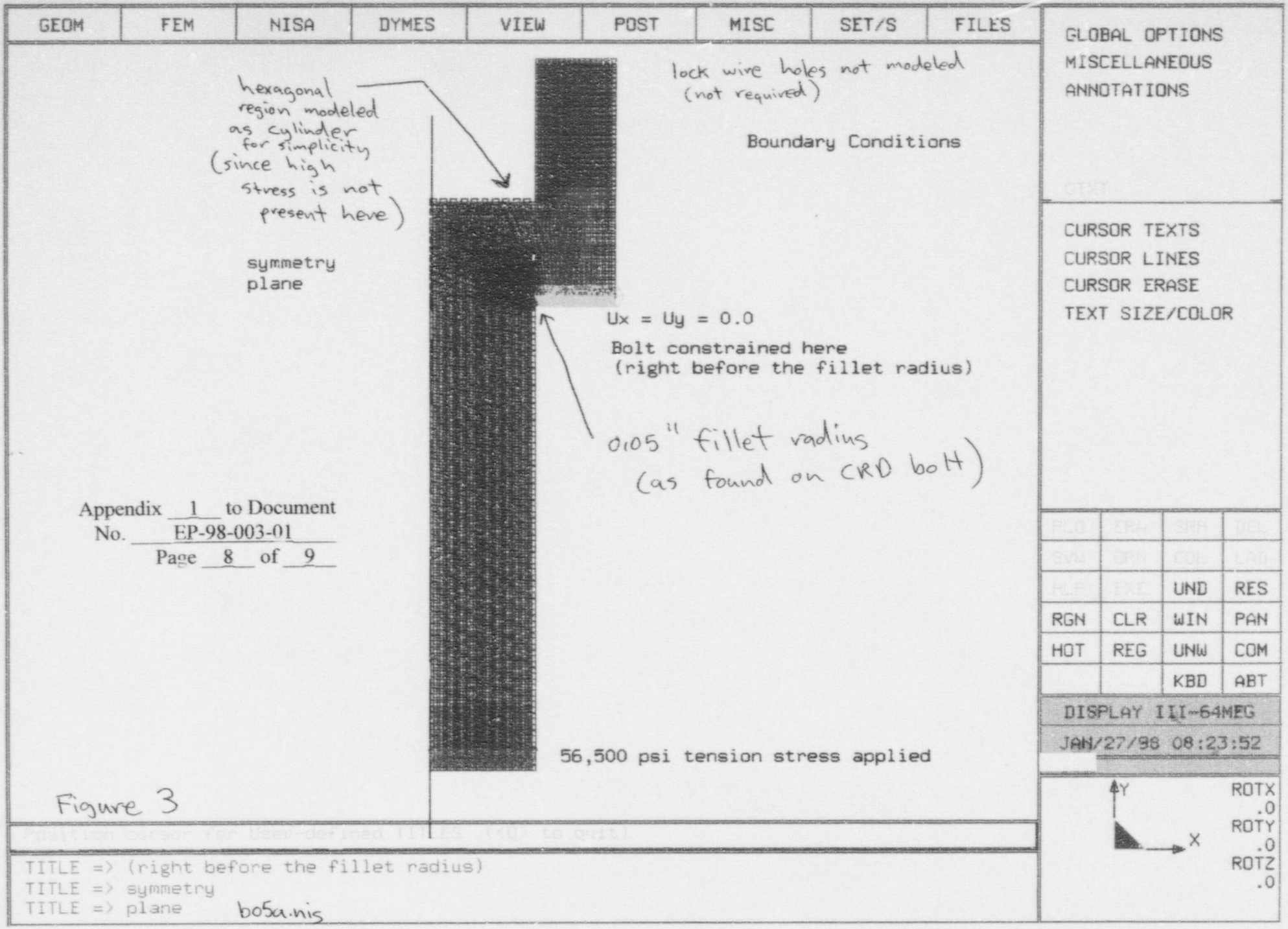

Appendix 1 to Document No. EP-98-003-01
Page 8 of 9

Figure 3

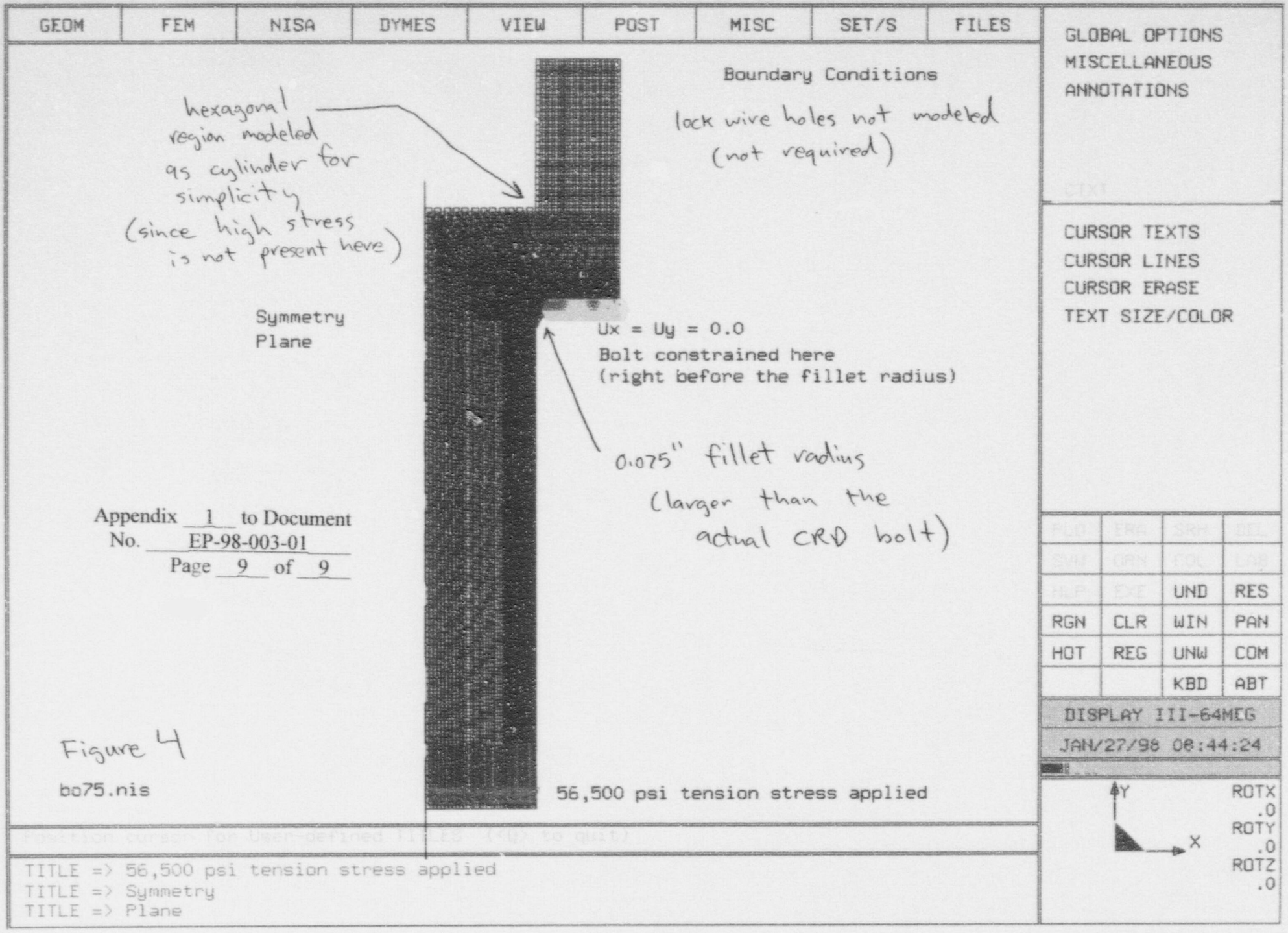

Appendix 1 to Document No. EP-98-003-01
Page 9 of 9

Figure 4

bo75.nis

Attachment 1: Section Stresses on Horizontal Plane A-A through Bolt Using Von Mises Stress (model *bo5a.nis*)

To calculate the average membrane stress across the section of the bolt, the trapezoidal method (from calculus) is used as follows:

There are a total of 31 data points (nodes or average of nodes) taken along Plane A-A.

ORIGIN := 1 n := 31 i := 1 .. n

Node No. $node_i :=$	x-distance (in.) $x_i :=$	Von Mises Stress (ksi) $S_{vm_i} :=$
2516	0	161.338
2524	0.0163108	92.890
2533.2534	0.0309101	66.892
2543	0.0447637	54.996
2552	0.0590185	50.216
2562	0.0728567	44.067
2572	0.0866949	39.711
2582.2504	0.1005885	38.430
2503	0.114478	37.315
2502	0.128311	34.804
2501	0.142144	32.696
2500	0.155978	30.883
2499	0.169811	29.289
2498	0.183644	27.860
2497	0.197478	26.562
2496	0.211311	25.366
2495.2464	0.225144	25.268
2494.2463	0.238978	24.158
2493.2462	0.252811	23.125
2492.2461	0.266644	22.163
2460	0.280478	22.055
2459	0.294311	21.193
2458	0.308144	20.403
2457	0.321978	19.685
2456	0.335811	19.041
2455	0.349644	18.475
2454	0.363478	17.988
2453	0.377311	17.586
2452	0.391144	17.271
2451	0.404978	17.047
2450	0.418811	16.912

$t := x_n$ Section Thickness

$t = 0.4188$

The average Von Mises membrane stress, S_{vm}, is

$$tS_{vm.avg} := \sum_{i=1}^{n-1} \left(\frac{1}{2}\right) \cdot \left(S_{vm_i} + S_{vm_{i+1}}\right) \cdot \left(x_{i+1} - x_i\right)$$

$$S_{vm.avg} := \frac{tS_{vm.avg}}{t}$$

$S_{vm.avg} = 34.2123$ Average stress across the section (membrane stress in ksi)

Linearized Stress Across Section (or Curve Fit Stress Profile)

$xd := 0, 0.005 .. 0.4205$

$k := 1$ ***n*th order of polynomial**

$B := regress(x, S_{vm}, k)$ $\quad B = \begin{bmatrix} 3 \\ 3 \\ 1 \\ 69.7762 \\ -163.1087 \end{bmatrix}$

$S(xd) := interp(B, x, S_{vm}, xd)$

The coefficients for the curve-fit of the stress profile are

$coeffs := submatrix(B, 4, length(B), 1, 1)$

$D := coeffs^T$ $\quad D = [\,69.7762 \quad -163.1087\,]$

$j := 1 .. k + 1$

$f_j := D^{\langle j \rangle}$

$h := 1 .. 100$

$c_h := if[h \le (k+1), f_h, 0]$

The Stress Function now has a range and value of

$$F(xd) := c_{11} \cdot (xd)^{10} + c_{10} \cdot (xd)^9 + c_9 \cdot (xd)^8 + c_8 \cdot (xd)^7 + c_7 \cdot (xd)^6 + c_6 \cdot (xd)^5 + c_5 \cdot (xd)^4 \ldots$$
$$+ c_4 \cdot (xd)^3 + c_3 \cdot (xd)^2 + c_2 \cdot (xd) + c_1$$

$F(0) = 69.7762$ $\quad S_{total} := F(0)$

Graph 1-1: Stress Profile Through the Bolt: Curve Fit of Stress Data

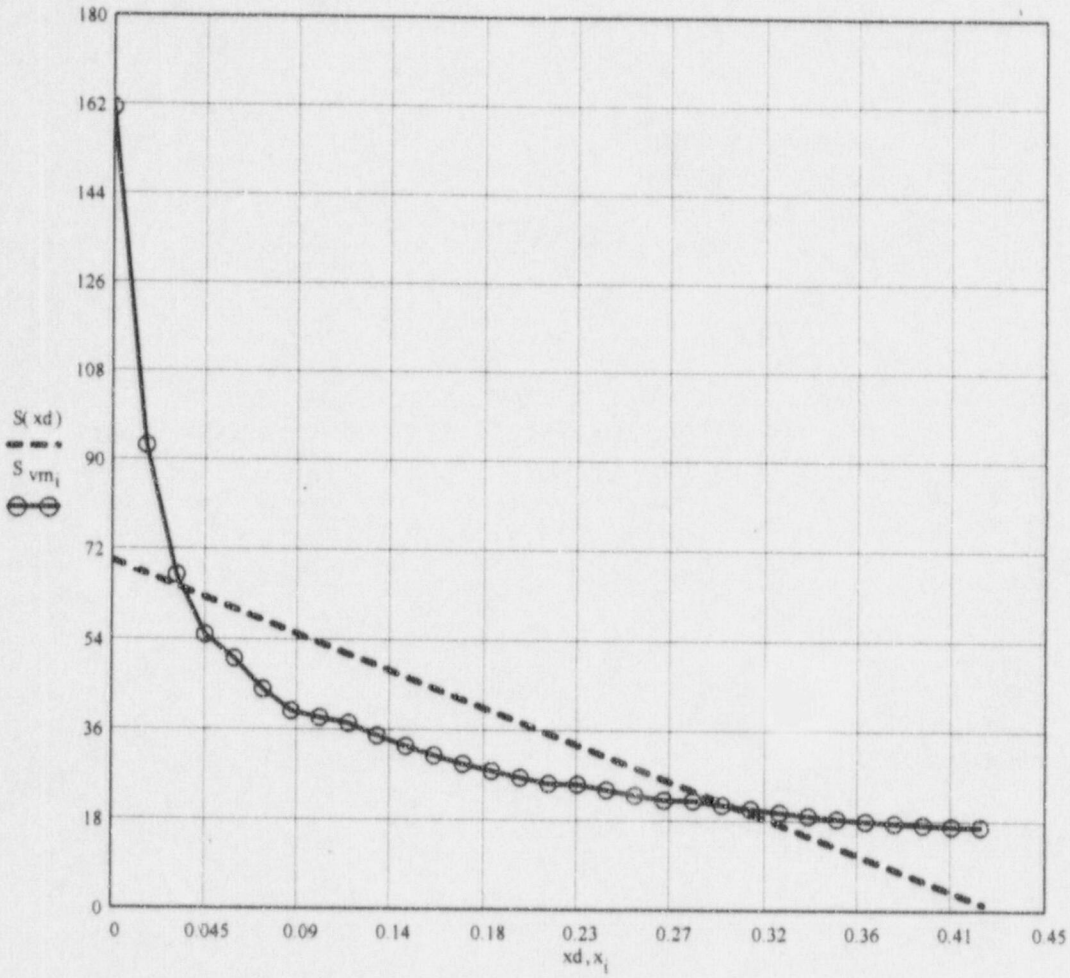

The function at xd = 0 corresponds (in the linear curve-fit case) to the intercept of the ordinate axis. This value is the membrane + bending (P_m+P_b) compenent of stress through the thickness of the component.

Thus, the individual stress values for membrane and bending (in units of ksi) are

$P_m := S_{vm.avg}$ $\quad P_m = 34.2123$

$P_b := S_{total} - S_{vm.avg}$ $\quad P_b = 35.5639$

$S_{total} := P_m + P_b$ $\quad S_{total} = 69.7762$ $\quad S_{tot}$).7762

The theoretical stress concentration factor at the horizontal plane of interest due to the notch is

$S_{peak} := S_{vm_i}$

$K_t := \frac{S_{peak}}{S_{tot}}$ $\quad K_t = 2.3122$

Strain Energy/Equivalent Area

The linearized curve and the actual stress profile cross at approximately 0.30 in. through the thickness. However, at a distance of 0.25 in., the stress profile is approximately linear, with a small slope. At this point, the equivalent area under a trapezoidal curve (sloping from a y-intercept to the stress at 0.25 in., then a constant linear value) is calculated.

The average Von Mises membrane stress, S_{vm}, is used in determining strain entergy.

$$\sigma\varepsilon := \sum_{i=1}^{n-1} \left(\frac{1}{2}\right) \cdot \left(S_{vm_i} + S_{vm_{i+1}}\right) \cdot \frac{\left(x_{i+1} - x_i\right)}{t}$$

approx. strain energy density calculated from the actual stress profile

$\sigma\varepsilon = 34.2123$ (in units of kip*in/in^3)

There are a pair of nodes located at approximately 0.25 in. (the cut plane passes through between nodes 2493 and 2462). The distance here is 0.252811 in.

$d := 0.252811$ in inches

The Von Mises stress here is

$\sigma_{0.25} := 23.125$ (units in ksi)

The area here forms a trapezoid, with the upper (y-intercept) stress as the only unknown if the area of the trapezoid is equated to the total strain energy across the thickness of the bolt, along Plane A-A.

The equation is determined by muliplying the strain energy density (from the actual stress profile through the bolt) by the thickness, and equating that with the area under a trapezoid of the stress versus the distance through the bolt at 0.25 in:

$$\sigma\varepsilon \cdot t = \frac{1}{2} \cdot \left(\sigma_o + \sigma_{0.25}\right) \cdot d$$

Solving for the only unknown, σ_o,

$$\sigma_o := 2 \cdot \frac{(\sigma\varepsilon \cdot t)}{d} - \sigma_{0.25}$$

$\sigma_o = 90.2285$

Thus, the function for this "new" stress profile is:

$$m := \frac{(\sigma_o - \sigma_{0.25})}{d}$$

$$\sigma_{new}(xd) := if\left[xd \le d, (\sigma_o - m \cdot xd), \sigma_{0.25}\right]$$

Graph 1-2: Strain Energy Linearization at 0.25 in. from Fillet

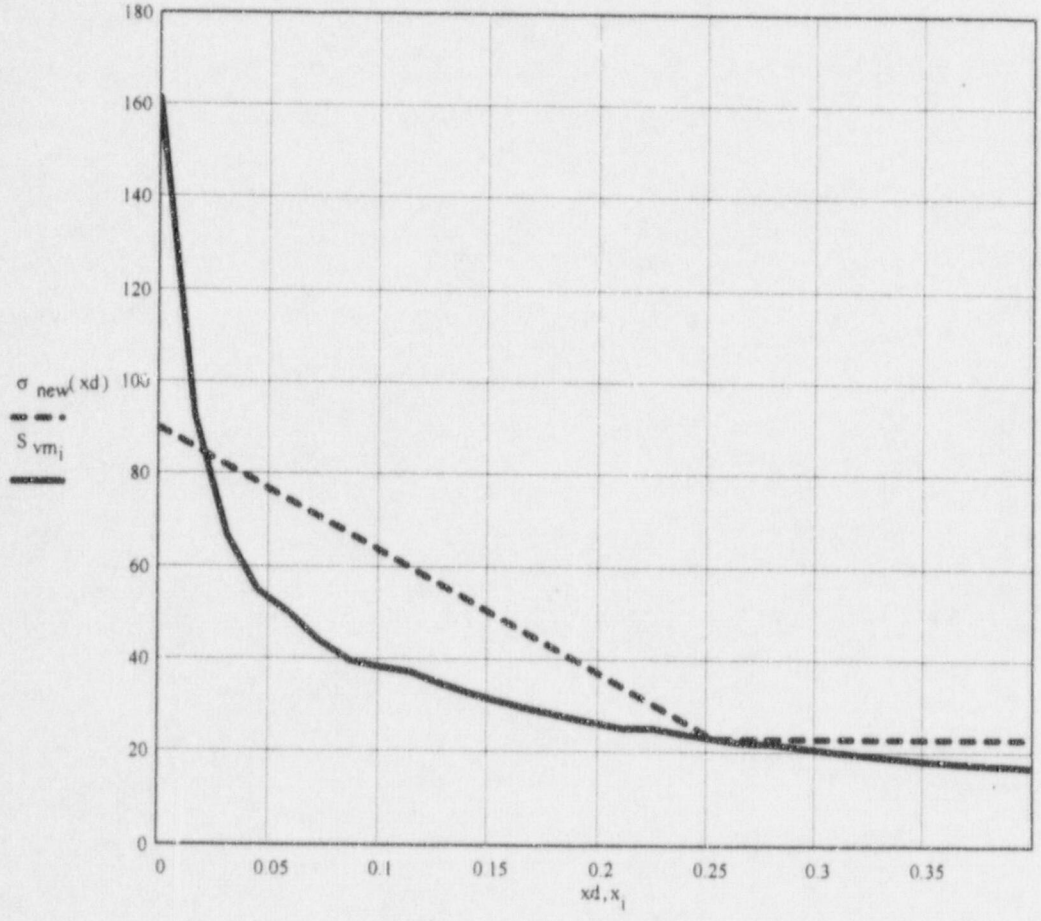

Graph 1-3: Comparison of the Three Stress Profiles

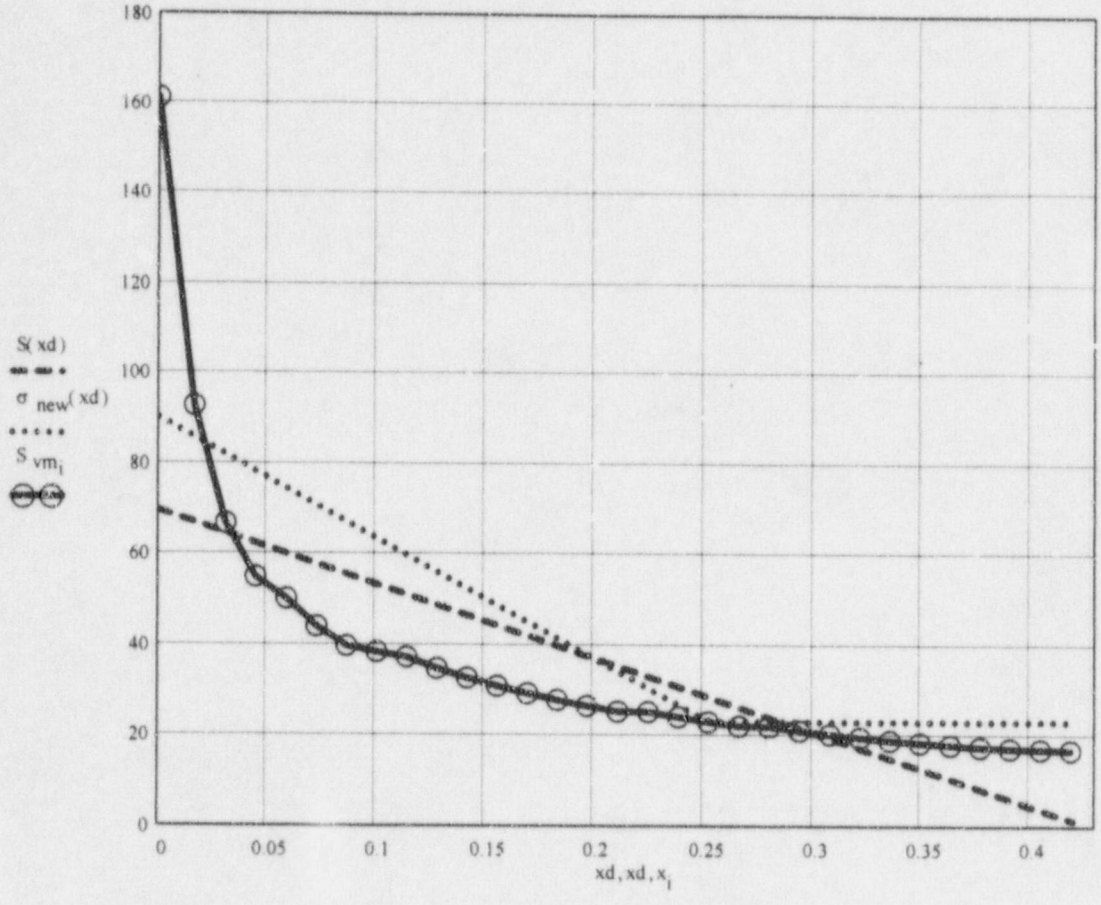

DISPLAY III - GEOMETRY MODELING SYSTEM (6.0.0) PRE/POST MODULE

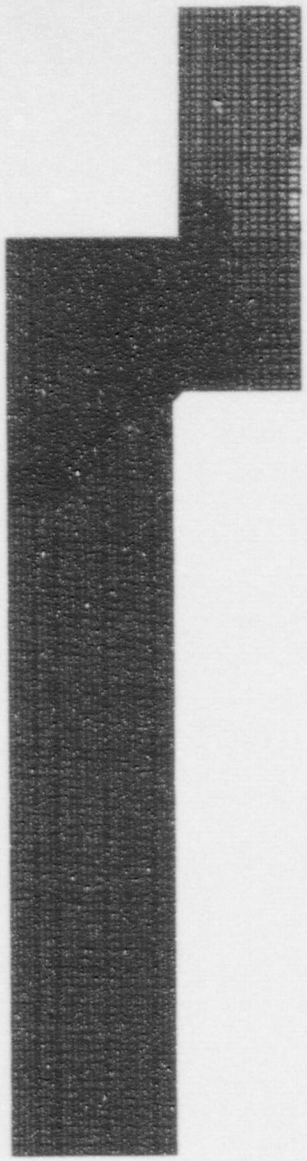

VON-MISES STRESS

VIEW : 347.1352
RANGE: 161337.7

(Band * 1.0E3)

161.3
149.8
138.3
126.8
115.3
103.8
92.34
80.84
69.34
57.84
46.34
34.85
23.35
11.85
.3471

EMRC-NISA/DISPLAY

JAN/05/98 07:35:00

Y
X

ROTX
.0
ROTY
.0
ROTZ
.0

Appendix 1, Attachment 1 to
Document No. EP-98-003-01
Page 7 of 10

Figure 1-1

b05a.nis: 0.83" bolt (1.5" head) subject to 56,500 psi tension stress (0.05" R)

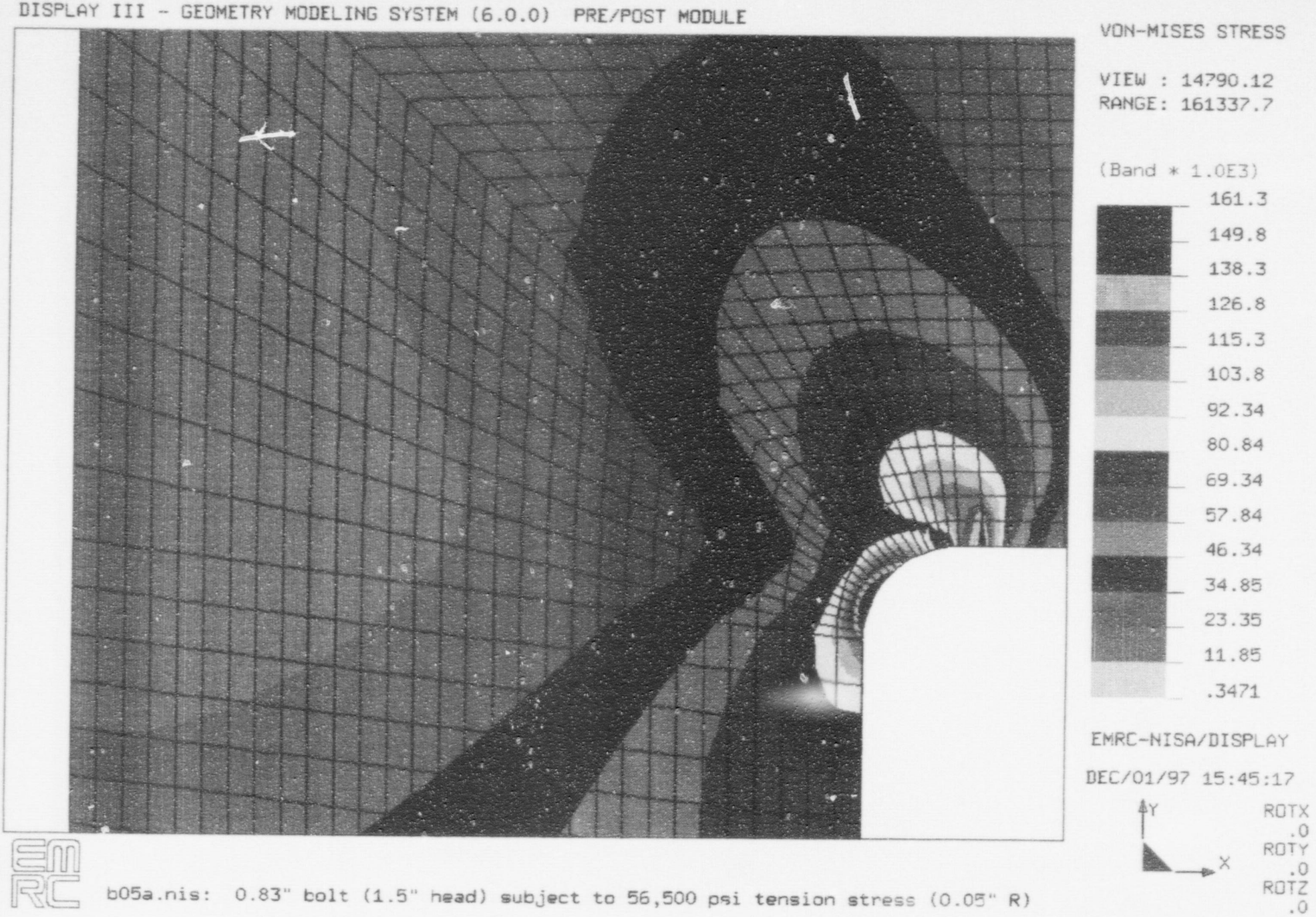
DISPLAY III - GEOMETRY MODELING SYSTEM (6.0.0) PRE/POST MODULE
VON-MISES STRESS
VIEW : 14790.12
RANGE: 161337.7
(Band * 1.0E3)
161.3
149.8
138.3
126.8
115.3
103.8
92.34
80.84
69.34
57.84
46.34
34.85
23.35
11.85
.3471
EMRC-NISA/DISPLAY
DEC/01/97 15:45:17
Y
X
ROTX
.0
ROTY
.0
ROTZ
.0
EMRC
b05a.nis: 0.83" bolt (1.5" head) subject to 56,500 psi tension stress (0.05" R)

Figure 1-2

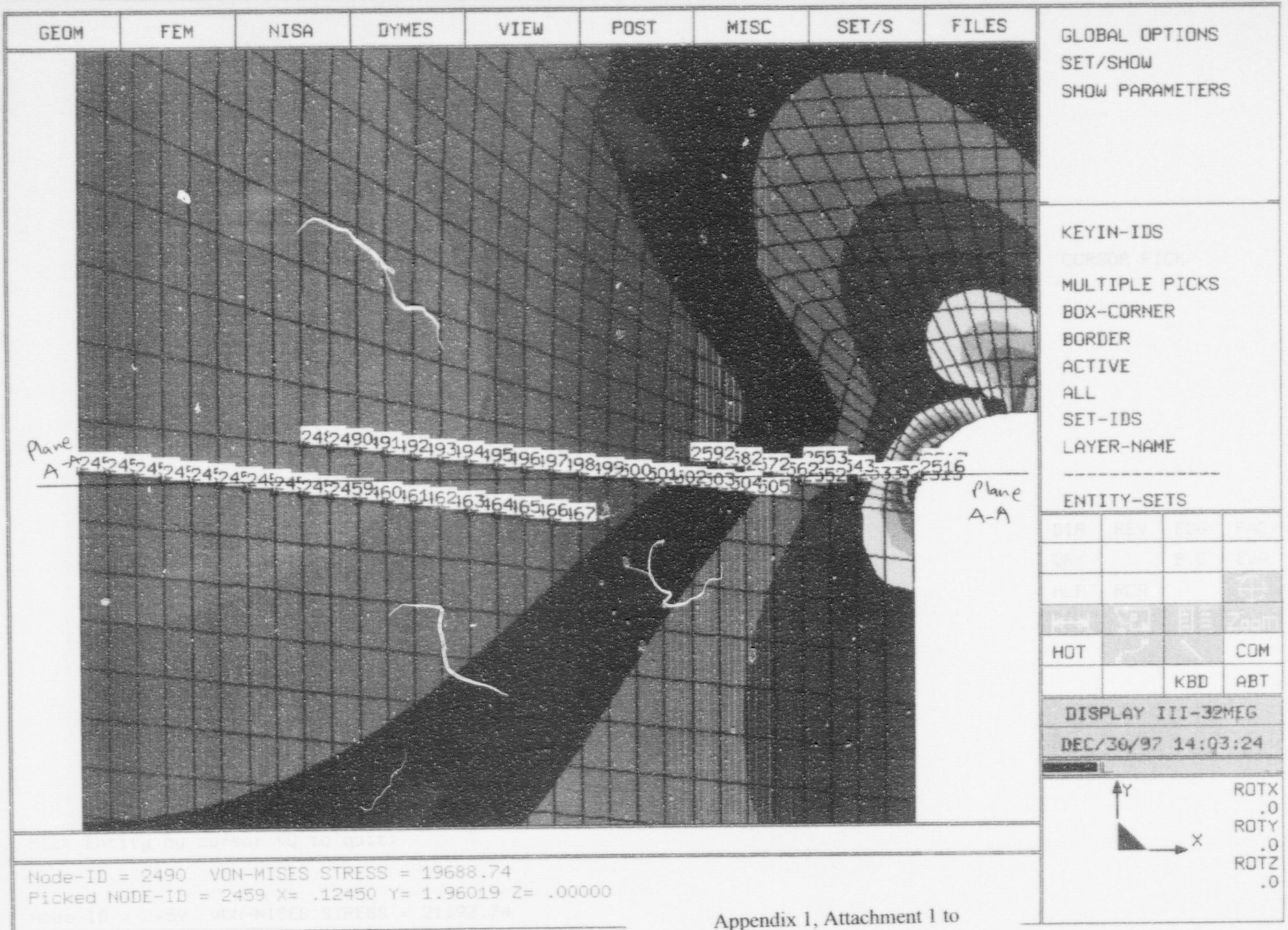

bosmis Figure 1-3

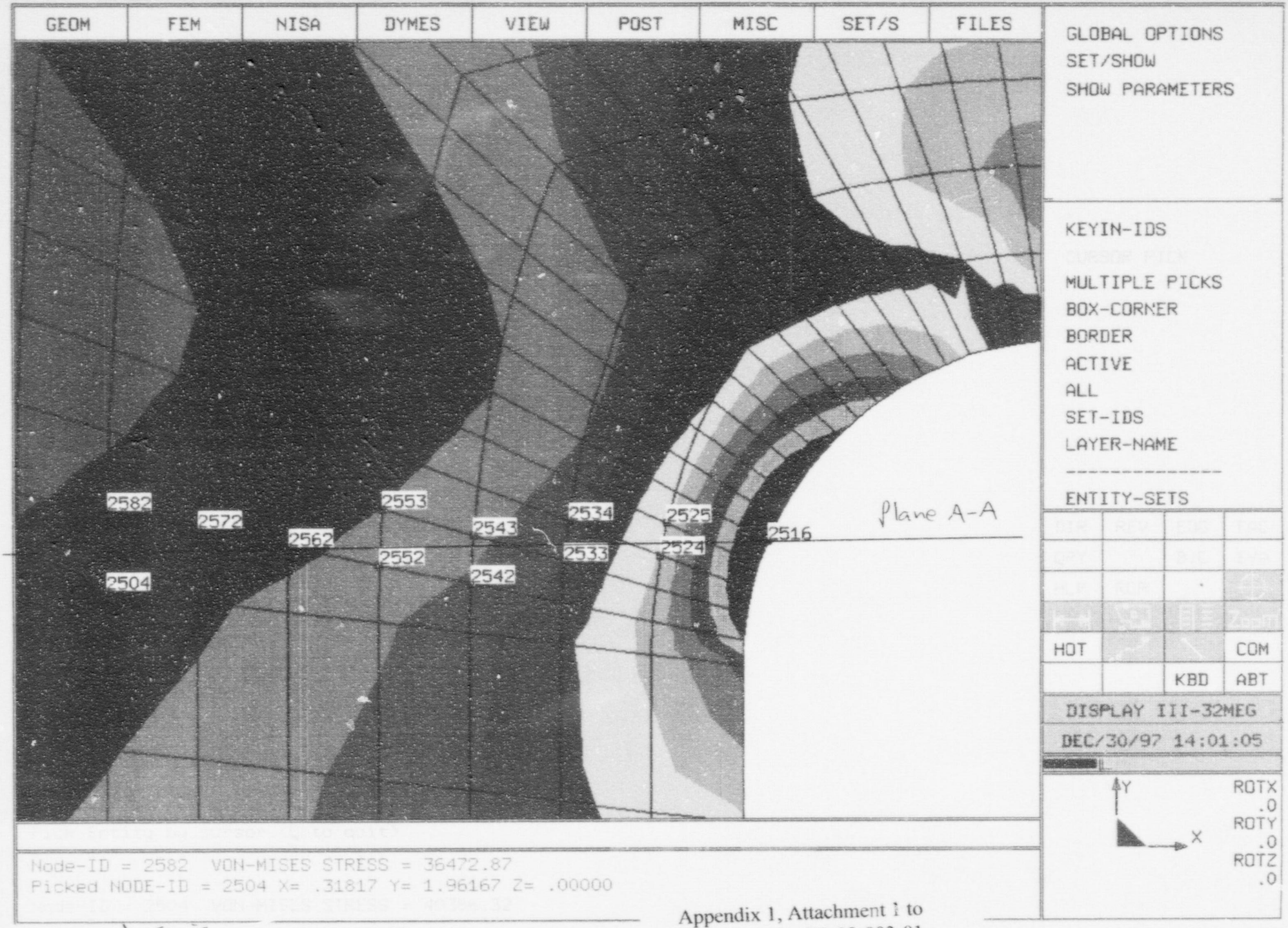

bosmis

Figure 1-4

DISPLAY III - GEOMETRY MODELING SYSTEM (6.0.0) PRE/POST MODULE

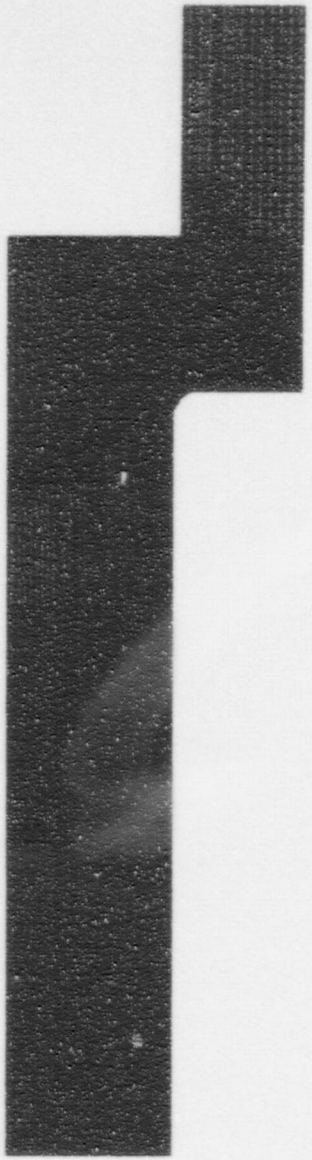

VON-MISES STRESS

VIEW : 397.3647
RANGE: 156782.4

(Band * 1.0E3)

156.8
145.6
134.4
123.3
112.1
100.9
89.76
78.59
67.42
56.25
45.08
33.91
22.74
11.57
.3974

EMRC-NISA/DISPLAY

DEC/01/97 10:21:23

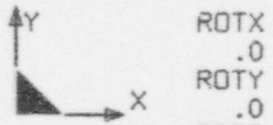

b075.nis: 0.83" bolt (1.5" head) subject to 56.5 ksi tension stress (0.075" R)

Figure 2-1

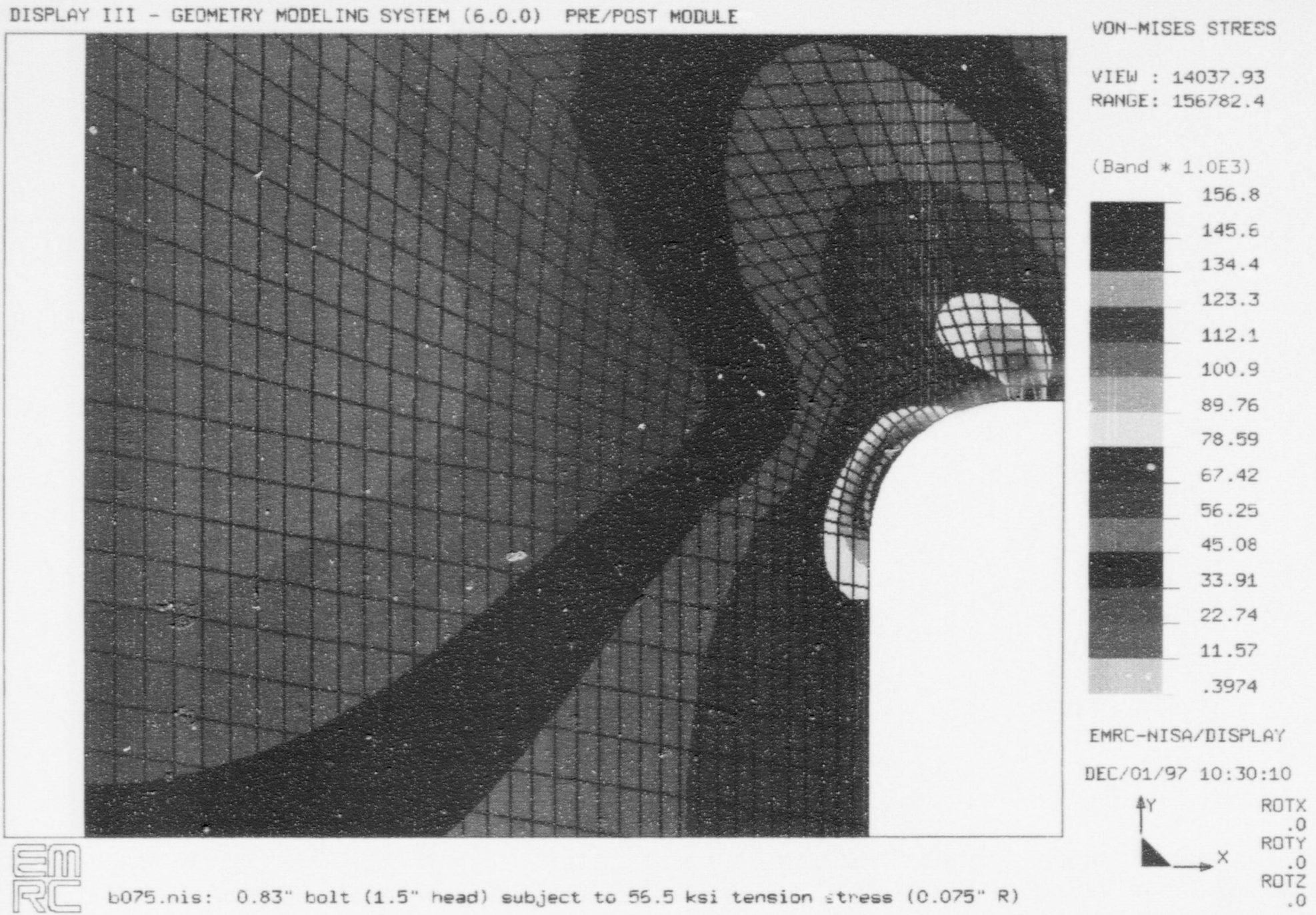
DISPLAY III - GEOMETRY MODELING SYSTEM (6.0.0) PRE/POST MODULE
VON-MISES STRESS
VIEW : 14037.93
RANGE: 156782.4
(Band * 1.0E3)
156.8
145.6
134.4
123.3
112.1
100.9
89.76
78.59
67.42
56.25
45.08
33.91
22.74
11.57
.3974
EMRC-NISA/DISPLAY
DEC/01/97 10:30:10
Y
X
ROTX
.0
ROTY
.0
ROTZ
.0
b075.nis: 0.83" bolt (1.5" head) subject to 55.5 ksi tension stress (0.075" R)

Figure 2-2

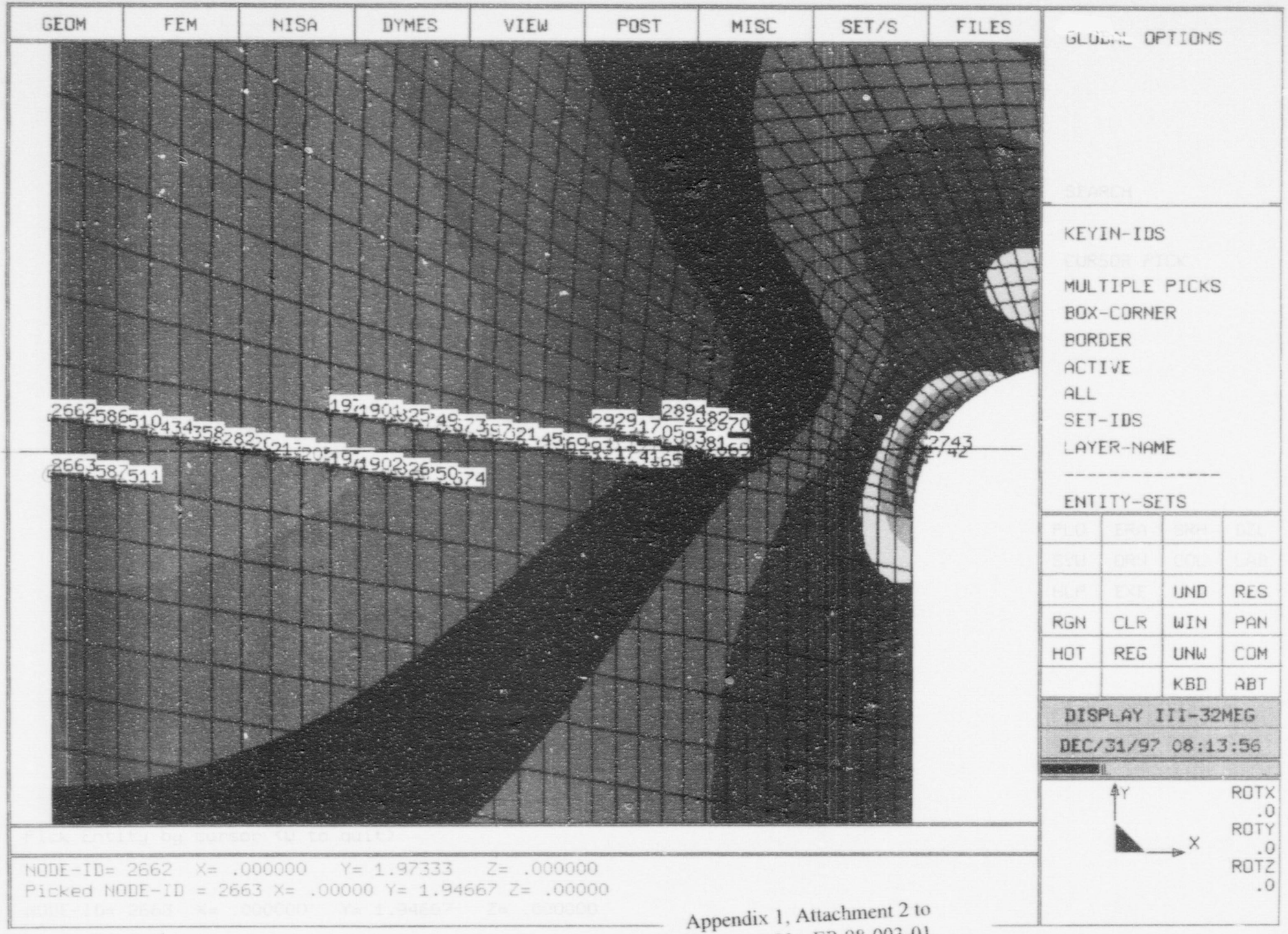

b075.mis
Figure 2-3

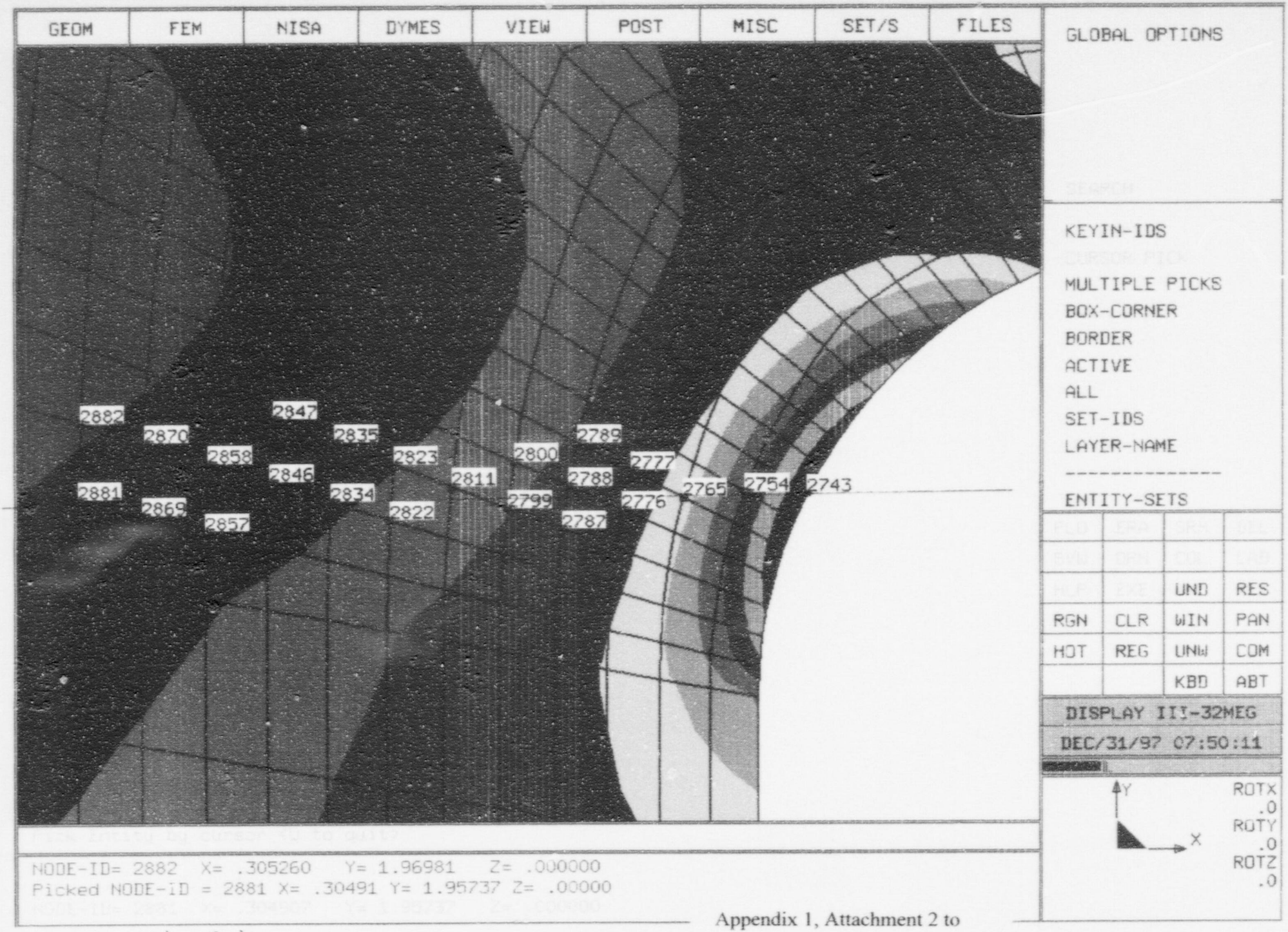

b075.nis

Figure 2-4

Attachment 2: Section Stresses on Horizontal Plane A-A through Bolt Using Von Mises Stress (model *bo75.nis*)

To calculate the average membrane stress across the section of the bolt, the trapezoidal method (from calculus) is used as follows:

There are a total of 36 data points (nodes or average of nodes) taken along Plane A-A.

ORIGIN := 1 n := 36 i := 1 .. n

Node No. $node_i :=$	x-distance (in.) $x_i :=$	Von Mises Stress (ksi) $S_{vm_i} :=$
2743	0.0	147.009
2754	0.0100371	110.823
2765	0.0199504	85.433
2776	0.0264478	71.364
2788	0.0384018	60.504
2799	0.0482995	55.575
2811	0.0573981	49.506
2822	0.0674182	47.700
2834	0.0769649	43.643
2846	0.0867444	40.306
2857	0.0971337	40.091
2869	0.107367	37.517
2881	0.117833	35.296
2893	0.128531	33.354
2905	0.139463	31.640
2917	0.150626	30.105
2929.1217	0.1620685	29.867
1293	0.173740	29.529
1369	0.185597	28.150
1445	0.197687	26.865
1521	0.21009	25.660
1597	0.222564	24.523
1673	0.235351	23.445
1749.1750	0.248370	23.408
1825.1826	0.261622	22.367
1902	0.275107	22.247
1978	0.288824	21.267
2054	0.302774	20.348
2130	0.316956	19.495
2206	0.331370	18.711
2282	0.346017	18.003
2358	0.360897	17.378
2434	0.376009	16.845
2510.2511	0.391354	17.260
2586.2587	0.406931	16.913
2662.2663	0.422740	16.683

$t := x_n$ Section Thickness

$t = 0.4227$

The average Von Mises membrane stress, S_{vm}, is

$$tS_{vm.avg} := \sum_{i=1}^{n-1} \left(\frac{1}{2}\right) \cdot \left(S_{vm_i} + S_{vm_{i+1}}\right) \cdot \left(x_{i+1} - x_i\right)$$

$$S_{vm.avg} := \frac{tS_{vm.avg}}{t}$$

$S_{vm.avg} = 33.5019$ Average stress across the section (membrane stress in ksi)

Linearized Stress Across Section (or Curve Fit Stress Profile)

$xd := 0, 0.005 .. 0.4205$

$k := 1$ ***n*th order of polynomial**

$B := regress(x, S_{vm}, k)$

$S(xd) := interp(B, x, S_{vm}, xd)$

$$B = \begin{bmatrix} 3 \\ 3 \\ 1 \\ 69.557 \\ -166.2468 \end{bmatrix}$$

The coefficients for the curve-fit of the stress profile are

$coeffs := submatrix(B, 4, length(B), 1, 1)$

$D := coeffs^T$ $D = \begin{bmatrix} 69.557 & -166.2468 \end{bmatrix}$

$j := 1 .. k+1$

$f_j := D^{<j>}$

$h := 1 .. 100$

$c_h := if\left[h \le (k+1), f_h, 0\right]$

The Stress Function now has a range and value of

$$F(xd) := c_{11}\cdot(xd)^{10} + c_{10}\cdot(xd)^{9} + c_{9}\cdot(xd)^{8} + c_{8}\cdot(xd)^{7} + c_{7}\cdot(xd)^{6} + c_{6}\cdot(xd)^{5} + c_{5}\cdot(xd)^{4} \ldots$$
$$+ c_{4}\cdot(xd)^{3} + c_{3}\cdot(xd)^{2} + c_{2}\cdot(xd) + c_{1}$$

$F(0) = 69.557$ $\qquad S_{total} := F(0)$

Graph 2-1: Stress Profile Through the Bolt: Curve Fit of Stress Data

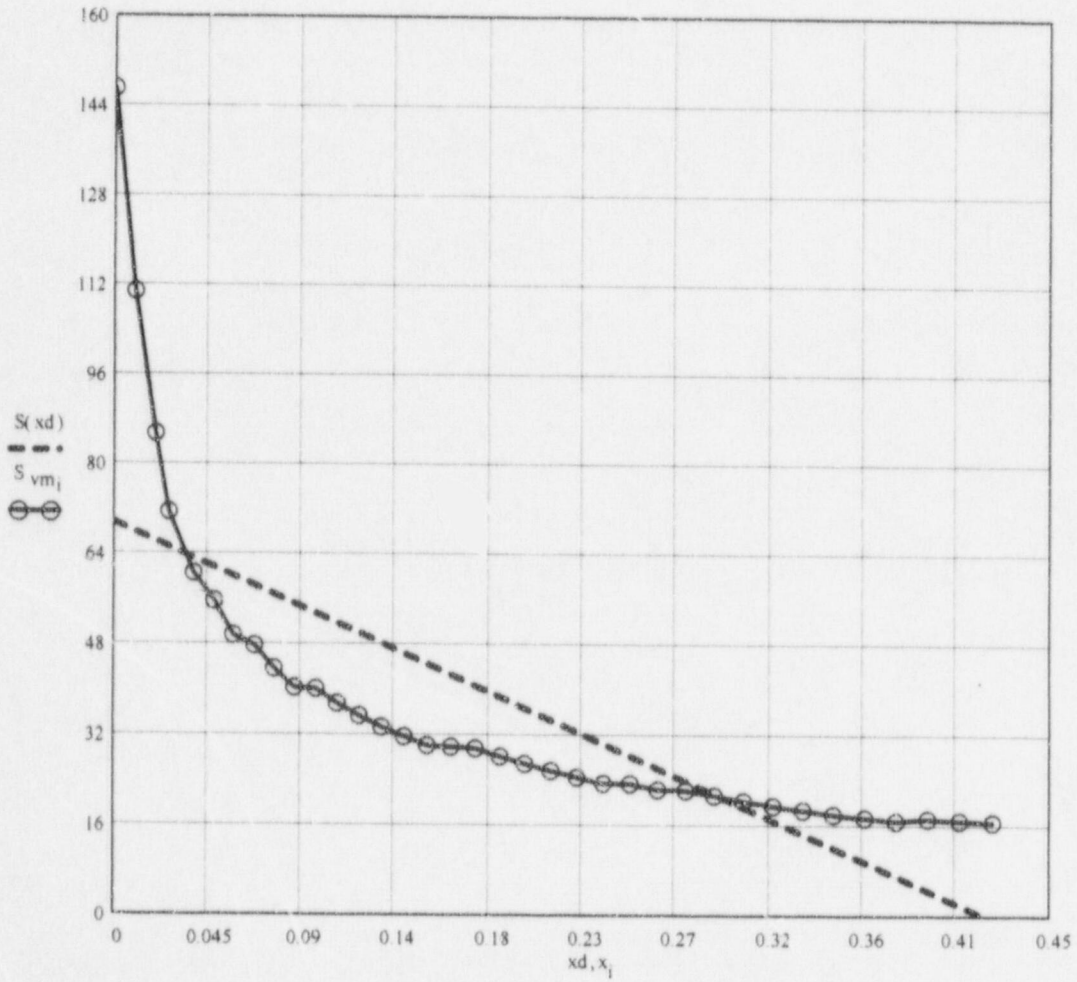

The function at xd = 0 corresponds (in the linear curve-fit case) to the intercept of the ordinate axis. This value is the membrane + bending (P_m+P_b) compenent of stress through the thickness of the component.

Thus, the individual stress values for membrane and bending (in units of ksi) are

$P_m := S_{vm.avg}$ $\quad P_m = 33.5019$

$P_b := S_{total} - S_{vm.avg}$ $\quad P_b = 36.0551$

$S_{total} := P_m + P_b$ $\quad S_{total} = 69.557$ $\quad S_{tot} := 69.557$

The theoretical stress concentration factor at the horizontal plane of interest due to the notch is

$\sigma_{peak} := S_{vm_1}$

$K_t := \frac{\sigma_{peak}}{S_{tot}}$ $\quad K_t = 2.1135$

Strain Energy/Equivalent Area

The linearized curve and the actual stress profile cross at approximately 0.30 in. through the thickness. However, at a distance of 0.25 in., the stress profile is approximately linear, with a small slope. At this point, the equivalent area under a trapezoidal curve (sloping from a y-intercept to the stress at 0.25 in., then a constant linear value) is calculated.

The average Von Mises membrane stress, S_{vm}, is used in determining strain entergy.

$$\sigma\varepsilon := \sum_{i=1}^{n-1} \left(\frac{1}{2}\right) \cdot \left(S_{vm_i} + S_{vm_{i+1}}\right) \cdot \frac{\left(x_{i+1} - x_i\right)}{t}$$

approx. strain energy density calculated from the actual stress profile

$\sigma\varepsilon = 33.5019$ (in units of kip*in/in^3)

There are a pair of nodes located at approximately 0.25 in. (the cut plane passes through between nodes 1749 and 1750). The distance here is 0.24837 in.

$d := 0.248370$ in inches

The Von Mises stress here is

$\sigma_{0.25} := 23.408$ (units in ksi)

The area here forms a trapezoid, with the upper (y-intercept) stress as the only unknown if the area of the trapezoid is equated to the total strain energy across the thickness of the bolt, along Plane A-A.

The equation is determined by muliplying the strain energy density (from the actual stress profile through the bolt) by the thickness, and equating that with the area under a trapezoid of the stress versus the distance through the bolt at approximately 0.25 in:

$$\sigma\varepsilon \cdot t = \frac{1}{2} \cdot \left(\sigma_o + \sigma_{0.25}\right) \cdot d$$

Solving for the only unknown, σ_o,

$$\sigma_o := 2 \cdot \frac{(\sigma\varepsilon \cdot t)}{d} - \sigma_{0.25}$$

$$\sigma_o = 90.6362$$

Thus, the function for this "new" stress profile is:

$$m := \frac{\left(\sigma_o - \sigma_{0.25}\right)}{d}$$

$$\sigma_{new}(xd) := \text{if}\left[xd \le d, \left(\sigma_o - m \cdot xd\right), \sigma_{0.25}\right]$$

Graph 2-2: Strain Energy Linearization at 0.25 in. from Fillet

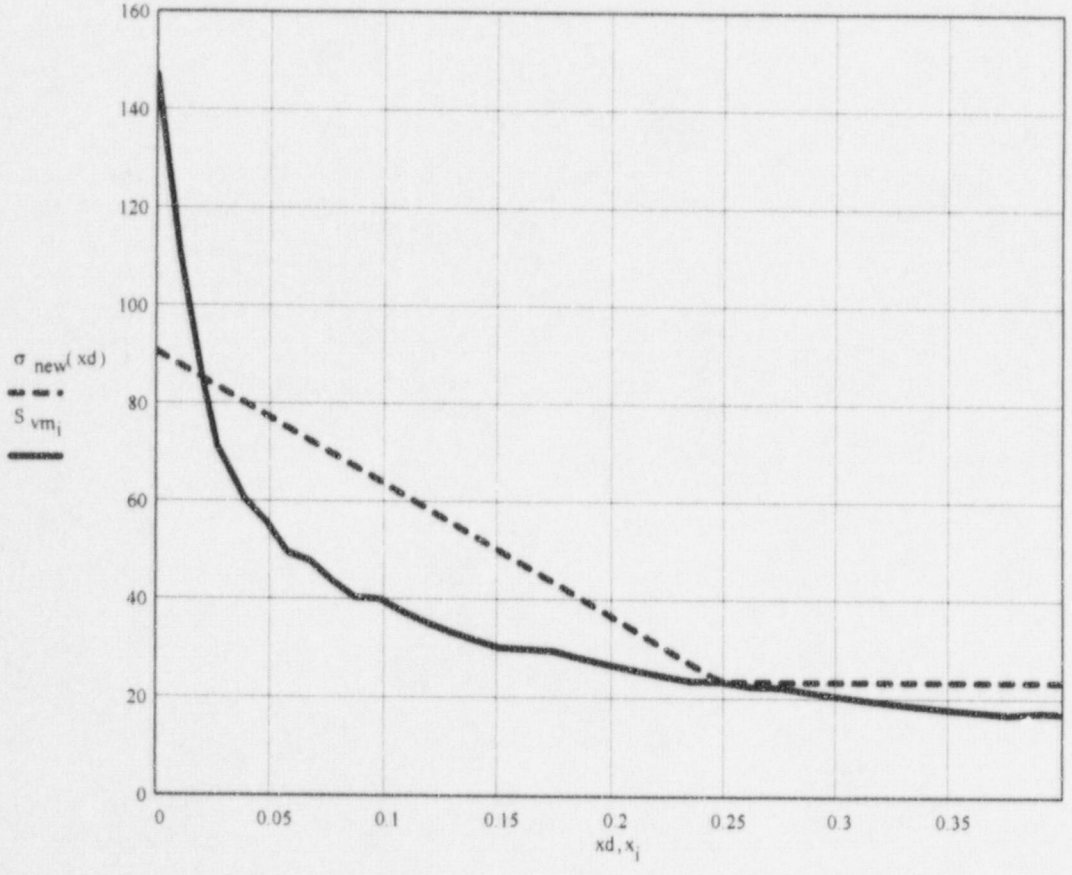

Graph 2-3: Comparison of the Three Stress Profiles

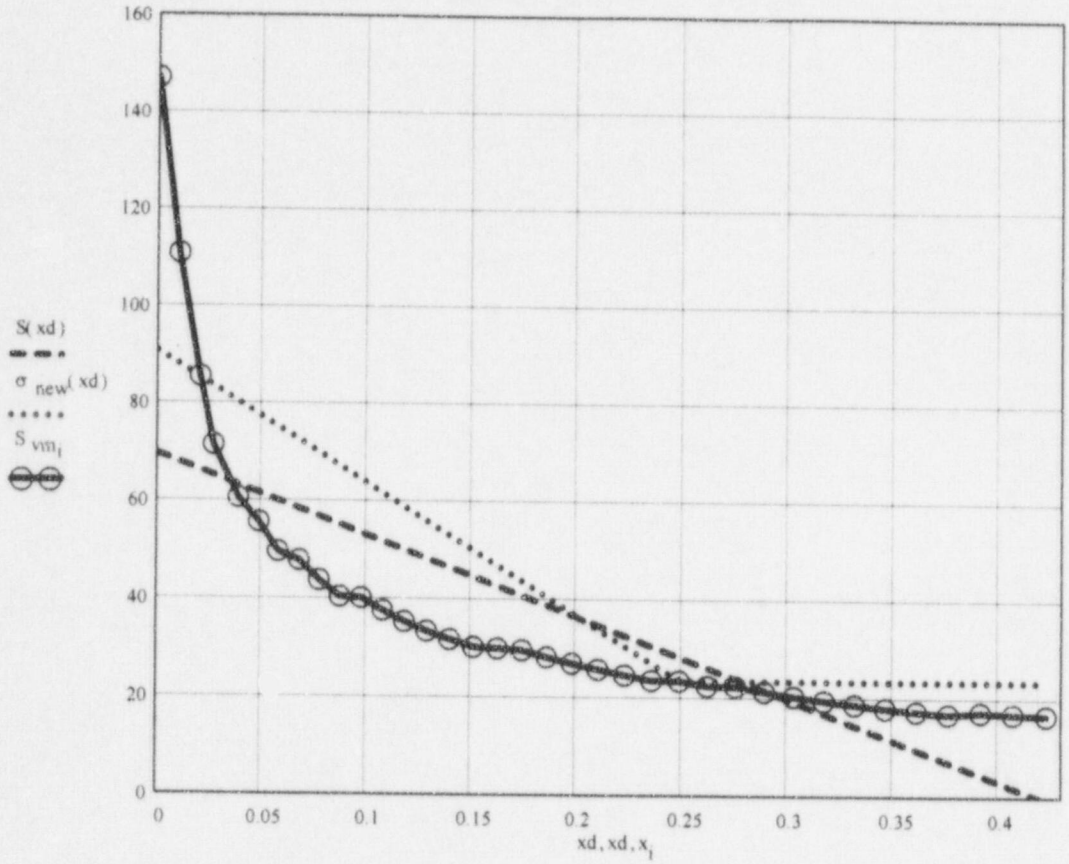

APPENDIX 2

Fracture Mechanics Evaluation of Flaws in Bolts

Comparisons of Stress Intensity factors for flaws in bolts:
Single Crack Solutions :- James-Mills, Liu , Daoud-Cartwright and Forman-Shivakumar.
Full Circumferential Crack :- Paris-Sih Solution for Notched Bar.

Solutions presented in this appendix are a compilation from various references. The appropriate references are provided for each solution. The nomenclature used in the various solutions are provided below.

General Nomenclature

S_0	Nominal Stress in Shank due to Bolt Preload {ksi}
P_m	Tension or Membrane Stress (ASME linearized in accordance with Section XI appendix "A". {ksi}
P_b	Bending Stress (ASME linearized in accordance with Section XI appendix "A". {ksi}
S_{peak}	Peak Stress at surface linearized by strain energy density method. {ksi}
S_{nom}	Nominal stress in the head-shank region interior obtained by linearization using strain energy density method. {ksi}
a_0	Initial Crack Depth. {inch}
D	Diameter of Bolt in the Shank region. {inch}

Notes :-
1) Other variables and constants used in the solutions are defined in the particular solution method.
2) Stresses used in this appendix are obtained from the results presented in appendix 1.
3) Material properties are from references cited in the body of this engineering report.

SOLUTION NUMBER :- I-A
Thread Root Region

James and Mills Correlation: For a Single Curved Crack in the Thread Root Region
{Empirical Equation that considers stress profile in the Thread Root Region}

REFERENCE:- James L. A. & Mills W. J. in Engineering Fracture Mechanics, Vol. 30,No. 5, 1988. "Review and Synthesis of Stress Intensity Factor Solutions Applicable to Cracks in Bolts".

$A_{jm} := 2.043$ $E_{jm} := 3.0469$

$B_{jm} := -31.332$ $F_{jm} := -19.504$

$C_{jm} := 0.6507$ $G_{jm} := 45.647$

$D_{jm} := 0.5367$

Stress Input

$S_0 := 56.5$ Nominal Tension Stress in Shank due to Preload {ksi}

Bolt Geometric data and Initial flaw depth :

$a_0 := 0.05$ Initial Flaw Depth {inch}

$a_{inc} := 0.005$ Increment for Flaw Depth {inch}

$D := 0.822$ Diameter of Shank {inch}

$i := 1 .. 40$ Loop Index

$a_i := a_{i-1} + a_{inc}$ Flaw Growth Simulation

Development of Equations for the determination of Applied Stress Intensity Factor as a Function of Flaw Depth

$$x_i := \frac{a_i}{D}$$ Normalized Flaw Depth

Magnification Factor

$$Y_{jm_i} := A_{jm} \cdot \exp\left(B_{jm} \cdot x_i\right) + C_{jm} + D_{jm} \cdot x_i + E_{jm} \cdot \left(x_i\right)^2 + F_{jm} \cdot \left(x_i\right)^3 + G_{jm} \cdot \left(x_i\right)^4$$

Stress Intensity Solution

$$K_{Ijmt_i} := S_0 \cdot Y_{jm_i} \cdot \sqrt{\pi \cdot a_i}$$

Tabular Results for James-Mills Correlation

a_i	x_i	Y_{jm_i}	K_{Ijmt_i}
0.055	0.067	0.946	22.227
0.06	0.073	0.907	22.257
0.065	0.079	0.876	22.362
0.07	0.085	0.851	22.537
0.075	0.091	0.831	22.778
0.08	0.097	0.815	23.077
0.085	0.103	0.802	23.429
0.09	0.109	0.793	23.827
0.095	0.116	0.786	24.265
0.1	0.122	0.781	24.737
0.105	0.128	0.778	25.24
0.11	0.134	0.776	25.769
0.115	0.14	0.775	26.319
0.12	0.146	0.775	26.889
0.125	0.152	0.776	27.476
0.13	0.158	0.778	28.077
0.135	0.164	0.78	28.69
0.14	0.17	0.782	29.316
0.145	0.176	0.785	29.952
0.15	0.182	0.789	30.598
0.155	0.189	0.793	31.255
0.16	0.195	0.797	31.921
0.165	0.201	0.801	32.598
0.17	0.207	0.806	33.285
0.175	0.213	0.811	33.985
0.18	0.219	0.817	34.696
0.185	0.225	0.822	35.422
0.19	0.231	0.828	36.163
0.195	0.237	0.835	36.92
0.2	0.243	0.842	37.696
0.205	0.249	0.849	38.492
0.21	0.255	0.857	39.31
0.215	0.262	0.865	40.153
0.22	0.268	0.873	41.023
0.225	0.274	0.883	41.922
0.23	0.28	0.892	42.853
0.235	0.286	0.903	43.819
0.24	0.292	0.914	44.823
0.245	0.298	0.925	45.867
0.25	0.304	0.938	46.956

Graphical Representation :- James-Mills Correlation

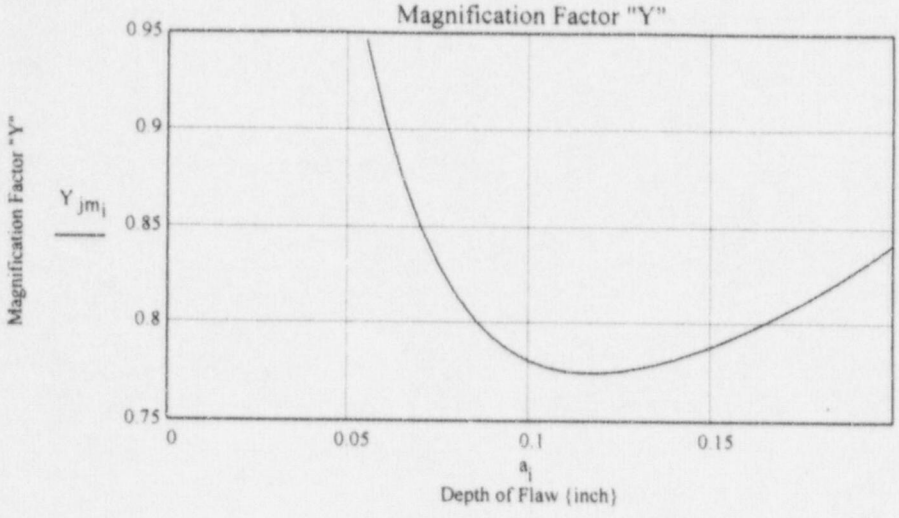

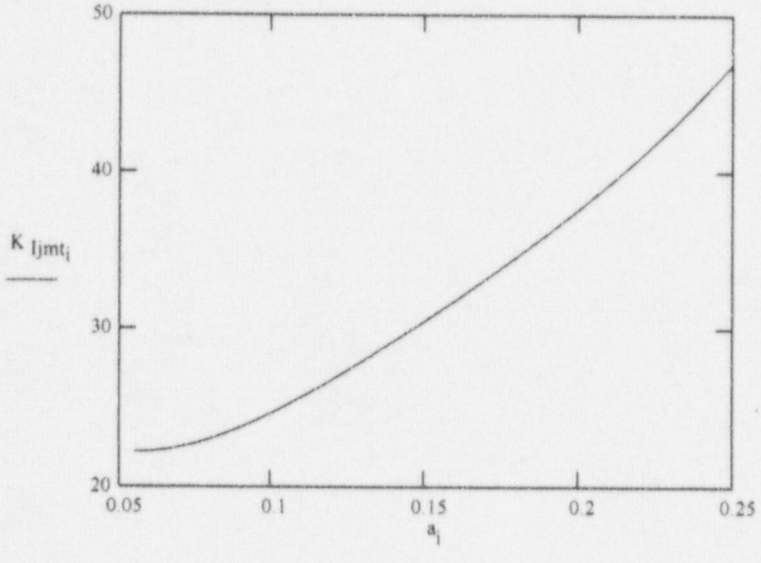

SOLUTION NUMBER :- I-B
Head to Shank Region

James and Mills Correlation: For a Single Curved Crack in the Shank-Head Region {Empirical Equation for tension and Bending in the head to shank region}

REFERENCE:- James L. A. & Mills W. J. in Engineering Fracture Mechanics, Vol. 30,No. 5, 1988. "Review and Synthesis of Stress Intensity Factor Solutions Applicable to Cracks in Bolts".

$C_{jm} := 0.6507$ $E_{jm} := 3.0469$ $G_{jm} := 45.647$

$D_{jm} := 0.5367$ $F_{jm} := -19.504$

$A_{jmb} := 0.631$ $C_{jmb} := -3.3365$ $E_{jmb} := -6.0021$

$B_{jmb} := 0.03488$ $D_{jmb} := 13.406$

Stress Input

$P_m := 34.212$ Nominal Tension Stress in Shank-Head Region due to Preload {ksi}

$P_b := 35.564$ Bending Stress in the Shank to Head Region due to Preload {ksi}

Bolt Geometric data and Initial flaw depth :

$a_0 := 0.00$ Initial Flaw Depth {inch}

$a_{inc} := 0.005$ Increment for Flaw Depth {inch}

$D := 0.822$ Diameter of Shank {inch}

$i := 1 .. 40$ Loop Index

$a_i := a_{i-1} + a_{inc}$ Flaw Growth Simulation

Development of Equations for the determination of Applied Stress Intensity Factor as a Function of Flaw Depth

$x_i := \frac{a_i}{D}$ Normalized Flaw Depth

Magnification Factor

$$Y_{jm_i} := C_{jm} + D_{jm} \cdot x_i + E_{jm} \cdot (x_i)^2 + F_{jm} \cdot (x_i)^3 + G_{jm} \cdot (x_i)^4$$

$$Y_{jmb_i} := A_{jmb} + B_{jmb} \cdot x_i + C_{jmb} \cdot (x_i)^2 + D_{jmb} \cdot (x_i)^3 + E_{jmb} \cdot (x_i)^4$$

Stress Intensity Solution

$$K_{Ijm_i} := P_m \cdot Y_{jm_i} \cdot \sqrt{\pi \cdot a_i}$$

$$K_{Ijmb_i} := P_b \cdot Y_{jmb_i} \cdot \sqrt{\pi \cdot a_i}$$

$$K_{Ihs_i} := K_{Ijm_i} + K_{Ijmb_i}$$

Tabular Results for James-Mills Correlation

a_i	x_i	Y_{jm_i}	Y_{jmb_i}	K_{Ijm_i}	K_{Ijmb_i}	K_{Ihs_i}
$5 \cdot 10^{-3}$	$6.083 \cdot 10^{-3}$	0.654	0.631	2.805	2.813	5.618
0.01	0.012	0.658	0.631	3.988	3.977	7.965
0.015	0.018	0.661	0.631	4.912	4.868	9.78
0.02	0.024	0.665	0.63	5.705	5.617	11.322
0.025	0.03	0.669	0.629	6.417	6.273	12.69
0.03	0.036	0.673	0.628	7.074	6.862	13.935
0.035	0.043	0.678	0.627	7.688	7.399	15.088
0.04	0.049	0.682	0.626	8.272	7.896	16.168
0.045	0.055	0.686	0.625	8.83	8.358	17.188
0.05	0.061	0.691	0.624	9.368	8.791	18.159
0.055	0.067	0.695	0.622	9.888	9.199	19.088
0.06	0.073	0.7	0.621	10.395	9.586	19.98
0.065	0.079	0.704	0.619	10.889	9.953	20.842
0.07	0.085	0.709	0.618	11.373	10.302	21.675
0.075	0.091	0.713	0.616	11.847	10.637	22.484
0.08	0.097	0.718	0.615	12.313	10.958	23.271
0.085	0.103	0.722	0.613	12.772	11.267	24.039
0.09	0.109	0.727	0.612	13.224	11.565	24.789
0.095	0.116	0.731	0.61	13.671	11.853	25.525
0.1	0.122	0.736	0.609	14.113	12.133	26.246
0.105	0.128	0.74	0.607	14.55	12.406	26.956
0.11	0.134	0.745	0.606	14.983	12.672	27.655
0.115	0.14	0.75	0.605	15.413	12.932	28.345
0.12	0.146	0.754	0.604	15.839	13.188	29.028
0.125	0.152	0.759	0.603	16.264	13.441	29.704
0.13	0.158	0.763	0.602	16.686	13.69	30.376
0.135	0.164	0.768	0.602	17.108	13.937	31.045
0.14	0.17	0.773	0.601	17.528	14.183	31.711
0.145	0.176	0.777	0.601	17.949	14.428	32.377
0.15	0.182	0.782	0.601	18.37	14.674	33.044
0.155	0.189	0.787	0.601	18.793	14.921	33.714
0.16	0.195	0.792	0.602	19.218	15.17	34.387
0.165	0.201	0.798	0.602	19.645	15.421	35.066
0.17	0.207	0.803	0.603	20.077	15.675	35.752
0.175	0.213	0.809	0.604	20.513	15.933	36.446
0.18	0.219	0.814	0.606	20.954	16.196	37.151
0.185	0.225	0.821	0.607	21.403	16.465	37.868
0.19	0.231	0.827	0.609	21.859	16.739	38.598
0.195	0.237	0.834	0.611	22.324	17.021	39.344
0.2	0.243	0.841	0.614	22.799	17.31	40.108

Graphical Representation :- James-Mills Correlation
Head to Shank Region

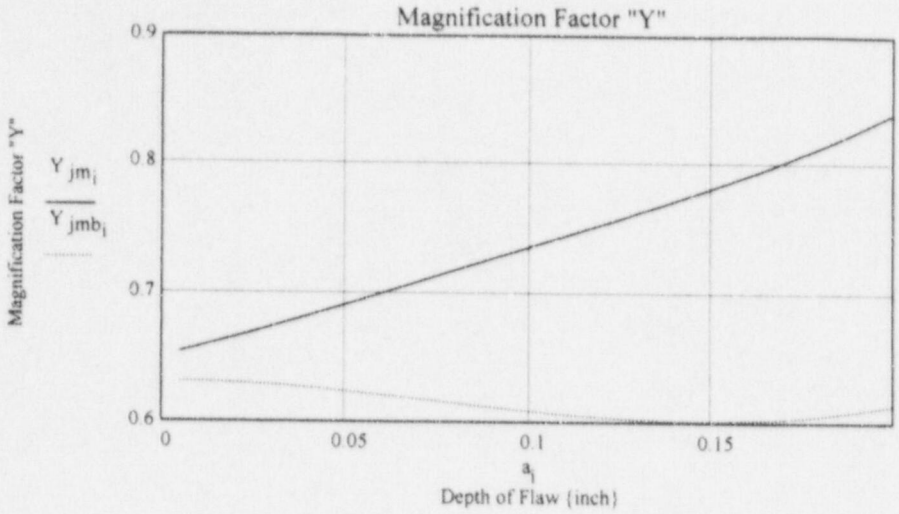

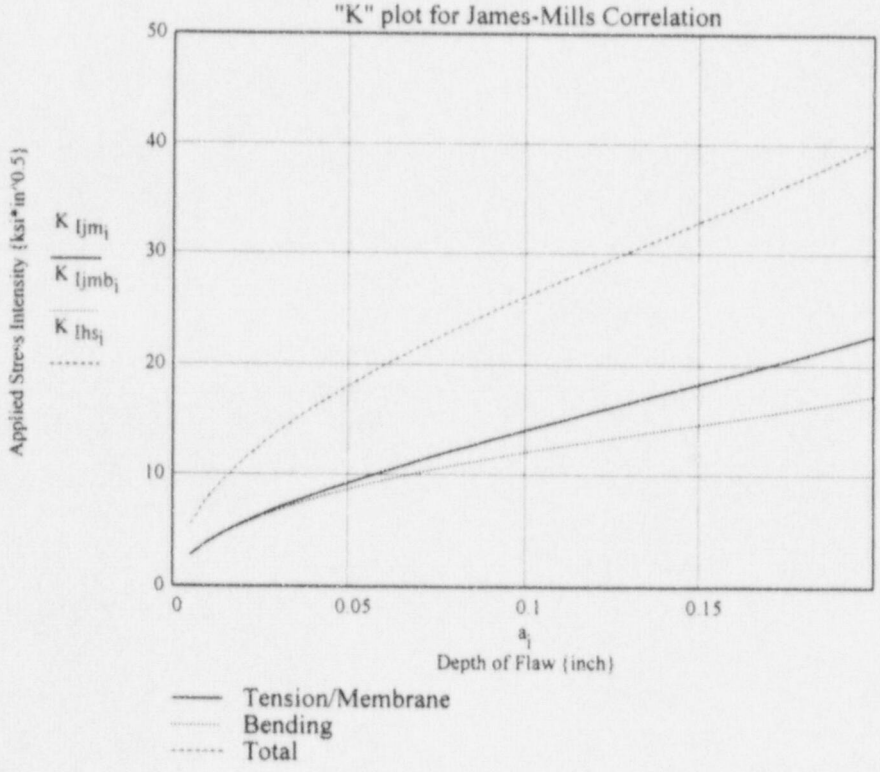

SOLUTION NUMBER :- I-C
Shank Region

James and Mills Correlation: For a Single Curved Crack in the Shank Region {Empirical equation modified in accordance with the Author's recommendation for regions removed from the thread root}

REFERENCE:- James L. A. & Mills W. . '. in Engineering Fracture Mechanics, Vol. 30,No. 5, 1988. "Review and Synthesis of Stress Intensity Factor Solutions Applicable to Cracks in Bolts".

$C_{jm} := 0.6507$ $E_{jm} := 3.0469$

$D_{jm} := 0.5367$ $F_{jm} := -19.504$

$G_{jm} := 45.647$

Stress Input

$S_0 := 56.5$ Nominal Tension Stress in Shank due to Preload {ksi}

Bolt Geometric data and Initial flaw depth :

$a_0 := 0.00$ Initial Flaw Depth {inch}

$a_{inc} := 0.005$ Increment for Flaw Depth {inch}

$D := 0.822$ Diameter of Shank {inch}

$i := 1 .. 40$ Loop Index

$a_i := a_{i-1} + a_{inc}$ Flaw Growth Simulation

Development of Equations for the determination of Applied Stress Intensity Factor as a Function of Flaw Depth

$x_i := \frac{a_i}{D}$ Normalized Flaw Depth

Magnification Factor

$$Y_{jm_i} := C_{jm} + D_{jm} \cdot x_i + E_{jm} \cdot (x_i)^2 + F_{jm} \cdot (x_i)^3 + G_{jm} \cdot (x_i)^4$$

Stress Intensity Solution

$$K_{Ijms_i} := S_0 \cdot Y_{jm_i} \cdot \sqrt{\pi \cdot a_i}$$

Tabular Results for James-Mills Correlation

a_i	x_i	Y_{jm_i}	K_{Ijms_i}
$5 \cdot 10^{-3}$	$6.083 \cdot 10^{-3}$	0.654	4.632
0.01	0.012	0.658	6.586
0.015	0.018	0.661	8.112
0.02	0.024	0.665	9.422
0.025	0.03	0.669	10.598
0.03	0.036	0.673	11.682
0.035	0.043	0.678	12.697
0.04	0.049	0.682	13.66
0.045	0.055	0.686	14.582
0.05	0.061	0.691	15.47
0.055	0.067	0.695	16.33
0.06	0.073	0.7	17.167
0.065	0.079	0.704	17.983
0.07	0.085	0.709	18.782
0.075	0.091	0.713	19.565
0.08	0.097	0.718	20.335
0.085	0.103	0.722	21.093
0.09	0.109	0.727	21.84
0.095	0.116	0.731	22.578
0.1	0.122	0.736	23.307
0.105	0.128	0.74	24.029
0.11	0.134	0.745	24.744
0.115	0.14	0.75	25.453
0.12	0.146	0.754	26.158
0.125	0.152	0.759	26.859
0.13	0.158	0.763	27.557
0.135	0.164	0.768	28.253
0.14	0.17	0.773	28.947
0.145	0.176	0.777	29.642
0.15	0.182	0.782	30.338
0.155	0.189	0.787	31.036
0.16	0.195	0.792	31.737
0.165	0.201	0.798	32.444
0.17	0.207	0.803	33.156
0.175	0.213	0.809	33.876
0.18	0.219	0.814	34.605
0.185	0.225	0.821	35.346
0.19	0.231	0.827	36.099
0.195	0.237	0.834	36.867
0.2	0.243	0.841	37.651

Graphical Representation :- James-Mills Correlation
Shank Region

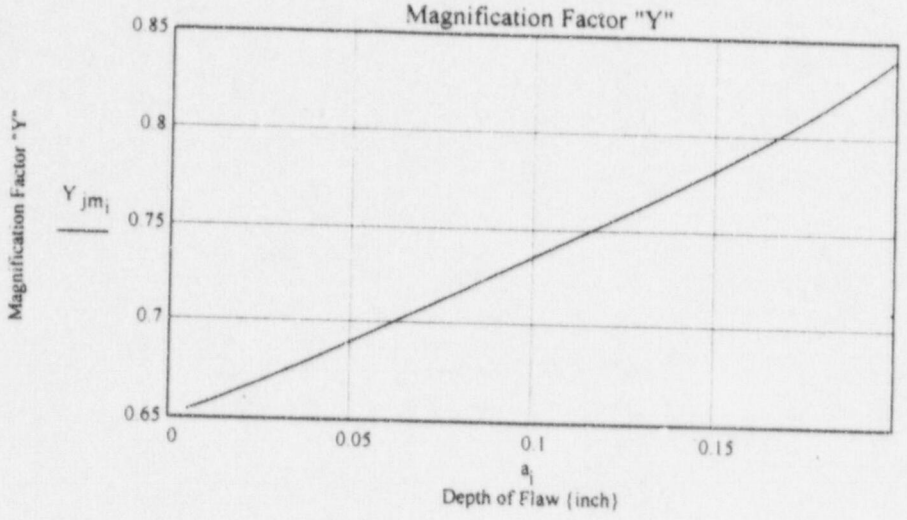

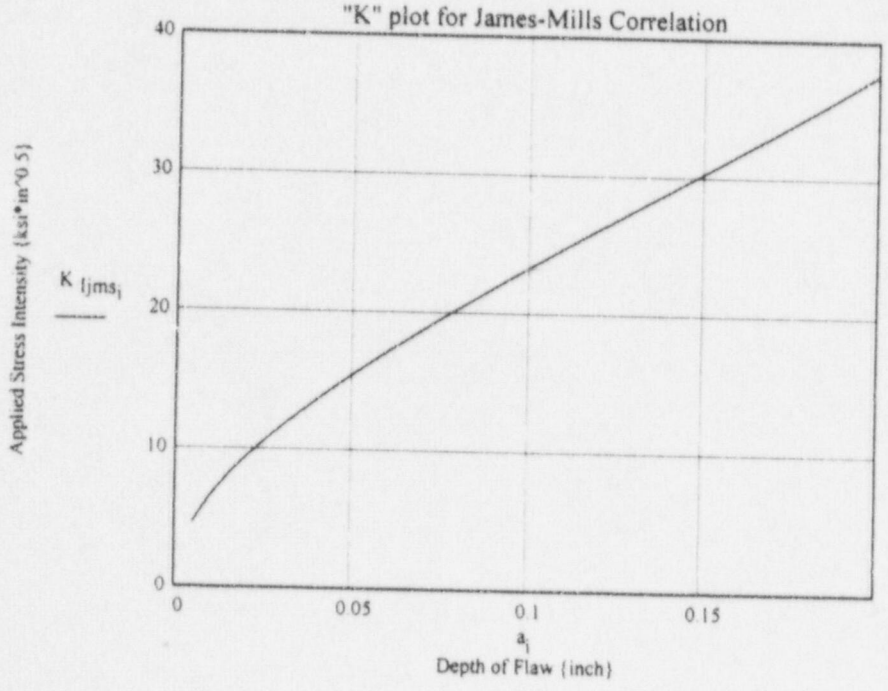

SOLUTION NUMBER. :-
II
Thread Root Region

Alan F. Liu correlation: Modification to James-Mills Correlation for magnification factors based on Test Data. Single Curved Crack

REFERENCE :- ASTM STP 1236 -Behavior of Fatigue Cracks in a Tension Bolt

$A_{al} := 2.4371$ $E_{al} := 2.4134$

$B_{al} := -36.5$ $F_{al} := -15.4491$

$C_{al} := 0.5154$ $G_{al} := 36.157$

$D_{al} := 0.4251$

Stress Input

$S_0 := 56.5$ Nominal Tension Stress in Shank due to Preload {ksi}

Bolt Geometric data and Initial flaw depth :

$a_0 := 0.05$ Initial Flaw Depth {inch}

$a_{inc} := 0.005$ Increment for Flaw Growth {inch}

$D := 0.822$ Diameter of Shank

$i := 1 .. 40$ Index for Loop

$a_i := a_{i-1} + a_{inc}$ Flaw Growth Simulation

Equations for the determination of the Applied Stress Intensity Factor as a function of Flaw depth.

$$x_i := \frac{a_i}{D}$$ Normalized Flaw Depth

Magnification Factor

$$Y_{al_i} := A_{al} \cdot \exp\left(B_{al} \cdot x_i\right) + C_{al} + D_{al} \cdot x_i + E_{al} \cdot \left(x_i\right)^2 + F_{al} \cdot \left(x_i\right)^3 + G_{al} \cdot \left(x_i\right)^4$$

Stress Intensity factor Solution

$$K_{Ial_i} := \dot{S}_0 \cdot Y_{al_i} \cdot \sqrt{\pi \cdot a_i}$$

Tabular Results for Alan Liu Correlation

a_i	x_i	Y_{al_i}	K_{Ial_i}
0.055	0.067	0.763	17.912
0.06	0.073	0.724	17.761
0.065	0.079	0.694	17.715
0.07	0.085	0.67	17.761
0.075	0.091	0.65	17.888
0.08	0.097	0.638	18.085
0.085	0.103	0.628	18.34
0.09	0.109	0.621	18.645
0.095	0.116	0.615	18.99
0.1	0.122	0.612	19.371
0.105	0.128	0.61	19.779
0.11	0.134	0.609	20.211
0.115	0.14	0.608	20.662
0.12	0.146	0.609	21.129
0.125	0.152	0.61	21.609
0.13	0.158	0.612	22.101
0.135	0.164	0.614	22.602
0.14	0.17	0.617	23.111
0.145	0.176	0.62	23.627
0.15	0.182	0.623	24.151
0.155	0.189	0.626	24.681
0.16	0.195	0.63	25.218
0.165	0.201	0.633	25.763
0.17	0.207	0.637	26.315
0.175	0.213	0.642	26.875
0.18	0.219	0.646	27.445
0.185	0.225	0.651	28.025
0.19	0.231	0.656	28.616
0.195	0.237	0.661	29.22
0.2	0.243	0.666	29.838
0.205	0.249	0.672	30.471
0.21	0.255	0.678	31.122
0.215	0.262	0.685	31.791
0.22	0.268	0.692	32.482
0.225	0.274	0.699	33.196
0.23	0.28	0.707	33.935
0.235	0.286	0.715	34.701
0.24	0.292	0.724	35.497
0.245	0.298	0.733	36.325
0.25	0.304	0.743	37.189

Graphical Representation :- Alan Liu Correlation

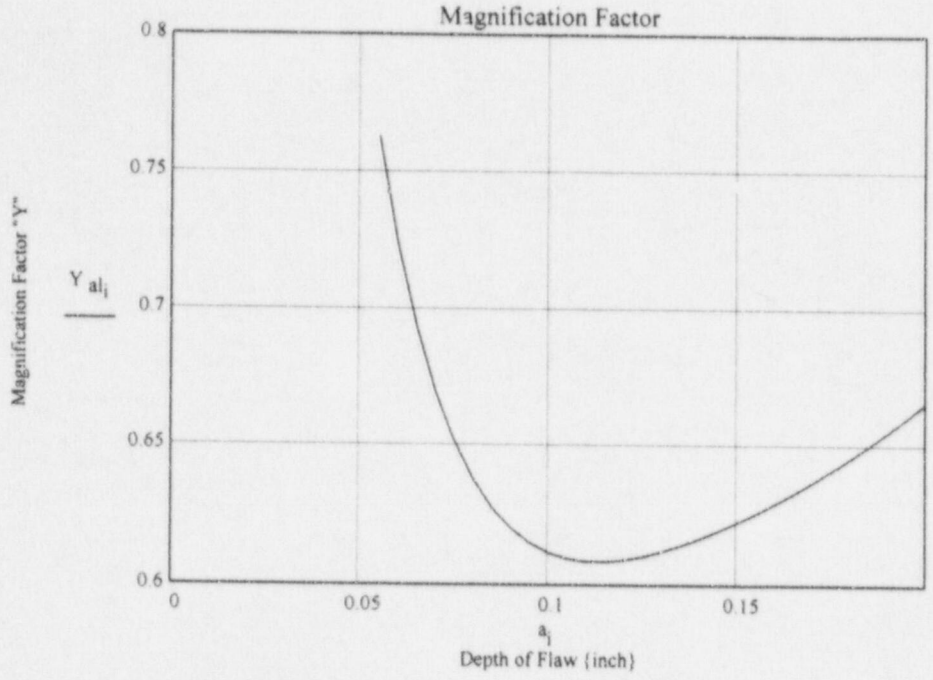

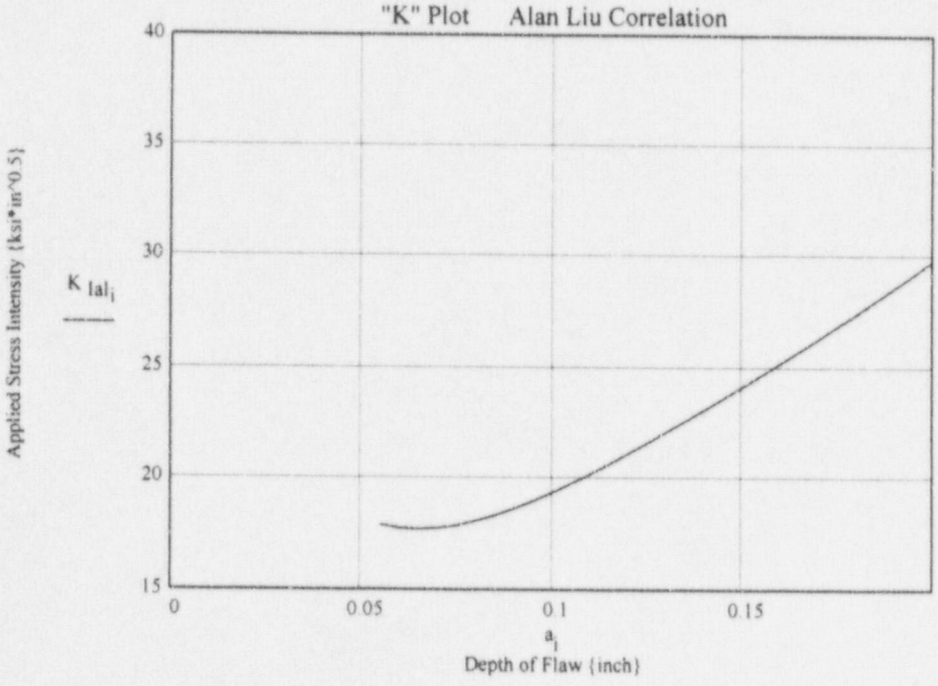

SOLUTION NUMBER :- III-A
Head to Shank Region

Forman - Shivakumar Correlation, for single Circular Crack in a Cylindrical Bar. For Constant Bending and Tension Stress. {Use ASME Sect. XI Appendix "A" Linearized stress profile.}

REFERENCE :- ASTM STP 905--"Growth Behavior of Surface Cracks in the Circumferential Plane of Solid and Hollow Cylinders"

Stress and Flaw Input data

$P_m := 34.212$	Tension or Membrane Stress{ksi}
$P_b := 35.564$	Bending Stress {ksi}
$a_0 := 0.0$	Initial Flaw Depth {inch}
$a_{inc} := 0.005$	Flaw Growth Increment {inch}
$i := 1 .. 40$	Index for Loop
$a_i := a_{i-1} + a_{inc}$	Flaw Growth Simulation
$\lambda_i := \frac{a_i}{D}$	Normalized Flaw Depth

Determination of Applied Stress Intensity Factor as a function of Flaw depth.

$$g_{\lambda_i} := 0.92 \cdot \left(\frac{2}{\pi}\right) \cdot \frac{\left[\frac{\tan\left(\pi \cdot \frac{\lambda_i}{2}\right)}{\left(\frac{\pi \cdot \lambda_i}{2}\right)}\right]^{0.5}}{\cos\left(\frac{\pi \cdot \lambda_i}{2}\right)}$$

Magnification factor

{Membrane/Tension}

$$F_{0\lambda_i} := g_{\lambda_i} \cdot \left[(0.752) + 2.02 \cdot \lambda_i + 0.37 \cdot \left[\left(1 - \sin\left(\frac{\pi \cdot \lambda_i}{2}\right)\right)^3\right]\right]$$

Magnification factor

{Bending}

$$F_{b\lambda_i} := g_{\lambda_i} \cdot \left[0.923 + 0.199 \cdot \left[\left(1 - \sin\left(\frac{\pi \cdot \lambda_i}{2}\right)\right)^4\right]\right]$$

Stress Intensity Factor Solution

$$K_{Isf_i} := \left[\left(P_m\right) \cdot F_{0\lambda_i} + P_b \cdot F_{b\lambda_i}\right] \cdot \sqrt{\pi \cdot a_i}$$

Tabular Results from Forman-Shivakumar Correlation.
{ASME Sect. XI Linearized $P_m + P_b$}

a_i	λ_i	$F_{0\lambda_i}$	$\bar{r}_{b\lambda_i}$	K_{Isf_i}
$5 \cdot 10^{-3}$	$6.083 \cdot 10^{-3}$	0.658	0.653	5.732
0.01	0.012	0.66	0.649	8.088
0.015	0.018	0.661	0.645	9.886
0.02	0.024	0.663	0.641	11.397
0.025	0.03	0.665	0.637	12.724
0.03	0.036	0.667	0.634	13.924
0.035	0.043	0.669	0.631	15.028
0.04	0.049	0.671	0.628	16.058
0.045	0.055	0.674	0.625	17.029
0.05	0.061	0.677	0.622	17.952
0.055	0.067	0.68	0.62	18.836
0.06	0.073	0.683	0.618	19.687
0.065	0.079	0.687	0.616	20.51
0.07	0.085	0.69	0.614	21.311
0.075	0.091	0.694	0.612	22.093
0.08	0.097	0.698	0.61	22.86
0.085	0.103	0.703	0.609	23.613
0.09	0.109	0.707	0.608	24.355
0.095	0.116	0.712	0.606	25.089
0.1	0.122	0.717	0.605	25.816
0.105	0.128	0.722	0.605	26.538
0.11	0.134	0.727	0.604	27.257
0.115	0.14	0.733	0.603	27.974
0.12	0.146	0.739	0.603	28.689
0.125	0.152	0.745	0.603	29.406
0.13	0.158	0.751	0.603	30.124
0.135	0.164	0.758	0.603	30.844
0.14	0.17	0.764	0.603	31.568
0.145	0.176	0.771	0.604	32.296
0.15	0.182	0.778	0.604	33.03
0.155	0.189	0.786	0.605	33.77
0.16	0.195	0.793	0.606	34.517
0.165	0.201	0.801	0.607	35.272
0.17	0.207	0.81	0.608	36.035
0.175	0.213	0.818	0.609	36.808
0.18	0.219	0.827	0.61	37.591
0.185	0.225	0.836	0.612	38.384
0.19	0.231	0.845	0.614	39.189
0.195	0.237	0.854	0.615	40.006
0.2	0.243	0.864	0.617	40.836

Graphical Representation :- Forman-Shivakumar Correlation
{ASME Sect. XI Linearized $P_m + P_b$}

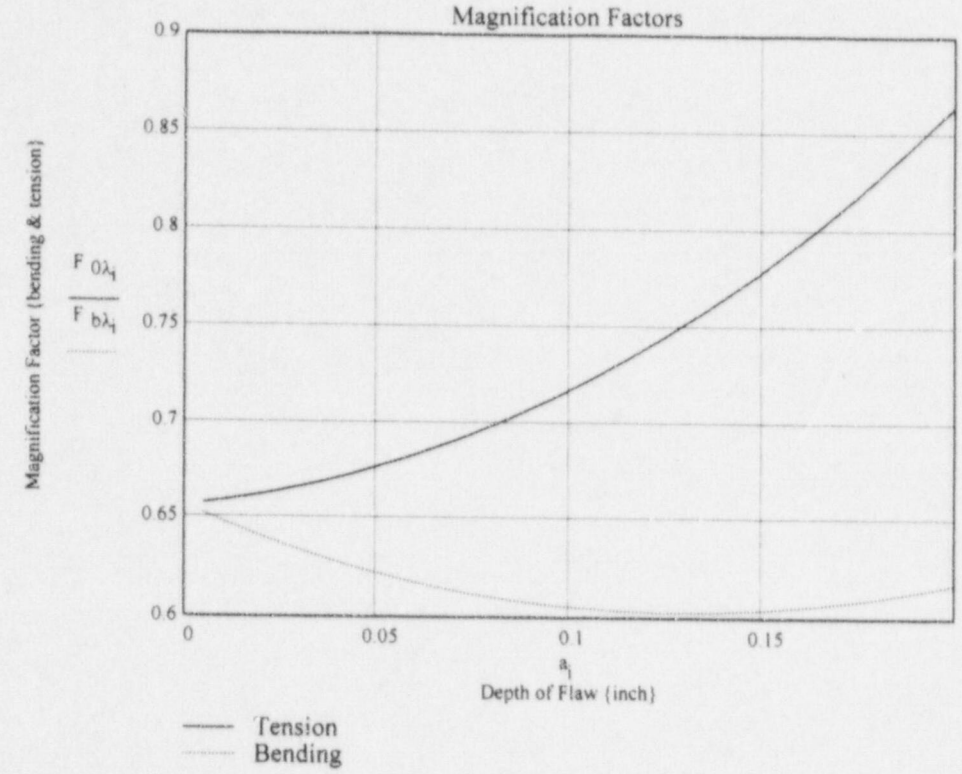

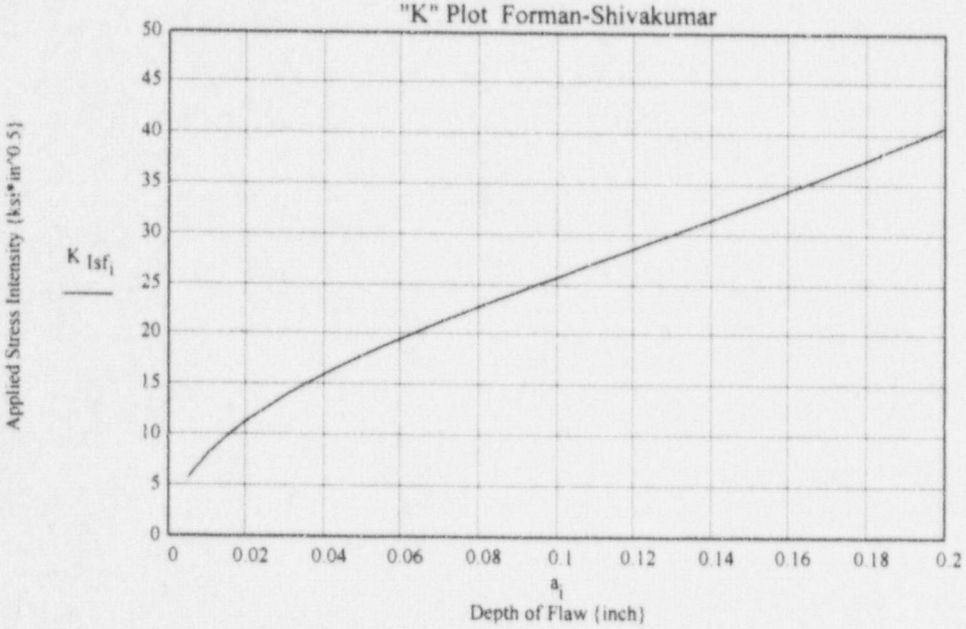

SOLUTION NUMBER :- III-B
Shank Region

Forman - Shivakumar Correlation, for single Circular Crack in a Cylindrical Bar. For Constant Bending and Tension Stress.{Use ASME Sect. XI Appendix "A" Linearized stress profile.}

REFERENCE :- ASTM STP 905--"Growth Behavior of Surface Cracks in the Circumferential Plane of Solid and Hollow Cylinders"

Stress and Flaw Input data

$S_0 := 56.5$ — Tension or Membrane Stress due to Bolt preload {ksi}

$a_0 := 0.0$ — Initial Flaw Depth {inch}

$a_{inc} := 0.005$ — Flaw Growth Increment {inch}

$i := 1 .. 40$ — Index for Loop

$a_i := a_{i-1} + a_{inc}$ — Flaw Growth Simulation

$\lambda_i := \frac{a_i}{D}$ — Normalized Flaw Depth

Determination of Applied Stress Intensity Factor as a function of Flaw depth.

$$g\lambda_i := 0.92 \cdot \left(\frac{2}{\pi}\right) \cdot \frac{\left[\frac{\tan\left(\pi \cdot \frac{\lambda_i}{2}\right)}{\left(\frac{\pi \cdot \lambda_i}{2}\right)}\right]^{0.5}}{\cos\left(\frac{\pi \cdot \lambda_i}{2}\right)}$$

Magnification factor

{Membrane/Tension}

$$F0\lambda_i := g\lambda_i \cdot \left[(0.752) + 2.02 \cdot \lambda_i + 0.37 \cdot \left[\left(1 - \sin\left(\frac{\pi \cdot \lambda_i}{2}\right)\right)^3\right]\right]$$

Stress Intensity Factor Solution

$$K_{Isfs_i} := \left(S_0 \cdot F0\lambda_i\right) \cdot \sqrt{\pi \cdot a_i}$$

Tabular Results from Forman-Shivakumar Correlation.
{Shank Region}

a_i	λ_i	$F_{0\lambda_i}$	K_{Isfs_i}
$5 \cdot 10^{-3}$	$6.083 \cdot 10^{-3}$	0.658	4.661
0.01	0.012	0.66	6.605
0.015	0.018	0.661	8.107
0.02	0.024	0.663	9.385
0.025	0.03	0.665	10.523
0.03	0.036	0.667	11.563
0.035	0.043	0.669	12.532
0.04	0.049	0.671	13.447
0.045	0.055	0.674	14.319
0.05	0.061	0.677	15.158
0.055	0.067	0.68	15.97
0.06	0.073	0.683	16.761
0.065	0.079	0.687	17.534
0.07	0.085	0.69	18.294
0.075	0.091	0.694	19.043
0.08	0.097	0.698	19.783
0.085	0.103	0.703	20.518
0.09	0.109	0.707	21.248
0.095	0.116	0.712	21.976
0.1	0.122	0.717	22.704
0.105	0.128	0.722	23.431
0.11	0.134	0.727	24.161
0.115	0.14	0.733	24.894
0.12	0.146	0.739	25.63
0.125	0.152	0.745	26.372
0.13	0.158	0.751	27.12
0.135	0.164	0.758	27.875
0.14	0.17	0.764	28.638
0.145	0.176	0.771	29.41
0.15	0.182	0.778	30.191
0.155	0.189	0.786	30.983
0.16	0.195	0.793	31.785
0.165	0.201	0.801	32.6
0.17	0.207	0.81	33.427
0.175	0.213	0.818	34.268
0.18	0.219	0.827	35.122
0.185	0.225	0.836	35.992
0.19	0.231	0.845	36.876
0.195	0.237	0.854	37.778
0.2	0.243	0.864	38.696

Graphical Representation :- Forman-Shivakumar
Correlation
{Shank Region}

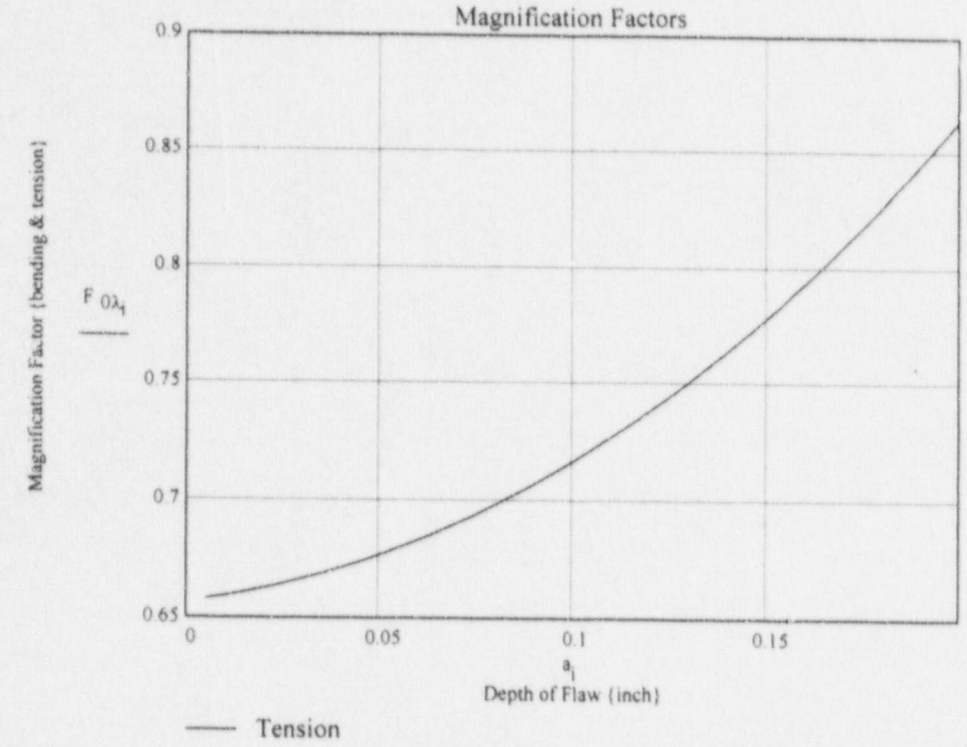

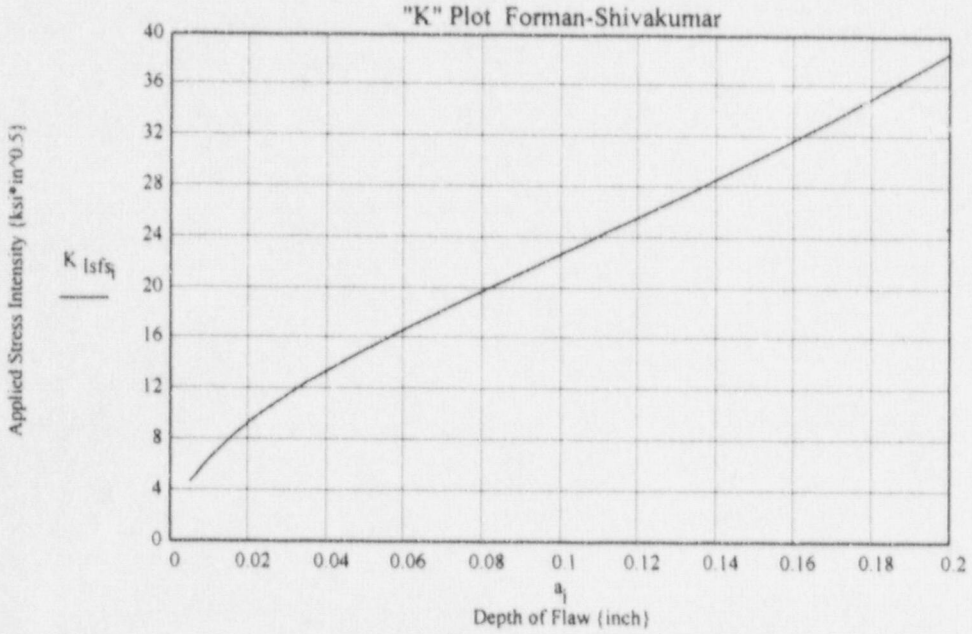

SOLUTION NUMBER :- IV

Forman - Shivakumar Correlation, REFERENCE:- ASTM STP 905-- Same Reference as Solution IIIA.

Bending stress modified to account for large surface stress at the fillet radius, from the FEA results for CRD bolt, using strain energy density method to determine a linearized equivalent stress profile.

Stress and Flaw Input Data

$S_{peak} := 90.229$ Linearized Peak Stress in Fillet Region {ksi}

$S_{nom} := 23.125$ Linearized Nominal Stress in the head-shank region {ksi}

$a_0 := 0.0$ Initial Flaw Depth {inch}

$a_{inc} := 0.005$ Increment for Flaw growth {inch}

$d_b := 0.25$ depth at which surface stress decays to nominal {inch}

$i := 1 .. 40$ Index for Loop

$a_i := a_{i-1} + a_{inc}$ Flaw Growth simulation

$\lambda_i := \frac{a_i}{D}$ Normalization of Flaw Depth

Modification of Bending Stress term to account for stress distribution at Fillet

$$J_{b_i} := \frac{S_{peak} - S_{nom}}{d_b} \cdot (d_b - a_i)$$

$$S_{b_i} := \text{if}(J_{b_i} \geq 0.0, J_{b_i} + S_{nom}, S_{nom})$$

Determination of Applied Stress Intensity Factor as a function of Flaw Depth

$$g_{\lambda_i} := 0.92 \cdot \left(\frac{2}{\pi}\right) \cdot \frac{\left[\frac{\tan\left(\pi \cdot \frac{\lambda_i}{2}\right)}{\frac{\pi \cdot \lambda_i}{2}}\right]^{0.5}}{\cos\left(\frac{\pi \cdot \lambda_i}{2}\right)}$$

Magnification Factor
{Membrane/Tension}

$$F_{0\lambda_i} := g_{\lambda_i} \cdot \left[(0.752) + 2.02 \cdot \lambda_i + 0.37 \cdot \left[\left(1 - \sin\left(\frac{\pi \cdot \lambda_i}{2}\right)\right)^3\right]\right]$$

Stress Intensity Solution

$$K_{Imsf_i} := \left(S_{b_i} \cdot F_{0\lambda_i}\right) \cdot \sqrt{\pi \cdot a_i}$$

Tabular Results from "Forman-Shivakumar" Correlation with modified bending stresses to account for the large stress at the Fillet of the CRD Bolt.

a_i	$F_{0\lambda_i}$	K_{Imsf_i}
$5 \cdot 10^{-3}$	0.658	7.333
0.01	0.66	10.234
0.015	0.661	12.369
0.02	0.663	14.096
0.025	0.665	15.554
0.03	0.667	16.818
0.035	0.669	17.93
0.04	0.671	18.919
0.045	0.674	19.806
0.05	0.677	20.607
0.055	0.68	21.332
0.06	0.683	21.989
0.065	0.687	22.587
0.07	0.69	23.131
0.075	0.694	23.626
0.08	0.698	24.075
0.085	0.703	24.481
0.09	0.707	24.848
0.095	0.712	25.177
0.1	0.717	25.471
0.105	0.722	25.731
0.11	0.727	25.958
0.115	0.733	26.154
0.12	0.739	26.319
0.125	0.745	26.455
0.13	0.751	26.561
0.135	0.758	26.638
0.14	0.764	26.687
0.145	0.771	26.708
0.15	0.778	26.7
0.155	0.786	26.664
0.16	0.793	26.6
0.165	0.801	26.507
0.17	0.81	26.386
0.175	0.818	26.235
0.18	0.827	26.055
0.185	0.836	25.845
0.19	0.845	25.605
0.195	0.854	25.333
0.2	0.864	25.029

Graphical Representation :- modified Forman-Shivakumar

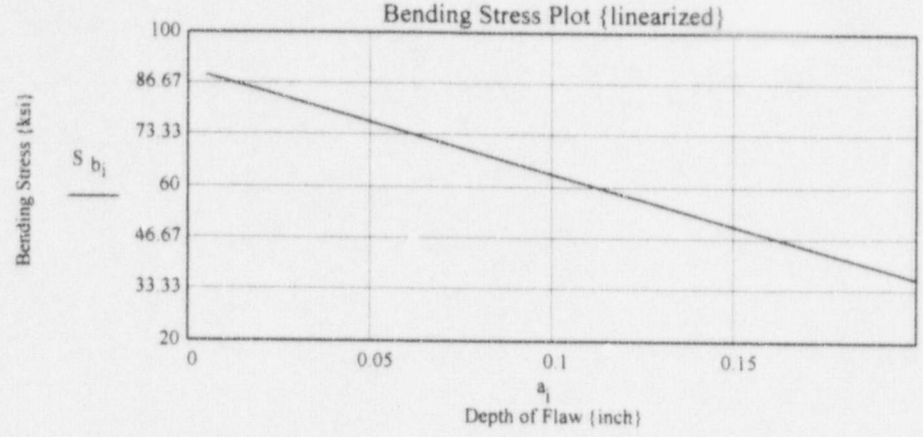

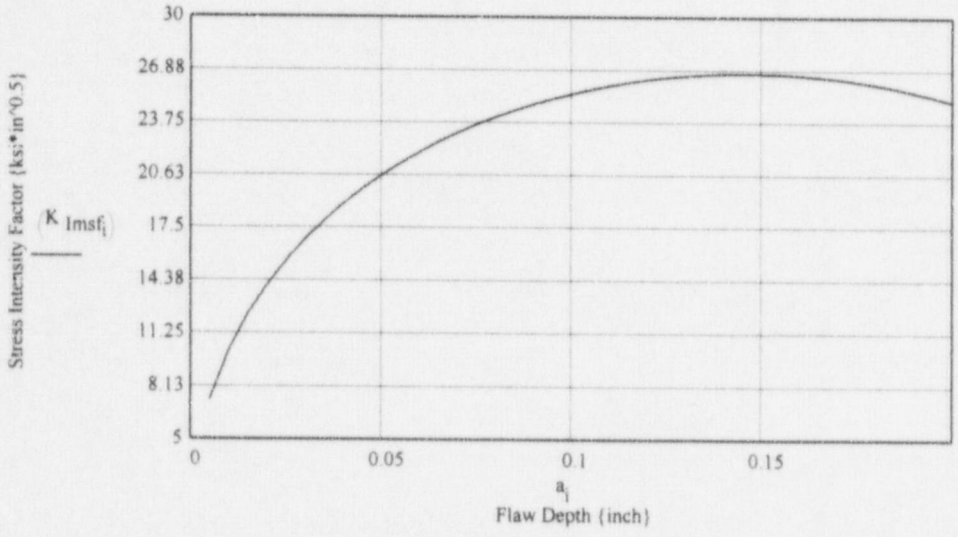

SOLUTION V-A
Head to Shank Region

SIF for rods in tension and bending with a single edge crack, (Straight Crack Front). Use of James & Mills approximation combined with Daoud & Cartwright for bending. Stress profile determined by linearization of FEA profile by strain energy density method.{Same profile as in solution IV}

Reference : SIF's for Cracks in Bolts; Engr. Fracture Mechanics, Vol. 30; No. 5. 1988.

Input Data

$S_{peak} := 90.229$ Linearized Peak Stress in Fillet region {ksi}

$S_{nom} := 23.125$ Linearized Nominal Stress in head-shank region {ksi}

$D := 0.822$ Diameter of Bolt in Shank region {inch}

$a_0 := 0.0$ Initial Crack depth {inch}

$d_b := 0.25$ Depth at which Surface Stress decays to Nominal {inch}

$a_{inc} := 0.005$ Increment for Crack Growth {inch}

$i := 1 .. 40$ Index for Loop

Simulation For Crack Growth

$a_i := a_{i-1} + a_{inc}$

$x_i := \frac{a_i}{D}$ Normalization of Crack Depth

Magnification Factors

Tension Magnification Factor :-

$$F_{t_i} := 0.926 - \left[1.771 \cdot x_i + (-26.421) \cdot (x_i)^2 - (-78.481) \cdot (x_i)^3 + (-87.911) \cdot (x_i)^4 \right]$$

Bending Magnification Factor :-

$$F_{b_i} := (1.04 - 3.64 \cdot x_i) + 16.86 \cdot (x_i)^2 - 32.59 \cdot (x_i)^3 + 28.41 \cdot (x_i)^4$$

Stress Distribution to account for the Fillet region Stress Gradient

Define the Stress Gradient as Bending Stress as :-

$$\sigma_{1b_i} := \frac{S_{peak} - S_{nom}}{d_b} \cdot (d_b - a_i)$$

$$\sigma_{b_i} := \text{if}\left[(d_b - a_i) \geq 0.0, \sigma_{1b_i}, 0.0 \right]$$

Applied Stress Intensity Factor as a Function of Crack Depth

$$K_{Icd_i} := \sqrt{\pi \cdot a_i} \cdot (S_{nom} \cdot F_{t_i} + \sigma_{b_i} \cdot F_{b_i})$$

Tabular results of Calculations from James-Mills approximation combined with Daoud-Cartwright

a_i	F_{t_i}	F_{b_i}	K_{Icd_i}
$5 \cdot 10^{-3}$	0.916	1.018	11.05
0.01	0.908	0.998	15.12
0.015	0.902	0.979	17.933
0.02	0.897	0.961	20.073
0.025	0.894	0.944	21.774
0.03	0.893	0.928	23.164
0.035	0.893	0.913	24.32
0.04	0.894	0.899	25.295
0.045	0.896	0.886	26.126
0.05	0.9	0.874	26.841
0.055	0.904	0.863	27.461
0.06	0.909	0.852	28.002
0.065	0.916	0.843	28.477
0.07	0.923	0.834	28.897
0.075	0.931	0.825	29.27
0.08	0.939	0.818	29.602
0.085	0.949	0.811	29.899
0.09	0.958	0.805	30.166
0.095	0.969	0.799	30.405
0.1	0.98	0.794	30.62
0.105	0.991	0.79	30.813
0.11	1.002	0.786	30.984
0.115	1.014	0.782	31.137
0.12	1.026	0.779	31.271
0.125	1.039	0.777	31.388
0.13	1.051	0.775	31.487
0.135	1.064	0.773	31.569
0.14	1.077	0.772	31.634
0.145	1.09	0.771	31.683
0.15	1.103	0.771	31.713
0.155	1.116	0.771	31.727
0.16	1.13	0.771	31.722
0.165	1.143	0.771	31.699
0.17	1.156	0.772	31.658
0.175	1.17	0.773	31.598
0.18	1.183	0.774	31.518
0.185	1.197	0.776	31.419
0.19	1.21	0.778	31.299
0.195	1.223	0.78	31.159
0.2	1.237	0.783	30.998

Graphical Representation :- Daoud-Cartwright & James-Mills

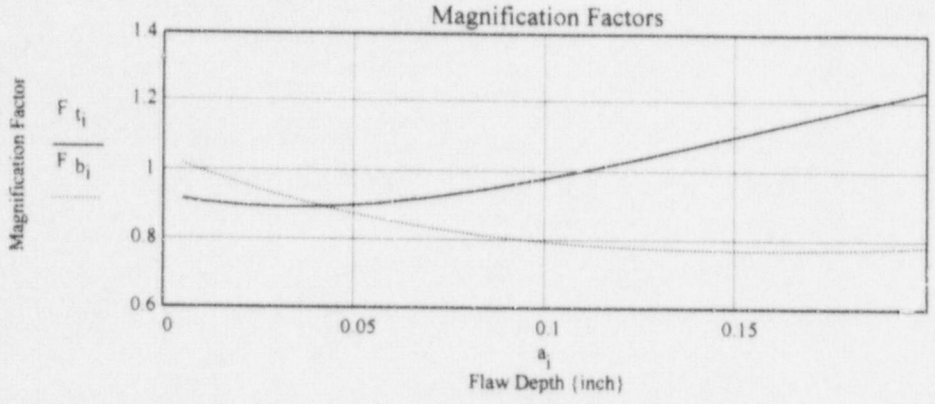

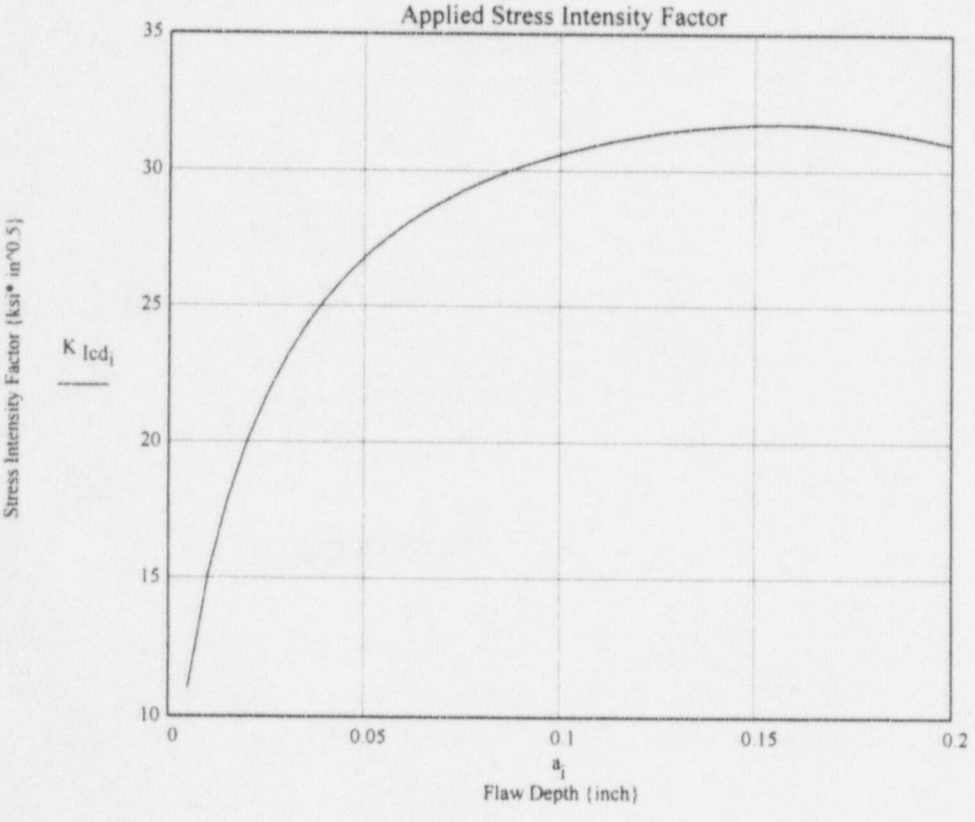

SOLUTION V-B
Shank Region

SIF for rods in tension with a single edge crack, (Straight Crack Front). Use of James & Mills approximation with tension stress caused by bolt preload in the Shank Region.

Reference : SIF's for Cracks in Bolts; Engr. Fracture Mechanics, Vol. 30; No. 5. 1988.

Input Data

$S_0 := 56.5$ Tension Stress in the Shank due to Preload {ksi}

$D := 0.822$ Diameter of Bolt in Shank region {inch}

$a_0 := 0.0$ Initial Crack depth {inch}

$d_b := 0.25$ Depth at which Surface Stress decays to Nominal {inch}

$a_{inc} := 0.005$ Increment for Crack Growth {inch}

$i := 1 .. 40$ Index for Loop

$a_i := a_{i-1} + a_{inc}$

$x_i := \frac{a_i}{D}$ Normalization of Crack Depth

Magnification Factors

$$F_{t_i} := 0.926 - \left[1.771 \cdot x_i + (-26.421) \cdot (x_i)^2 - (-78.481) \cdot (x_i)^3 + (-87.911) \cdot (x_i)^4\right]$$

Applied Stress Intensity Factor as a Function of Crack Depth

$$K_{Iscjm_i} := \sqrt{\pi \cdot a_i} \cdot (S_0 \cdot F_{t_i})$$

Tabular results of Calculations from James-Mills for Straight Crack Front

a_i	F_{t_i}	K_{Iscjm_i}
$5 \cdot 10^{-3}$	0.916	6.488
0.01	0.908	9.095
0.015	0.902	11.063
0.02	0.897	12.71
0.025	0.894	14.163
0.03	0.893	15.488
0.035	0.893	16.725
0.04	0.894	17.902
0.045	0.896	19.037
0.05	0.9	20.144
0.055	0.904	21.232
0.06	0.909	22.309
0.065	0.916	23.382
0.07	0.923	24.454
0.075	0.931	25.529
0.08	0.939	26.609
0.085	0.949	27.698
0.09	0.958	28.795
0.095	0.969	29.902
0.1	0.98	31.02
0.105	0.991	32.149
0.11	1.002	33.289
0.115	1.014	34.441
0.12	1.026	35.603
0.125	1.039	36.776
0.13	1.051	37.96
0.135	1.064	39.153
0.14	1.077	40.356
0.145	1.09	41.568
0.15	1.103	42.789
0.155	1.116	44.018
0.16	1.13	45.254
0.165	1.143	46.498
0.17	1.156	47.748
0.175	1.17	49.006
0.18	1.183	50.27
0.185	1.197	51.541
0.19	1.21	52.818
0.195	1.223	54.103
0.2	1.237	55.394

Graphical Representation :- James-Mills for a Straight Crack Front

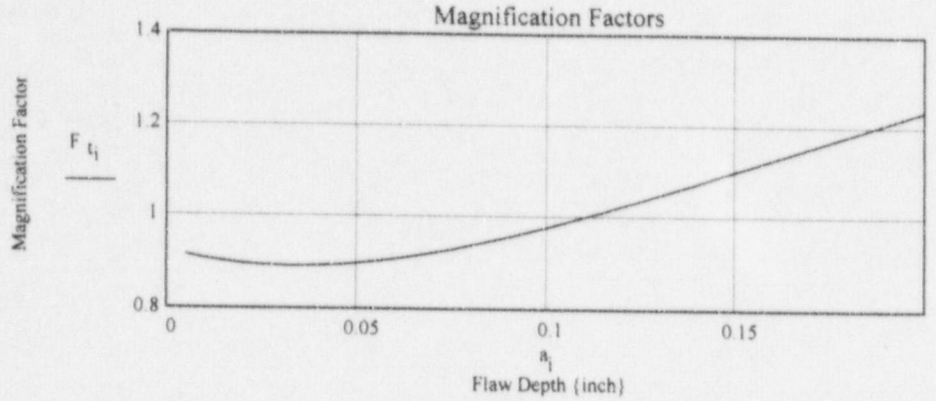

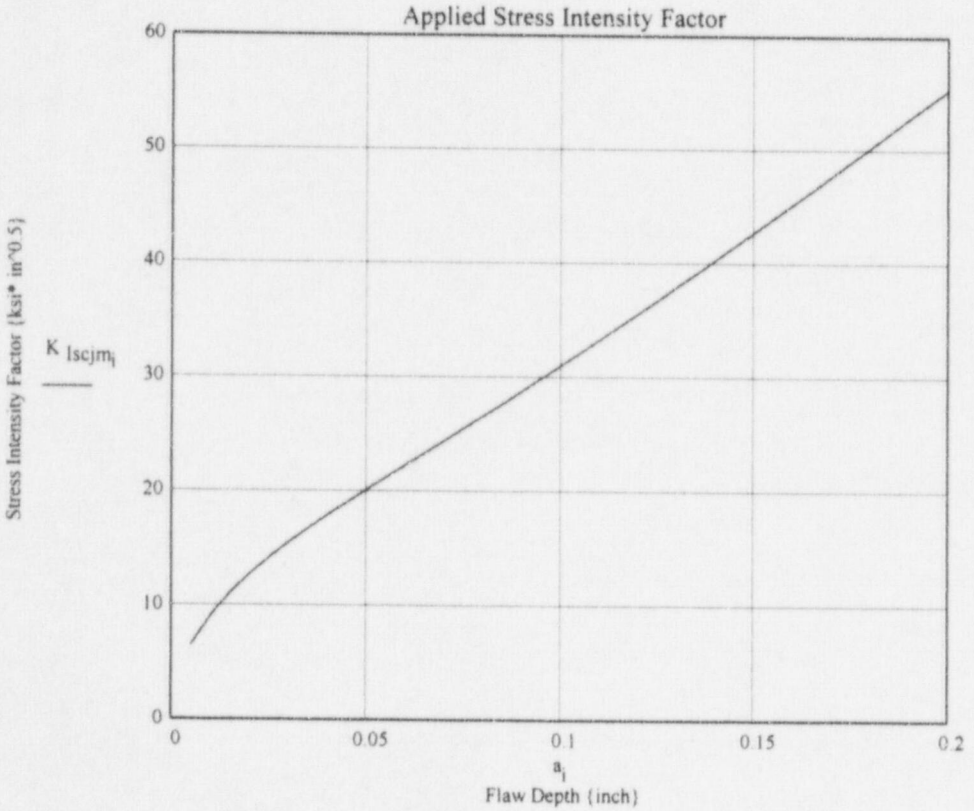

SOLUTION NUMBER :- VI-A
Head to Shank Region

Paris-Sih Circumferentially Cracked Bar in Tension;
REFERENCE:- ASTM STP 381, "Stress Analysis of Cracks"

Paris Equation With Curve fitted values for Influence Coefficients obtained from ASTM STP 381

Stress Input

$S_{nom} := 23.125$ Linearized Nominal Stress in head-shank region {ksi}

$S_{peak} := 90.229$ Linearized Peak Stress in Fillet Region {ksi}

Bolt geometric data and initial Flaw depth

$D := 0.822$ Diameter of Shank {inch}

$a_0 := 0.0$ Initial Flaw Depth {inch}

$a_{inc} := 0.005$ Increment for Flaw Growth {inch}

$d_b := 0.25$ Depth at which Surface Stress decays to Nominal {inch}

$i := 1 .. 40$ Index for Loop

$a_i := a_{i-1} + a_{inc}$ Flaw Growth Simulation

$d_i := D - 2 \cdot a_i$ Reduced Diameter due to Flaw {inch}

$x_i := \frac{2 \cdot a_i}{D}$ Flaw Depth Normalization

Equation for modifying the stress term to account for stress distribution at the fillet in the shank-to-head region of the bolt.

$$SS_i := \left[\frac{S_{peak} - S_{nom}}{d_b} \cdot (d_b - a_i) \right]$$

Stress modified to account for stress distribution from FEA. The fillet stress concentration is represented by a linear fit.

$$S_i := if(SS_i \geq 0.0, SS_i + S_{nom}, S_{nom})$$

Curve Fit equation for Influence coefficients from Paris-Sih paper in ASTM STP 381.

$$HT_i := \left[\left[0.0003 + 7.2879 \cdot x_i - 140.7368 \cdot (x_i)^2 \right] + 1714.21 \cdot (x_i)^3 - 12801.2885 \cdot (x_i)^4 \right]$$

$$F_{1dD_i} := HT_i + \left[\left[59075.1219 \cdot (x_i)^5 \right] - \left[168504.1995 \cdot (x_i)^6 \right] + \left[288396.4712 \cdot (x_i)^7 \right] - \left[270720.9370 \cdot (x_i)^8 \right] \right]$$

$$F_{dD_i} := F_{1dD_i} + 106884.1602 \cdot (x_i)^9$$

Applied Stress Intensity Solutions:

I :- Constant Stress {Tension} on cross-section

$$K_{I_i} := \frac{S_{peak}}{\left(\frac{d_i}{D}\right)^2} \cdot (\pi \cdot D)^{0.5} \cdot 0.24$$

Peak Stress {S} at fillet Radius considered to act across the shank cross-sectional area

II :- Stress distribution at Fillet Radius approximated and actual Stress distribution on the cross-section considered {S}

$$K_{IIp_i} := \frac{S_i}{\left(\frac{d_i}{D}\right)^2} \cdot (\pi \cdot D)^{0.5} \cdot F_{dD_i}$$

Tabular Results from Paris-Sih Correlation.

a_i	$\frac{d_i}{D}$	F_{dD_i}	K_{Iip_i}	K_{I_i}
$5 \cdot 10^{-3}$	0.988	0.071	10.386	35.662
0.01	0.976	0.115	16.993	36.556
0.015	0.964	0.143	21.323	37.485
0.02	0.951	0.161	24.333	38.45
0.025	0.939	0.175	26.618	39.453
0.03	0.927	0.186	28.519	40.495
0.035	0.915	0.195	30.213	41.579
0.04	0.903	0.203	31.771	42.707
0.045	0.891	0.21	33.209	43.882
0.05	0.878	0.216	34.519	45.106
0.055	0.866	0.221	35.686	46.382
0.06	0.854	0.225	36.706	47.713
0.065	0.842	0.228	37.586	49.102
0.07	0.83	0.23	38.344	50.553
0.075	0.818	0.231	39.009	52.068
0.08	0.805	0.233	39.615	53.653
0.085	0.793	0.233	40.194	55.312
0.09	0.781	0.234	40.774	57.048
0.095	0.769	0.235	41.376	58.868
0.1	0.757	0.236	42.009	60.776
0.105	0.745	0.237	42.671	62.778
0.11	0.732	0.238	43.351	64.881
0.115	0.72	0.239	44.03	67.092
0.12	0.708	0.24	44.687	69.417
0.125	0.696	0.241	45.3	71.865
0.13	0.684	0.241	45.854	74.446
0.135	0.672	0.241	46.342	77.167
0.14	0.659	0.24	46.773	80.041
0.145	0.647	0.24	47.165	83.078
0.15	0.635	0.239	47.552	86.292
0.155	0.623	0.238	47.976	89.696
0.16	0.611	0.238	48.481	93.305
0.165	0.599	0.238	49.105	97.136
0.17	0.586	0.239	49.867	101.209
0.175	0.574	0.241	50.754	105.543
0.18	0.562	0.243	51.709	110.161
0.185	0.55	0.244	52.618	115.089
0.19	0.538	0.244	53.305	120.356
0.195	0.526	0.243	53.529	125.992
0.2	0.513	0.238	53.002	132.034

Graphical Representation :- Paris-Sih Correlation

NOTE

1) Solid Curve based on the actual stress distribution from FEA results.

2) Dashed Curve based on assuming the Peak surface stress from FEA to be constant stress acting on the cross-section of the shank.

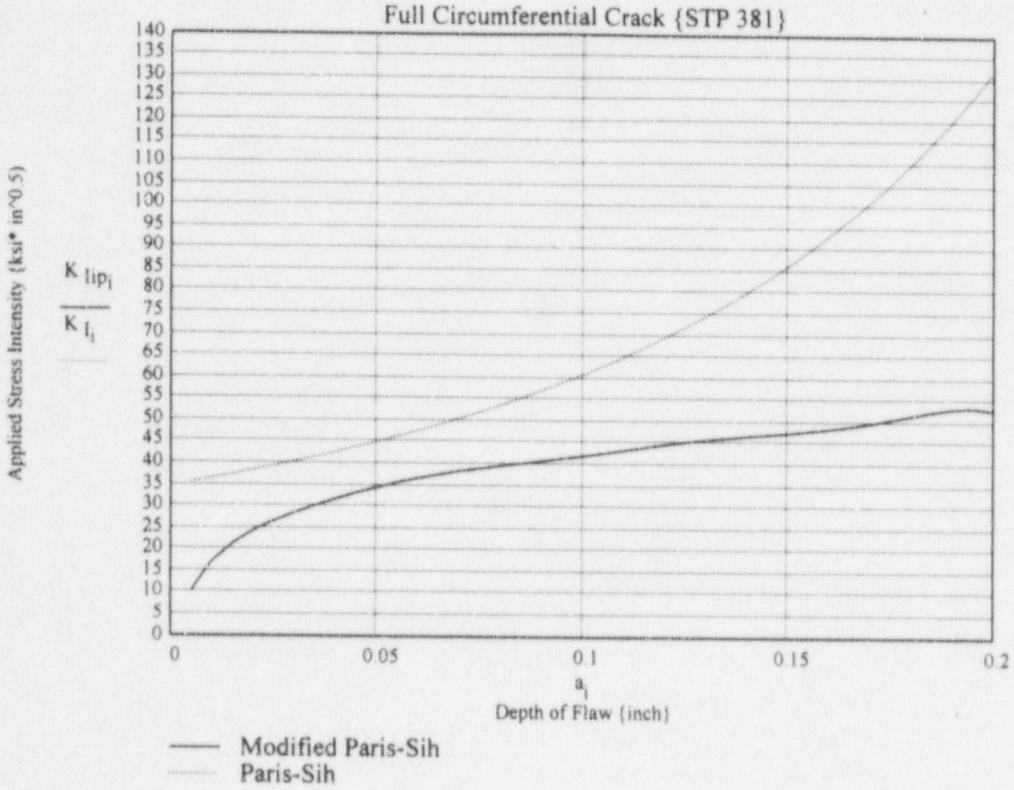

SOLUTION NUMBER :-
VI-B
Shank Region

Paris-Sih Circumferentially Cracked Bar in Tension;
REFERENCE:- ASTM STP 381, "Stress Analysis of Cracks"

Paris Equation With Curve fitted values for Influence Coefficients obtained from ASTM STP 381

Stress Input

$S_0 := 56.5$ Tension Stress in Shank Region due to Bolt Preload {ksi}

Bolt Geometric Data and Initial Flaw depth

$D := 0.822$ Diameter of Shank {inch}

$a_0 := 0.0$ Initial Flaw Depth {inch}

$a_{inc} := 0.005$ Increment for Flaw Growth {inch}

$i := 1 .. 40$ Index for Loop

$a_i := a_{i-1} + a_{inc}$ Flaw Growth Simulation

$d_i := D - 2 \cdot a_i$ Reduced Diameter due to Flaw {inch}

$x_i := \frac{2 \cdot a_i}{D}$ Flaw Depth Normalization

Curve Fit equation for Influence coefficients from Sih-Paris paper in ASTM STP 381.

$$HT_i := \left[\left[0.0003 + 7.2879 \cdot x_i - 140.7368 \cdot (x_i)^2\right] + 1714.21 \cdot (x_i)^3 - 12801.2885 \cdot (x_i)^4\right]$$

$$F_{1dD_i} := HT_i + \left[\left[59075.1219 \cdot (x_i)^5\right] - \left[168504.1995 \cdot (x_i)^6\right] + \left[288396.4712 \cdot (x_i)^7\right] - \left[270720.9370 \cdot (x_i)^8\right]\right]$$

$$F_{dD_i} := F_{1dD_i} + 106884.1602 \cdot (x_i)^9$$

Applied Stress Intensity Solution:

Constant Stress {Tension} on Shank cross-section

$$K_{Is_i} := \frac{S_0}{\left(\frac{d_i}{D}\right)^2} \cdot (\pi \cdot D)^{0.5} \cdot F_{dD_i}$$

Peak Stress {S} at fillet Radius considered to act across the shank cross-sectional area

Tabular Results from Paris-Sih Correlation.

a_i	$\frac{d_i}{D}$	F_{dD_i}	K_{Is_i}
$5 \cdot 10^{-3}$	0.988	0.071	6.602
0.01	0.976	0.115	10.967
0.015	0.964	0.143	13.975
0.02	0.951	0.161	16.201
0.025	0.939	0.175	18.007
0.03	0.927	0.186	19.608
0.035	0.915	0.195	21.118
0.04	0.903	0.203	22.582
0.045	0.891	0.21	24.009
0.05	0.878	0.216	25.392
0.055	0.866	0.221	26.717
0.06	0.854	0.225	27.979
0.065	0.842	0.228	29.177
0.07	0.83	0.23	30.325
0.075	0.818	0.231	31.442
0.08	0.805	0.233	32.553
0.085	0.793	0.233	33.687
0.09	0.781	0.234	34.868
0.095	0.769	0.235	36.116
0.1	0.757	0.236	37.445
0.105	0.745	0.237	38.858
0.11	0.732	0.238	40.349
0.115	0.72	0.239	41.908
0.12	0.708	0.24	43.517
0.125	0.696	0.241	45.158
0.13	0.684	0.241	46.819
0.135	0.672	0.241	48.494
0.14	0.659	0.24	50.192
0.145	0.647	0.24	51.937
0.15	0.635	0.239	53.77
0.155	0.623	0.238	55.747
0.16	0.611	0.238	57.933
0.165	0.599	0.238	60.392
0.17	0.586	0.239	63.174
0.175	0.574	0.241	66.293
0.18	0.562	0.243	69.703
0.185	0.55	0.244	73.275
0.19	0.538	0.244	76.771
0.195	0.526	0.243	79.824
0.2	0.513	0.238	81.942

Graphical Representation :- Paris-Sih Correlation in Shank Region

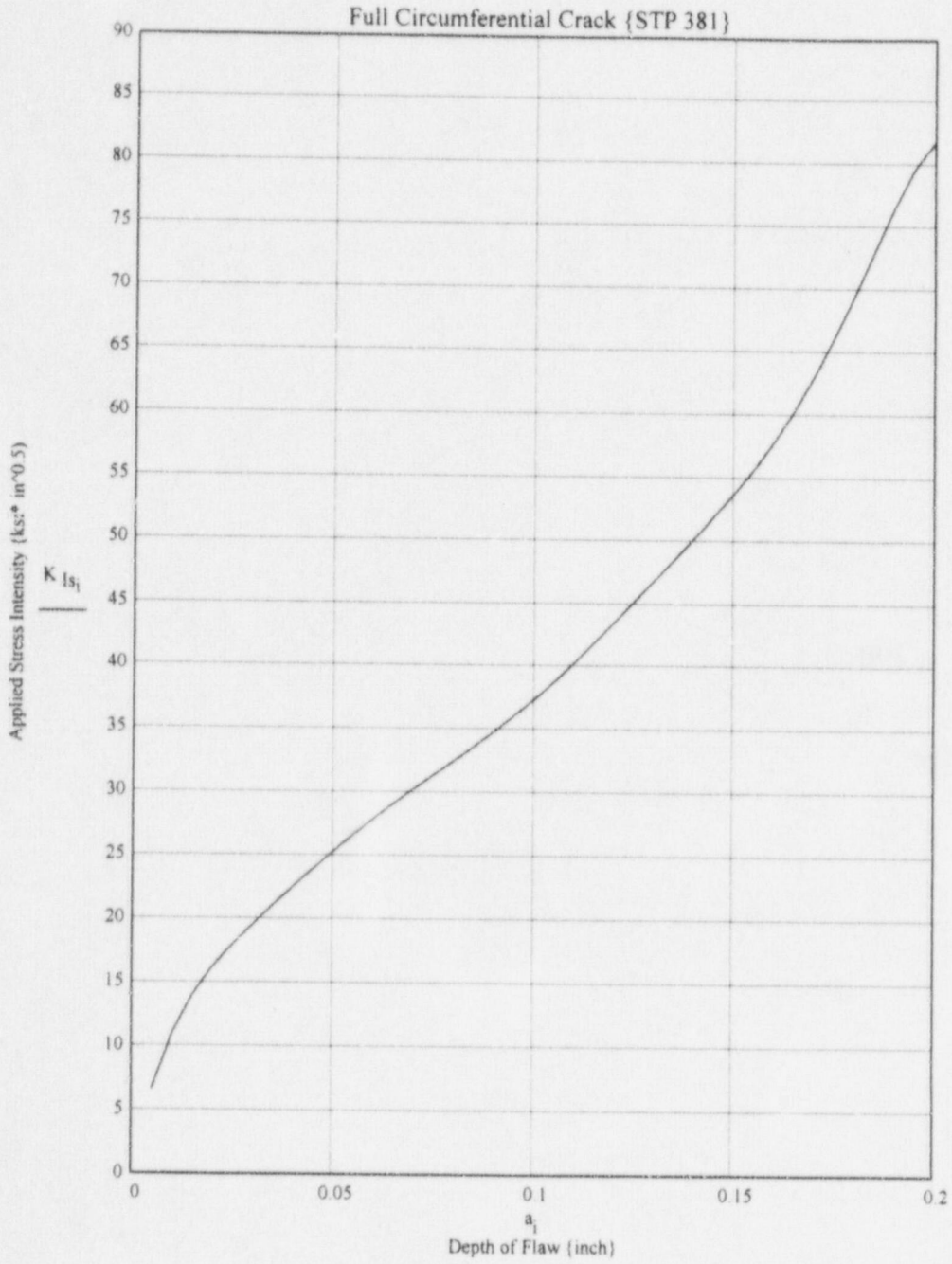

SOLUTION VII
Head to Shank Region

SIF for rods in tension and bending with Paris-Sih formulation for tension and Daoud- Cartwright solution for bending. The tension solution is for full circumferential notched bar and the bending solution is for a single (straight crack front) crack. This superposition method is in accordance with WRC bulletin 175 "Toughness requirements for Bolting", paragraph "B".

References : SIF's for Cracks in Bolts; Engr. Fracture Mechanics, Vol. 30; No. 5. 1988., ASTM STP 381, & WRC Bulletin 175.

Input Data

$P_m := 34.212$ Linearized Membrane Stress in Fillet region {ksi}

$P_b := 35.564$ Linearized Bending Stress in head-shank region {ksi}

$D := 0.822$ Diameter of Bolt in Shank region {inch}

$a_0 := 0.0$ Initial Crack depth {inch}

$a_{inc} := 0.005$ Increment for Crack Growth {inch}

$i := 1 .. 40$ Index for Loop

Simulation For Crack Growth

$a_i := a_{i-1} + a_{inc}$

$d_i := D - 2 \cdot a_i$

$x_i := \frac{a_i}{D}$ Normalization of Crack Depth

Bending Magnification Factor (Daoud-Cartwright):-

$$F_{b_i} := (1.04 - 3.64 \cdot x_i) + 16.86 \cdot (x_i)^2 - 32.59 \cdot (x_i)^3 + 28.41 \cdot (x_i)^4$$

Curve Fit equation for Influence coefficients from Paris-Sih paper in ASTM STP 381.

$$HT_i := \left[\left[0.0003 + 7.2879 \cdot x_i - 140.7368 \cdot (x_i)^2\right] + 1714.21 \cdot (x_i)^3 - 12801.2885 \cdot (x_i)^4\right]$$

$$F_{1dD_i} := HT_i + \left[\left[59075.1219 \cdot (x_i)^5\right] - \left[168504.1995 \cdot (x_i)^6\right] + \left[288396.4712 \cdot (x_i)^7\right] - \left[270720.9370 \cdot (x_i)\right.\right.$$

$$F_{dD_i} := F_{1dD_i} + 106884.1602 \cdot (x_i)^9$$

K_I from Paris-Sih Formulation for Tension Stress

$$K_{Ips_i} := \frac{P_m}{\left(\frac{d_i}{D}\right)^2} \cdot (\pi \cdot D)^{0.5} \cdot F_{dD_i}$$

K_I from Daoud-Cartwright for Bending Stress

$$K_{Idc_i} := \sqrt{\pi \cdot a_i} \cdot \left(P_b \cdot F_{b_i}\right)$$

K_I combined in the Shank Region

$$K_{Ipd_i} := K_{Ips_i} + K_{Idc_i}$$

Tabular Results for combined Paris-Sih & Daoud-Cartwright

a_i	K_{Ips_i}	K_{Idc_i}	K_{Ipd_i}
$5 \cdot 10^{-3}$	2.242	4.54	6.782
0.01	4.098	6.292	10.39
0.015	5.658	7.558	13.216
0.02	6.985	8.567	15.551
0.025	8.131	9.409	17.54
0.03	9.142	10.133	19.275
0.035	10.053	10.769	20.822
0.04	10.896	11.336	22.232
0.045	11.694	11.85	23.543
0.05	12.466	12.32	24.785
0.055	13.227	12.754	25.981
0.06	13.99	13.159	27.149
0.065	14.761	13.541	28.302
0.07	15.547	13.903	29.451
0.075	16.352	14.25	30.602
0.08	17.178	14.583	31.762
0.085	18.027	14.906	32.934
0.09	18.9	15.221	34.121
0.095	19.796	15.529	35.325
0.1	20.717	15.832	36.549
0.105	21.661	16.132	37.793
0.11	22.63	16.429	39.059
0.115	23.625	16.725	40.35
0.12	24.648	17.02	41.668
0.125	25.701	17.315	43.016
0.13	26.787	17.611	44.398
0.135	27.909	17.909	45.818
0.14	29.074	18.208	47.282
0.145	30.286	18.51	48.797
0.15	31.553	18.815	50.368
0.155	32.881	19.122	52.003
0.16	34.28	19.433	53.712
0.165	35.757	19.747	55.504
0.17	37.324	20.065	57.389
0.175	38.991	20.387	59.378
0.18	40.77	20.713	61.483
0.185	42.672	21.043	63.715
0.19	44.711	21.378	66.09
0.195	46.902	21.718	68.619
0.2	49.258	22.062	71.32

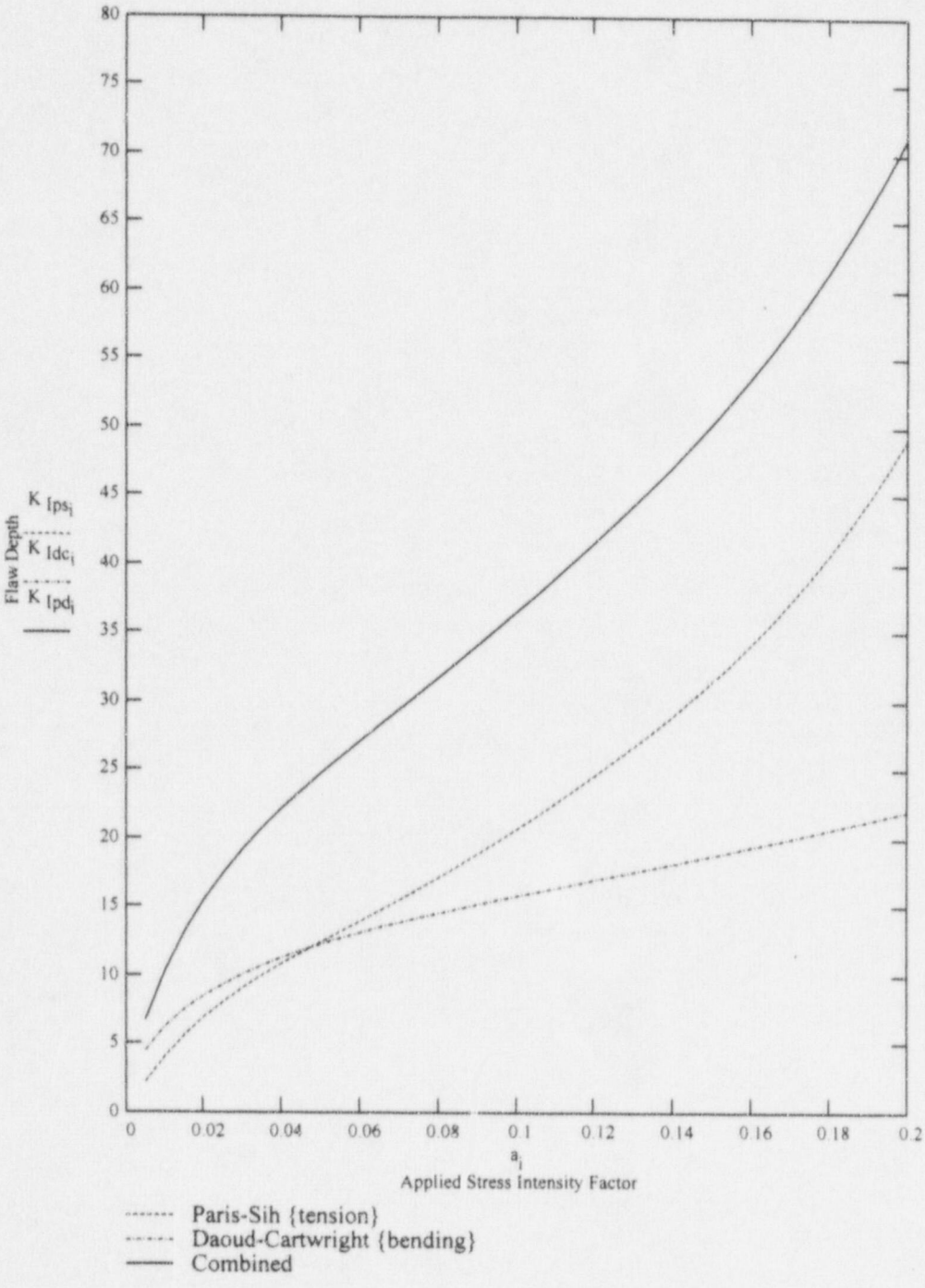
80
75
70
65
60
55
50
45
40
35
30
25
20
15
10
5
0
0
0.02
0.04
0.06
0.08
0.1
0.12
0.14
0.16
0.18
0.2
Flaw Depth
K Ipsi
K Idci
K Ipdi
ai
Applied Stress Intensity Factor
Paris-Sih {tension}
Daoud-Cartwright {bending}
Combined

SOLUTION VIII
Head to Shank Region

SIF for rods in tension and bending with Paris-Sih formulation for tension and Besuner solution for bending. Both the tension and bending solutions are fro a notched bar geometry. This superposition method is in accordance with WRC bulletin 175 "Toughness requirements for Bolting", paragraph "B".

References :Requirements and Guidelines for Component Support Materials Under Unresolved Safety Issue A-12; EPRI NP-3528, & WRC Bulletin 175.

Input Data

$P_m := 34.212$ Linearized Membrane Stress in Fillet region {ksi}

$P_b := 35.564$ Linearized Bending Stress in head-shank region {ksi}

$D := 0.822$ Diameter of Bolt in Shank region {inch}

$b := \frac{D}{2.0}$ Outside radius of bolt (inch)

$a_0 := 0.0$ Initial Crack depth {inch}

$a_{inc} := 0.005$ Increment for Crack Growth {inch}

$i := 1..40$ Index for Loop

Simulation For Crack Growth

$a_i := a_{i-1} + a_{inc}$

$c_i := b - a_i$

$x_i := \frac{c_i}{b}$ Normalization of Crack Depth

Influence Functions

$$F_{mepri_i} := 0.5 \cdot (x_i)^{-1.5} \cdot \left[1 + \left[0.5 \cdot x_i + \left[0.374 \cdot (x_i)^2 - 0.363 \cdot (x_i)^3 + 0.731 \cdot (x_i)^4\right]\right]\right]$$

$$F_{bepri_i} := 0.375 \cdot (x_i)^{-2.5} \cdot \left[1 + 0.5 \cdot x_i + 0.375 \cdot (x_i)^2 + 0.3125 \cdot (x_i)^3 + 0.2734 \cdot (x_i)^4 + 0.537 \cdot (x_i)^5\right]$$

SIF Solutions for Tension and Bending

$$K_{Itepri_i} := P_m \cdot F_{mepri_i} \cdot \sqrt{\pi \cdot a_i}$$

$$K_{Ibepri_i} := P_b \cdot F_{bepri_i} \cdot \sqrt{\pi \cdot a_i}$$

$$K_{Iepri_i} := K_{Itepri_i} + K_{Ibepri_i}$$

i	a_i	c_i	K_{Iepri_i}
1	$5 \cdot 10^{-3}$	0.406	9.859
2	0.01	0.401	14.008
3	0.015	0.396	17.247
4	0.02	0.391	20.031
5	0.025	0.386	22.539
6	0.03	0.381	24.864
7	0.035	0.376	27.06
8	0.04	0.371	29.167
9	0.045	0.366	31.211
10	0.05	0.361	33.212
11	0.055	0.356	35.188
12	0.06	0.351	37.153
13	0.065	0.346	39.117
14	0.07	0.341	41.092
15	0.075	0.336	43.088
16	0.08	0.331	45.113
17	0.085	0.326	47.176
18	0.09	0.321	49.286
19	0.095	0.316	51.452
20	0.1	0.311	53.682
21	0.105	0.306	55.984
22	0.11	0.301	58.368
23	0.115	0.296	60.843
24	0.12	0.291	63.419
25	0.125	0.286	66.106
26	0.13	0.281	68.917
27	0.135	0.276	71.862
28	0.14	0.271	74.955
29	0.145	0.266	78.21
30	0.15	0.261	81.642
31	0.155	0.256	85.268
32	0.16	0.251	89.106
33	0.165	0.246	93.177
34	0.17	0.241	97.502
35	0.175	0.236	102.107
36	0.18	0.231	107.019
37	0.185	0.226	112.268
38	0.19	0.221	117.888
39	0.195	0.216	123.919
40	0.2	0.211	130.403

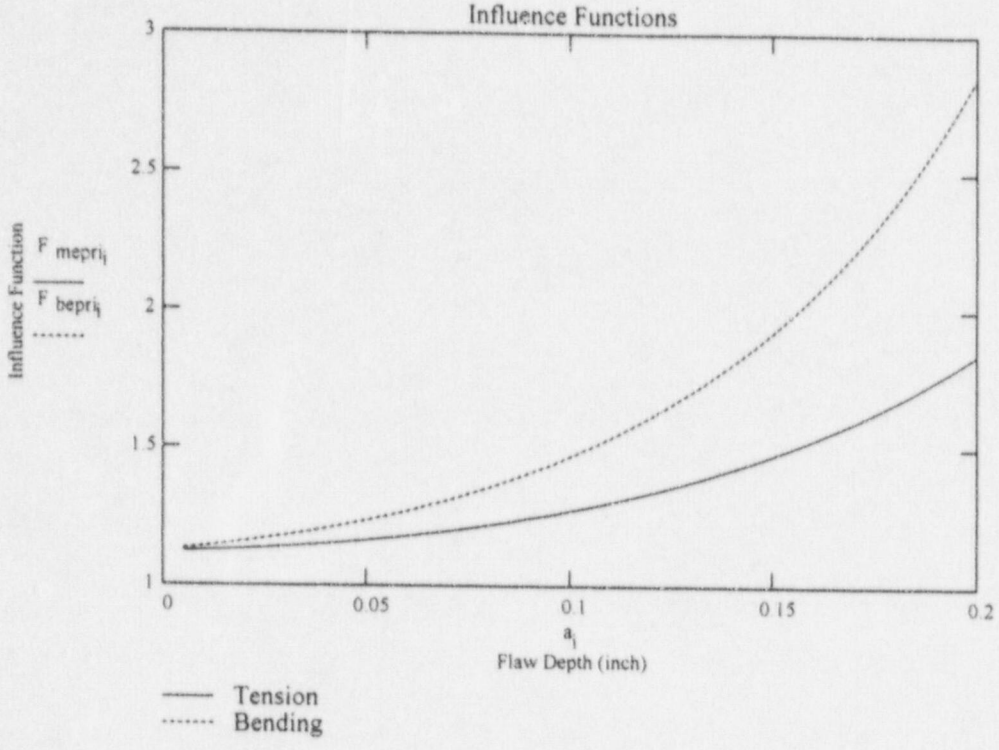
Influence Functions
Influence Function
F mepri_i / F bepri_i
3
2.5
2
1.5
1
0
0.05
0.1
0.15
0.2
a_i
Flaw Depth (inch)
Tension
Bending

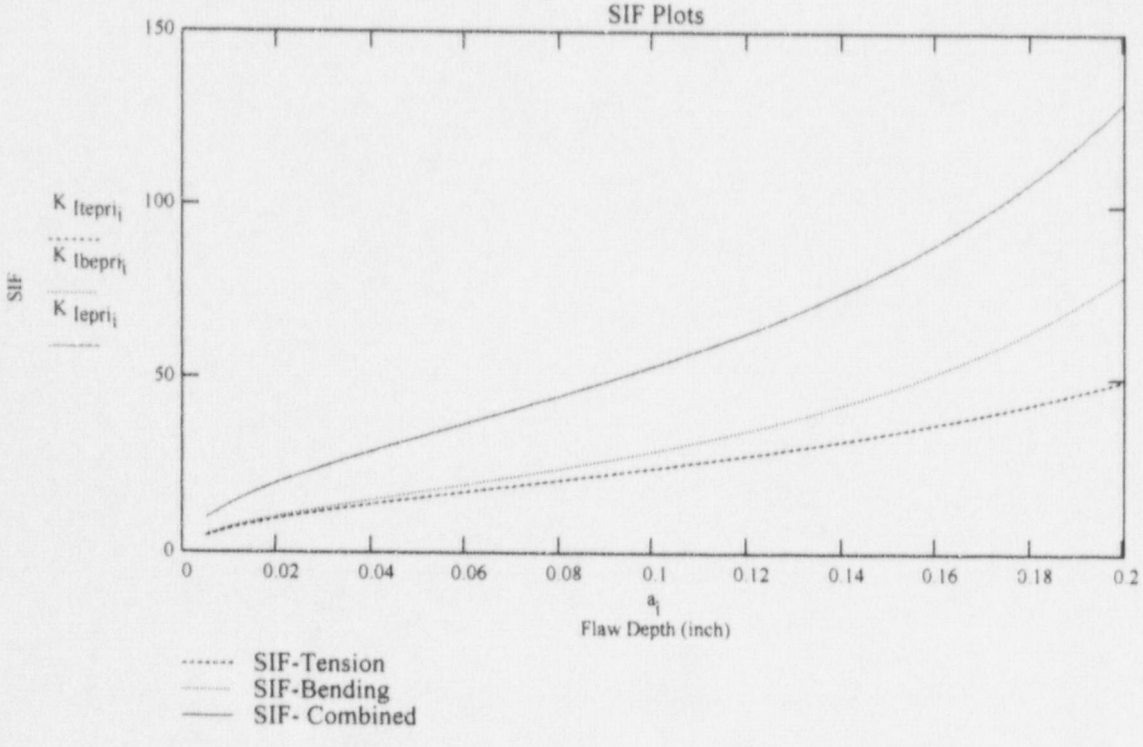
SIF Plots
SIF
K Itepri_i
K Ibepri_i
K Iepri_i
150
100
50
0
0
0.02
0.04
0.06
0.08
0.1
0.12
0.14
0.16
0.18
0.2
a_i
Flaw Depth (inch)
SIF-Tension
SIF-Bending
SIF- Combined

Determination of ASME Section XI Allowable Fracture Toughness K_{Ic}

Material Fracture Toughness for Initiation {K_{Ic}} -- ksi * $in^{0.5}$

$$K_{Ic} := 130.00$$

Material Stress Corrosion Cracking Threshold Stress Intensity Factor {K_{Iscc}} -- ksi * $in^{0.5}$

$$K_{Iscc} := 130.00$$

Use the lower of the material toughness value to determine the ASME allowable:

$$K_{IASME} := \frac{130}{\sqrt{2}}$$

$$i := 1 .. 40$$

$$K_{Iasme_i} := K_{IASME}$$

$$K_{IASME} = 91.924$$

Plot Number: 1

Graphical Comparison of Results from "K" solutions for Head to Shank Region

***Note** : Paris-Sih correlation is for a Full Circumferential Crack (360 degrees) whereas the other correlations are for Part-Circumferential Cracks.*

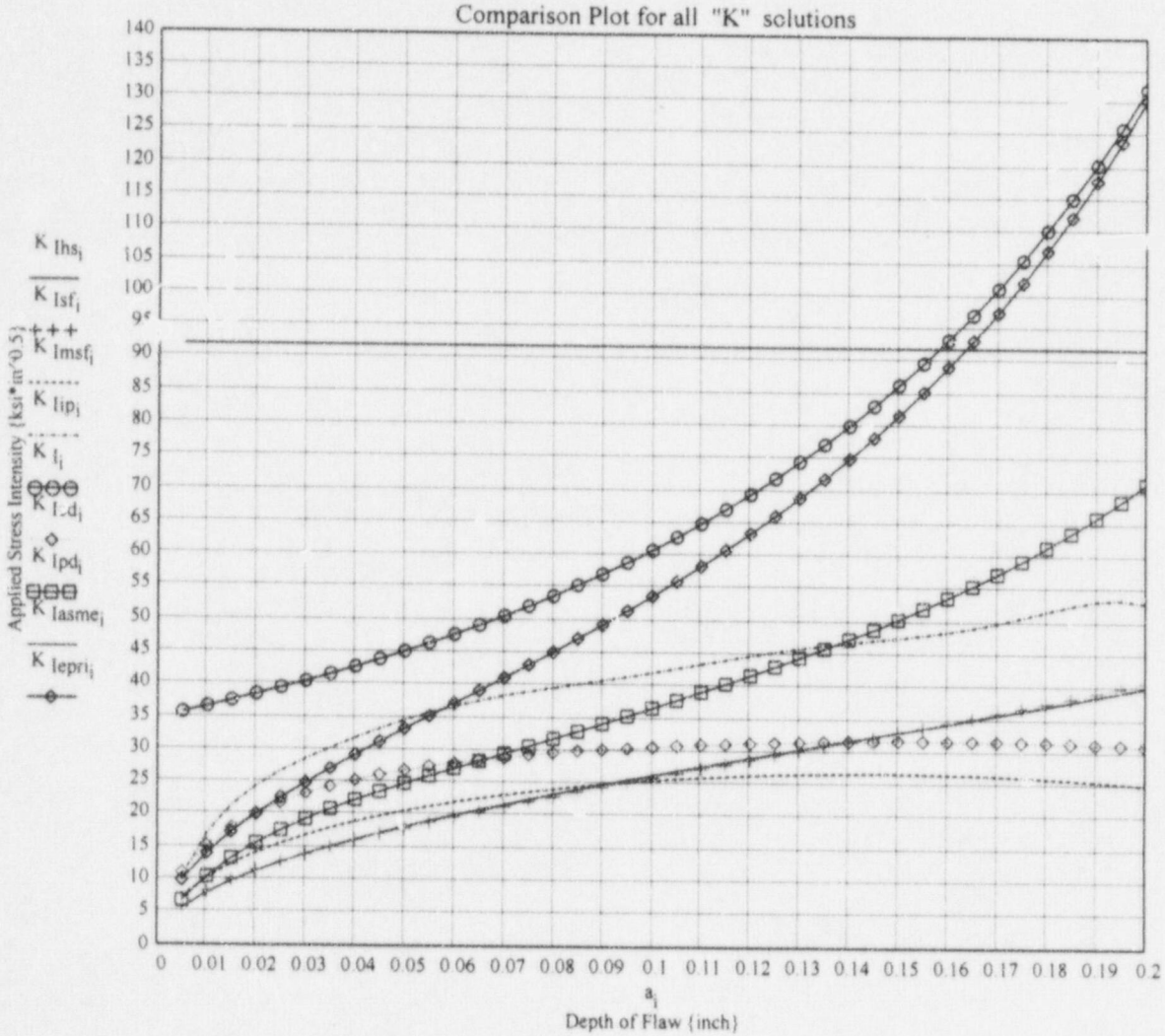

Plot Number: 2

Graphical Comparison of Results from "K" solutions for Thread Root Region

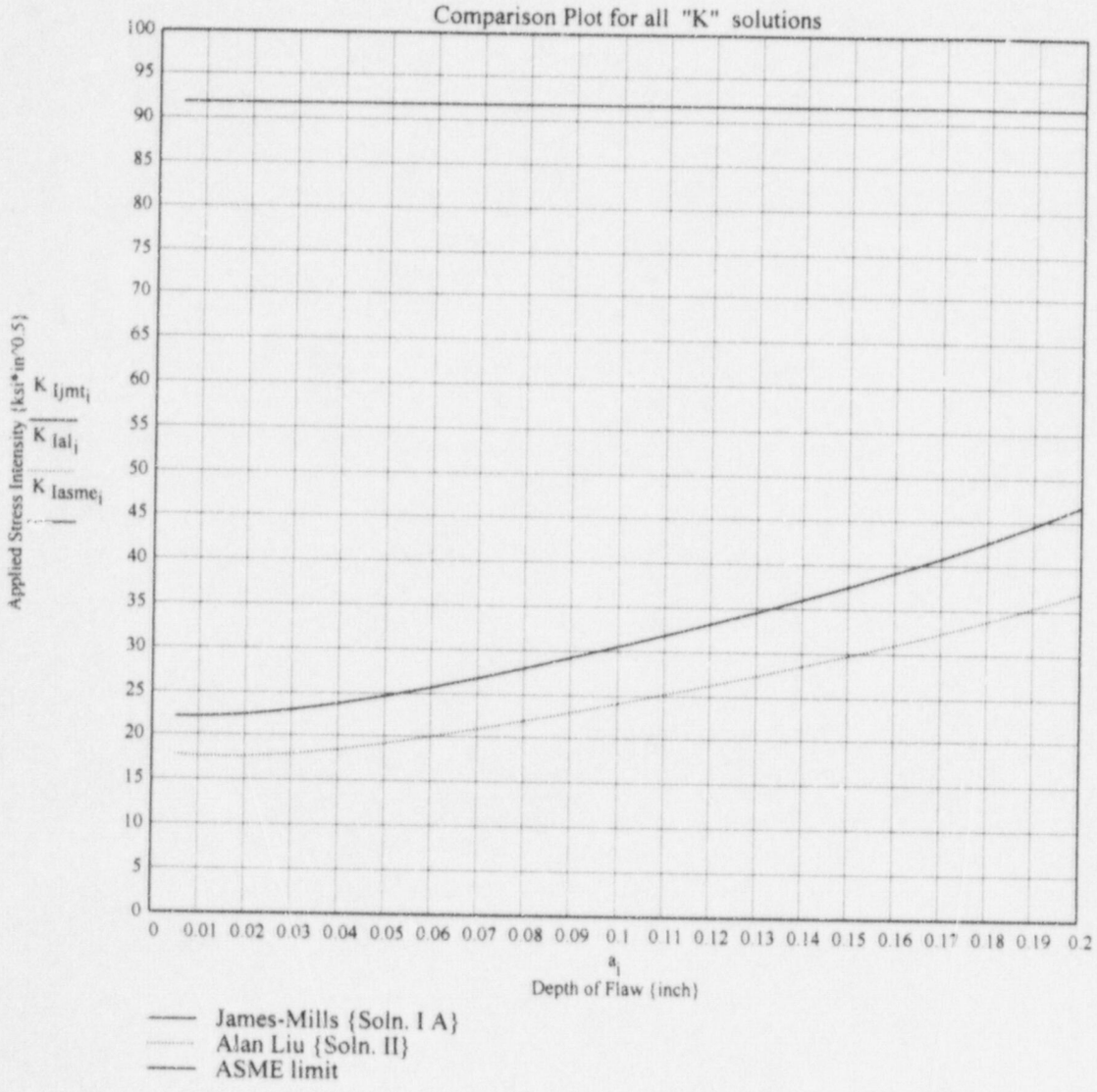

Plot Number: 3

Comparison of Graphical Results from "K" solutions for Shank Region

***Note** : Paris-Sih correlation is for a Full Circumferential Crack (360 degrees) whereas the other correlations are for Part-Circumferential Cracks.*

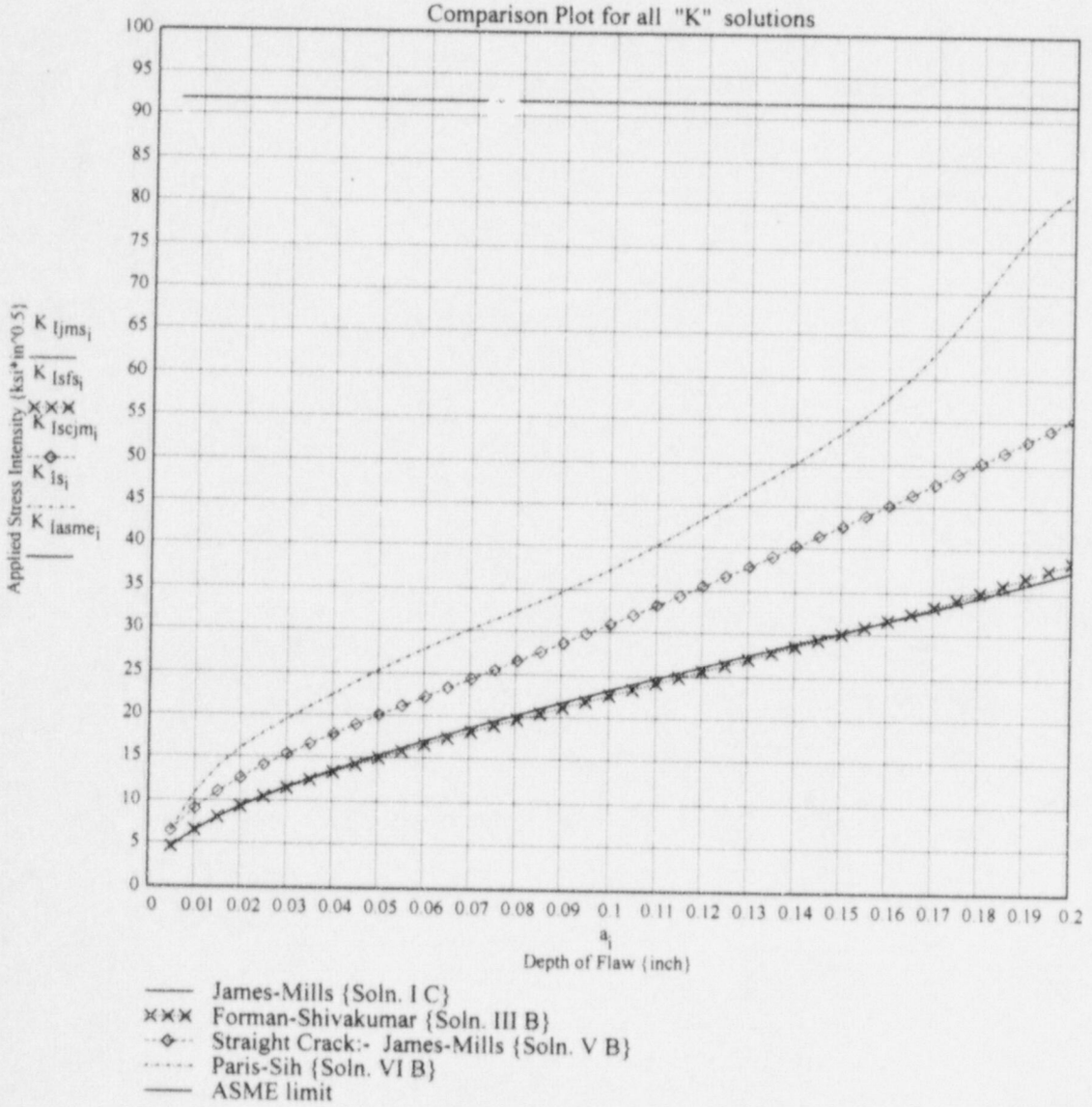

Appendix 3

Evaluation of Bolted Joint

Appendix 3

Bolted Joint Calculations: CRD Cap Screw Evaluation

Nomenclature

D_B = Larger of Bolt Head or Washer Diameter (inch)
L_G = Grip Length of Bolt (inch)
T_H = Height of Bolt Head (inch)
L_t = Length of Threads (inch)
L_B = Length of Bolt Shank (inch)
L_G = Grip Length of Bolt (inch)
D_{sh} = Diameter of Bolt Shank (inch)
T_N = Heigth of Nut or Length of Threads for CRD cap Screw (inch)
A_s = Tensile Area of Threads (inch^2)
A_B = Crossectional Area of Bolt Shank (inch^2)
A_N = Crossectional area of Shank at Notch/Falw (inch ^{2})
L_{be} = Equivalent length of Bolt Shank (inch)
L_{se} = Equivalent length of Threads (inch)
L_N = Width/length of circumferential Notch/Flaw (inch)
d_n = Depth of Notch/Flaw (inch)
E = Youngs Modulus (ksi)
K_B = Stifness of Bolt (kip/inch)
A_C = Crossectional Area of the Equivalent Cylinder used) represent Joint Stiffness (kip/inch)
T = Total Joint Thickness- for CRD cap screw taken as l gth of Shank (inch)
D_H = Diameter of Bolt Hole (inch)
D_J = Effective Diameter of Equivalent Cylinder of Joint under Preload (inch)
K_J = Stiffness of Joint (inch)
F_P =Prevailing or Residual Preload (kip)
L_X = Exte nal Load on Bolt (kip)
L_{Xcrit} = Critical External Load required to cause Joint Separation (kip)
ΔF_B = Additional Load on Bolt due to External Load (kip)
Φ_k = Load Factor (dimensionless)
F_{Pi} = Initial Preload at Installation (kip)
RF_{ipl} = Reduction Factor for Initial Preload immediately after tightening (%)
RF_{eli} = Reduction Factor due to Elastic Interactions (%)
RF_{ltr} = Reduction Factor for Long Term Relaxation of Bolt atTemperature (%)
D_{bf} = Diameter of Bolt Shank at Location of Notch/Flaw (ALLOWABLE) (inch)
a_f = Allowable depth of Notch/Flaw to meet requirements (inch)
P_{acc} =Maximum Internal Pressure causing external load on Bolt (ksi)
D_{nozz} = Diameter of CRD Nozzle (inch)
N = Number of Bolts
F_{tp} = Total Preload on Bolt ; including external load (kip)
σ_i = Total stress in Bolt at initial Preload (ksi)
σp = Prevailing Stress in Bolt due to Prevailing Preload (ksi)
σpe = Stress in Bolt Due to Prevailing Preload + External Bolt load (ksi)
S_m = Allowable ASME Stress at temperature (ksi)

See Figure 1 for explanation of Bolt and Joint Nomenclature

CALCULATIONS FOR BOLTED JOINT

INPUT DATA (References in Parenthesis)

$D_B := 1.8125$ (Ref. 22 & 26)

$L_G := 3.44$ (Ref. 3 & 22)

$T_H := 1.00$ (Ref. 3 & 22)

$L_t := 2.06$ (Ref. 3 & 22)

$L_B := 3.44$ (Ref. 3 & 22)

$D_{sh} := 0.822$ (Ref. 3 & 22)

$T_N := 2.05$ (Ref. 3 & 22)

$A_S := 0.462$ (Ref. 3 , 8 & 22)

$D_H := 1.0$ (Ref. 27)

$F_{Pi} := 30.0$ (Ref. 1, 2 & 3)

$RF_{ipl} := 7.0$ (Ref. 8)

$RF_{eli} := 15.0$ (Ref. 8)

$RF_{ltr} := 20.$ (Ref. 9)

$P_{acc} := 5.872$ (Ref. 25)

$D_{n,z} := 4.912$ (Ref. 27)

$N := 8$ (Ref. 27)

Input Below from Report.

$L_N := 0.05$

$d_n := 0.120$

$E := 30.\cdot 10^3$

$T := 3.44$

$\sigma_i := 69.78$

$S_m := 29.5$

Joint Stiffness Calculation

Reference : 8 Equation 5.20 pp 152

Calculation for $D_B < D_J < 3\ D_B$ Use $D_J/D_B = 2.0$

$$A_C := \frac{\pi}{4}\cdot\left(D_B^{\,2} - D_H^{\,2}\right) + \frac{\pi}{8}\cdot(1.0)\cdot\left(\frac{D_B\cdot T}{5} + \frac{T^2}{100}\right) \qquad A_C = 2.331$$

$$K_J := \frac{E\cdot A_C}{T} \qquad K_J = 2.033\cdot 10^4$$

Bolt Stiffness Calculations
Case 1 Nominal Bolt

$$L_{be} := L_B + \frac{T_H}{2} \qquad L_{be} = 3.94$$

$$L_{se} := L_G - L_B + \frac{T_N}{2} \qquad L_{se} = 1.03$$

$$A_{B1} := \frac{\pi\cdot D_{sh}^{\,2}}{4} \qquad A_{B1} = 0.531$$

$$K_{B1} := \frac{1}{\frac{L_{be}}{E\cdot A_{B1}} + \frac{L_{se}}{E\cdot A_S}} \qquad K_{B1} = 3.108\cdot 10^3$$

Bolt Stiffness Calculation
Case 2: Bolt Shank completely degraded by 0.120 inch

$$L_{be} := L_B + \frac{T_H}{2} \qquad L_{be} = 3.94$$

$$L_{se} := L_G - L_B + \frac{T_N}{2} \qquad L_{se} = 1.03$$

$$A_{B2} := \frac{\pi \cdot (D_{sh} - 2 \cdot d_n)^2}{4} \qquad A_{B2} = 0.266$$

$$K_{B2} := \frac{1}{\frac{L_{be}}{E \cdot A_{B2}} + \frac{L_{se}}{E \cdot A_S}} \qquad K_{B2} = 1.761 \cdot 10^3$$

Bolt Stiffness Calculation
Case 3: A Full Circumferential Notch in the Middle of the Shank

$$L_{be} := L_B + \frac{T_H}{2} - L_N \qquad L_{be} = 3.89$$

$$L_{se} := L_G - L_B + \frac{T_N}{2} \qquad L_{se} = 1.03$$

$$A_N := \frac{\pi \cdot (D_{sh} - 2 \cdot d_n)^2}{4} \qquad A_N = 0.266$$

$$A_{B3} := \frac{\pi \cdot D_{sh}^2}{4} \qquad A_{B3} = 0.531$$

$$K_{B3} := \frac{1}{\frac{L_{be}}{E \cdot A_{B3}} + \frac{L_{se}}{E \cdot A_S} + \frac{L_N}{E \cdot A_N}} \qquad K_{B3} = 3.078 \cdot 10^3$$

Calculation of Prevailing Preload & and Stress in Bolt

$$F_p := F_{pi} \cdot \left(1 - \frac{RF_{ipl}}{100}\right) \cdot \left(1 - \frac{RF_{eli}}{100}\right) \cdot \left(1 - \frac{RF_{ltr}}{100}\right) \qquad F_p = 18.972$$

$$\sigma_p := \sigma_i \cdot \left[\left(1 - \frac{RF_{ipl}}{100}\right) \cdot \left(1 - \frac{RF_{eli}}{100}\right) \cdot \left(1 - \frac{RF_{ltr}}{100}\right)\right] \qquad \sigma_p = 44.129$$

Calculation of Loads required for Joint Separation

Case 1 {Nominal Bolt}

$$L_{Xcrit1} := F_p \cdot \left(1 + \frac{K_{B1}}{K_J}\right) \qquad L_{Xcrit1} = 21.872$$

Case 2 {Fully Degraded Bolt Shank}

$$L_{Xcrit2} := F_p \cdot \left(1 + \frac{K_{B2}}{K_J}\right) \qquad L_{Xcrit2} = 20.615$$

Case 3 { Bolt Shank with a circumferential Notch in the middle}

$$L_{Xcrit3} := F_p \cdot \left(1 + \frac{K_{B3}}{K_J}\right) \qquad L_{Xcrit3} = 21.844$$

Calculation of Load Factor using Bolt Stiffness from Case 3

$$\Phi_k := \frac{K_{B3}}{K_{B3} + K_J} \qquad \Phi_k = 0.131$$

Calculation of Bolt External Load due to Accident Pressure

$$Forc := \frac{P_{acc} \cdot (D_{nozz})^2 \cdot \pi}{4} \qquad Forc = 111.274$$

$$L_X := \frac{Forc}{N} \qquad L_X = 13.909$$

$$\Delta F_B := L_X \cdot \Phi_k \qquad \Delta F_B = 1.829$$

$$F_{tp} := F_P + \Delta F_B \qquad F_{tp} = 20.801$$

$$M := \frac{F_{tp}}{F_P} \qquad M = 1.096$$

The External Load on the Bolted Joint Smaller than the due to Accident Maximum Pressure is smaller than the critical external load to cause Joint Sepration; That is:

L_X (13.909 kip) < L_{Xcrit} (20.615 kip)
Therefore Joint Separation is Precluded.

Calculation of Allowable Notch/Flaw Depth to sustain Total Bolt Load

$$\sigma_{pe} := \sigma_p \cdot M \qquad \sigma_{pe} = 48.383$$

$$D_{bf} := \sqrt{\frac{\sigma_{pe}}{3 \cdot S_m}} \cdot D_{sh} \qquad D_{bf} = 0.608$$

$$a_f := \frac{D_{sh} - D_{bf}}{2} \qquad a_f = 0.107$$

The allowable Notch/Flaw depth for a full circumferential Notch is 107 mils

Figure 1 : General Bolt Dimensions

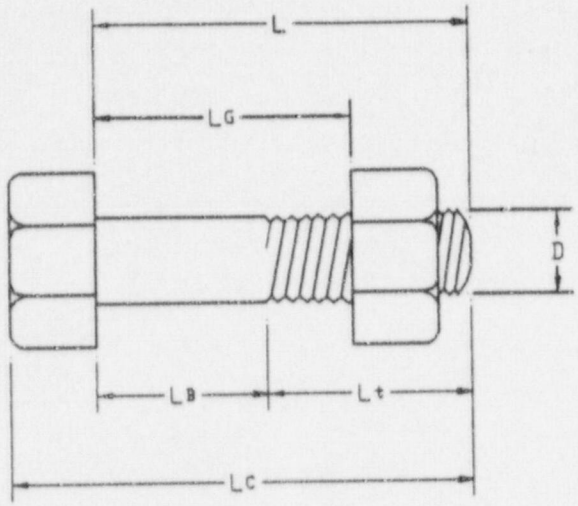

Figure 2 : Effective Bolt Dimensions for Use in Calculations

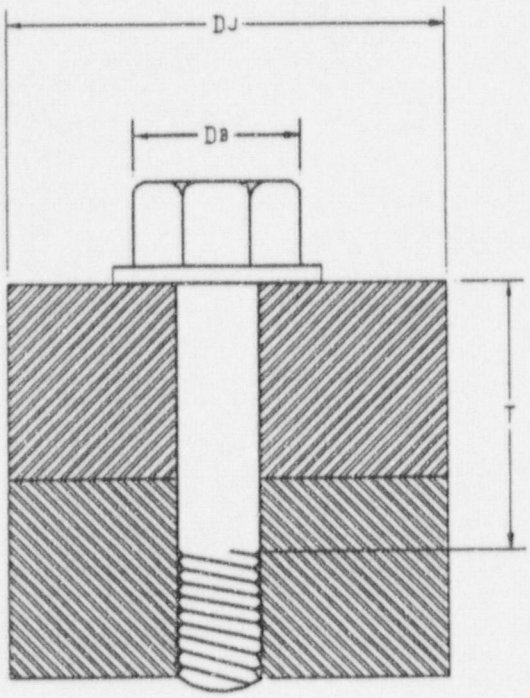

Appendix 4

Mechanical testing and Evaluation of Circumferentially Notched CRD Capscrew Material

APPENDIX 4
Mechanical Testing and Evaluation of Circumferentially Notched CRD Capscrew Material

INTRODUCTION :

The bolted joint and fracture mechanics evaluation of CRD capscrews showed that the limiting flaw depths, for a full circumferential flaw subjected to a maximum load, were 107 mils and 150 mils respectively. Based on these evaluations a limiting flaw depth of 107 mils was used to establish the inspection criteria. The purpose of the mechanical testing was to ensure that the limiting flaw depth determined by analysis is conservative and provides assurance against premature failure of the capscrew. The CRD capscrew material of interest is ASME SA 193 Gr. B7. Additional bolts with the same specification and of similar dimensions were procured for mechanical testing. The details of the testing performed and an evaluation of the test results are presented in the following sections.

DETAILS of TESTING :

A comparison of the procured bolts and the CRD capscrew is shown below.

Attribute	CRD Capscrew	Procured Bolts
Material Specification	ASME SA 193 Gr. B7	ASME SA 193 Gr. B7
Overall Length (in)	6.5	8.5
Thread Length (in)	2.0	2.5
Thread Size	1.0" x 8 UNC	7/8" x 9 UNC
Shank Length (in)	3.375	5.25
Shank Diameter (in)	0.823	0.850

The CRD capscrews were custom manufactured for the application, hence the procured bolts were selected such that the shank diameters were reasonably close. The shank length of the procured bolts were longer in order to accommodate a clip-on extensometer having a one inch (1.00") gauge length.

Two bolts from the procured set were subjected to tension testing in accordance with the Standard ASTM E-8 method. The results from the tension testing are as follows:

Property	Specimen 1	Specimen 2	Average
Yield Strength (ksi)	121.9	122.9	122.4
Tensile Strength (ksi)	135.4	136.6	135.0
Elongation (%)	20.3	20.9	20.6
Reduction in Area (%)	61.0	60.0	60.5

The tension properties of the CRD capscrew material from references 1 through 3 were compared to the test data above. This comparison is shown below:

Property	**Procured Bolt**	**CRD Capscrew Material**	
		Reference 1	Reference 2 & 3
Yield Strength (ksi)	122.4	127.2	120.9
Tensile Strength (ksi)	135.0	144.5	131.4
Elongation (%)	20.6	N/A	21
Reduction in Area (%)	60.5	N/A	60.6

The comparison presented above demonstrates that the mechanical properties of the procured bolts are similar to the material for the CRD capscrews. Therefore mechanical testing of notched bolts would effectively simulate the behavior of notches in the CRD capscrews.

Additional tension testing of bolts in the as-is condition, using two procured bolts and one CRD capscrew removed from service at GGNS, were performed to compare the applied load versus strain behavior. An increasing load to a value of 56.0 kips was applied and the strain recorded. Upon reaching the maximum load the specimen was unloaded and the strain recorded. Figure 1 shows the load-strain trace for the two procured bolts and figure 2 shows the load-strain trace for the GGNS CRD capscrew. A comparison of the two figures showed that the behavior was similar in that the strain at a load of 50.0 kips was between 0.0029 in/in and 0.0031 in/in. This test along with the tension properties comparison, clearly demonstrates that the behavior of the procured bolt is representative of the CRD capscrew material. Therefore, using the procured bolts to perform notch testing will enable characterization of the CRD capscrew material and, hence, provide the necessary information for verification of flaw depth limits obtained by analytical methods.

A "V" groove notch, (60° included angle and 10 mil root radius), were machined in the middle of the shank. The notch depths were 100 mils, 125 mils and 150 mils. These depths were selected to cover the range of the depths used in the analytical evaluations. The maximum applied load was based on the initial preload of the CRD capscrew, corrected for test temperature with respect to the normal operating temperature. The load correction to account for temperature correction was obtained by taking a ratio of the room temperature yield strength and the at temperature yield strength. The yield strengths used in the ratio were obtained from Section II of the ASME Boiler and Pressure Vessel Code (reference 4) for the CRD capscrew material. The maximum load was determined as follows:

$$\text{Maximum Load} = 30.0 \times (105.0/88.5)$$
$$= 35.59 \text{ or } 36.0 \text{ kips.}$$

The gauge length for the extensometer was one (1.0) inch, and the notch was located in the middle of the extensometer. The extensometer was functional for the entire test including both the loading and the unloading sequence. For each notch depth two specimens were tested, for a total of six tests. The load-strain traces from the test are provided in figures 3 through 5. The traces in these figures clearly show that the strain behavior is linear for both loading and unloading and that upon complete unloading no residual strain is observed. This behavior is characteristic of a linear elastic behavior and indicates that the notch effect is not pronounced.

The two specimens with a 150 mil deep notch were used to evaluate the onset of elastic-plastic behavior. These specimens were loaded incrementally in tension until the strain trace showed a clear departure from linearity. At this point the unloading sequence commenced with the extensometer functional. Thus the complete load-strain trace for the full cycle was obtained. The results of this test sequence is presented in figure 6. Figure 6 shows that the departure from linearity of the strain trace occurs at a nominal strain of 0.0030 in/in and is clearly discernible at a strain value of 0.0032 in/in. The residual strain was approximately 0.00025 in/in. The residual strain is indicative of the onset of plastic deformation in the notch region. At the departure from linearity of the strain trace the applied load was 46.0 kips.

EVALUATION :

The test results, presented in the previous section were evaluated using nominal stress and strain concepts and by Neuber's rule (reference 5) for notch analysis.

The effect of notch depth on measured strain, at the maximum load of 36.0 kips, was obtained from figures 1 through 5 and graphically presented in figure 7. Also presented in figure 7 is a linear regression line with a slope of 9.11 E -05. The extremely small value of the slope is indicative of a near horizontal line, which implies that the notch depth from 0 to 150 mils has insignificant effect on measured strain. Since the applied load was representative of the initial preload at temperature, this observation demonstrates that a bolt with a 150 mil deep notch will sustain a tensile load of 36.0 kips without an overload failure.

The stress at the notch root was computed by dividing the maximum load of 36.0 kips by the cross-sectional area at the notch. The results of the notch root stress as a function of notch depth is presented in figure 8. From this figure and the tensile data presented earlier, it appears the notch root stress reaches yield strength level at a depth of 117 mils. This simplistic analysis shows that at the limiting flaw depth of 107 mils, the stresses at the root of the notch will remain below yield strength.

The evaluation of stress and strain at notches is most often performed using Neuber's rule. Neuber's rule states (reference 5):

> *"The geometric mean of the stress and strain concentration factors remain equal to the elastic stress concentration factor during plastic deformation."*

This rule is mathematically defined as:

$$k_{tn} = \sqrt{k_\sigma \times k_\varepsilon} \quad \text{--------- (1)}$$

where: k_{tn} = elastic stress concentration factor
k_σ = stress concentration factor ; {local stress @ notch/ nominal stress}
or σ/S
k_ε = strain concentration factor; {local strain @ notch/nominal strain}
or ε/e

Neuber's rule applies only in the deformation regime prior to full plastic yielding of the net section. In the notch region subjected to loading there are three deformation stages possible, namely; elastic, elastic-plastic and fully plastic. For the evaluation of the CRD capscrews the stage of full plastic deformation is undesirable and hence to be avoided. Thus the analysis and testing was undertaken to define a safe flaw depth such that the onset of full plastic deformation is precluded. For these reasons the final stage, the full plastic deformation, will not be discussed. The evaluation of the other two deformation mechanisms, described in reference 5, are summarized below :

1) Linear elastic deformation: When no localized yielding has occurred at the notch root, the notch stress (σ) is related to the nominal stress "S" by the elastic stress concentration factor k_{tn} as follows:

$$\sigma = k_{tn} \times S \quad \text{-------(2)}$$

similarly the notch strain can be defined by:

$$\varepsilon = [S \times k_{tn}]/ E \quad \text{-----(3); where E is the Modulus of Elasticity}$$

In this regime of deformation both the stress and strain remain below their respective values at yield in a uniaxial tension test.

2) Elastic-Plastic Deformation (Local Yielding): With an increase in the applied load, local yielding at the notch root occurs when the stresses reach the material's yield strength. At this point only a small volume fraction of the material in the notch region has yielded. Eventually, as the load is increased to a substantially higher level, net-section yielding occurs. The applicability of Neuber's rule in the elastic-plastic deformation regime is limited to a state prior to the net section yielding. The deformation in this regime is quantified by (reference 5):

$$\sigma \times \varepsilon = [k_{tn} \times S]^2/E \quad \text{-----(4)}$$

For elastic-perfectly plastic material the strains prior to net section yielding can be determined by the formulation in reference 5, which is:

$$\varepsilon_{yn} = [k_{tn} \times S]^2/[\sigma_{ys} \times E] \qquad \text{-----(5)}$$

where: ε_{yn} = notch strain past local yield but prior to net section yield,
σ_{ys} = material yield strength.

In the above equation it is important to note that the notch strains will be higher than the uniaxial yield strain; i.e. $\varepsilon_{yn} \geq \sigma_{ys}/E$.
In order to determine the notch stress and strain behavior for the test specimens a Ramberg-Osgood material behavior was used. The Ramberg-Osgood model provides for strain hardening and hence provides for proper characterization of material behavior. The model is defined as (reference 5):

$$\varepsilon = (\sigma/E) + (\sigma/H)^{1/n} \qquad \text{-----(6)}$$

where : H = strength coefficient
n = strain hardening exponent.

The Ramberg-Osgood coefficients (H and n) were determined by using the stress strain data from the tension tests (provided in figure 9) and performing a linear regression using equation 6. The method used is described in reference 5. The Ramberg-Osgood coefficients obtained were as follows: H= 250.41 ksi and n = 0.131.
In order to ensure the validity of these coefficients, values for a similar material obtained from reference 6 were compared. The material in reference 6 for which the values were available was SAE 4130 having two different thermo-mechanical treatments. However it was essential to ascertain that the coefficients obtained from test data for the present effort was in reasonable agreement with the published values. This comparison is presented below :

Material	**Condition**	**"n"**	**"H" (ksi)**
SA 193 - B7	Quenched & Tempered	0.131	250.41
SAE 4130	Annealed	0.118	169.4
SAE 4130	Quenched & Temper Rolled	0.156	154.5

The above comparison shows that the values for the coefficients appear reasonable and the differences are attributable to the differences in the material chemistry and thermo-mechanical treatment. These martensitic steels are characterized by low strain hardening exponents and high strength coefficients.

When the stress-strain relationship described by equation 6 is substituted in equation 4, the resulting stress-strain at the notch with respect to the applied load becomes (reference 5):

$$[k_{tn} \times S]^2 = \sigma^2 + \sigma \times E \times (\sigma/H)^{1/n} \qquad \text{-----(7)}$$

Equations 6 and 7 were numerically evaluated by using Mathcad worksheets which are included as Attachment 1 to this Appendix.

The elastic stress concentration factor (k_{tn}) for the various notch depths was obtained from reference 7. For the notch geometry and depths tested the value for the elastic stress concentration factor was found to be nearly constant at a value of 4.9.

The upper bound for the notch strain, for the test specimens, at an applied load of 36.0 kips can be obtained from equation 5. This strain, considering an elastic-perfectly plastic material, is 0.0266 in/in.

Results from the analysis presented in Attachment 1 to this Appendix shows that for an applied load of 36.0 kips the notch strain is 0.0202 in/in. This value when compared with that from equation 5 suggests, for the notch depths of interest (100 to 150 mils) at an applied load of 36.0 kips, that any yielding would be very localized and net section yielding is precluded.

The nominal strains obtained from the test of the 150 mil notch specimen (figure 6) and the notch strains from Attachment 1 can be used to determine strain concentration factors at various load levels as shown below :

Applied Load (kips)	**Nominal Strain (in/in)**	**Notch Strain (in/in)**	k_ε
36.0	0.0023	0.0202	8.78
43.04	0.0029	0.0273	9.41
47.43	0.0031	0.0322	10.39

The strain concentration factors below net section yield load (46.0 kips) are reasonably close. Once the load is increased past the net-section yielding, the strain concentration factors tends to diverge in accordance with theoretical predictions (reference 5). The notch strain at the estimated

maximum preload value of 36.0 kips is 62.5% of the notch strain at net-section yield load of 46.0 kips. This shows that based on a notch analysis, net-section yielding at estimated maximum preload is precluded.
Similar analysis for the 100 mil and 125 mil notch specimens show the strain concentration factors at an applied load of 36.0 kips to be 8.18 and 8.43 respectively. These values compare favorably with 8.78 for the 150 mil notch specimen. This comparison shows that the effect of notch depth, in the range tested, is not significant.

CONCLUSIONS :

Based on the testing results and the evaluations presented in the previous sections the following conclusions are made:

1) The load-strain trace maintain a linear relationship up to the maximum load of 36.0 kips for all notch depths tested.
2) At the maximum load of 36.0 kips the nominal (measured) strains are not affected by the notch depth. The slope of a linear regression line, on the plot for measured strain as a function of notch depth, was extremely small.
3) For an applied load of 36.0 kips the notch stress, based on net section area, would reach material yield strength at a notch depth of 117 mils.
4) The elastic stress concentration factor, for the various notch depths investigated, remained constant at a value of 4.9.
5) The calculated notch strains for the applied load of 36.0 kips are above the strain at yield in a uniaxial test. Therefore, localized yielding at the notch root is expected to occur for notch depths above 117 mils. However, the calculated notch strain is below the limiting value calculated assuming an elastic-perfectly behavior.
6) Notch analysis using the elastic stress concentration factor of 4.9, using Neuber's rule and a Ramberg-Osgood material relationship, shows that for an applied load of 36.0 kips the notch strains remain below the notch strain required for net-section yield. Therefore, for the deepest notch depth evaluated, net-section yielding is precluded at the expected bolt preload of 36.0 kips at room temperature which is equivalent to 30.0 kips at the operating temperature.

REFERENCES :

1) Grand Gulf Nuclear Station Engineering Report, GGNS-92-0033, Revision 0. 1992.
2) River Bend Nuclear Station, RBS CR 92-410.
3) River Bend Nuclear Station, RBS CR 96-310.
4) ASME Boiler and Pressure Vessel Code, Section II Part D, 1992 Edition.
5) "Mechanical Behavior of Materials"; Norman E. Dowling, Prentice Hall, Englewood Cliffs, NJ 07632. 1993.
6) "Failure of Materials in Mechanical Design: Analysis, Prediction, Prevention"; Second Edition, Jack A. Collins; John Wiley & Sons Inc.; New York, NY. 1993.
7) "Peterson's Stress Concentration Factors"; Second Edition; Walter D. Pilkey, John Wiley & Sons Inc.; New York, NY. 1997.

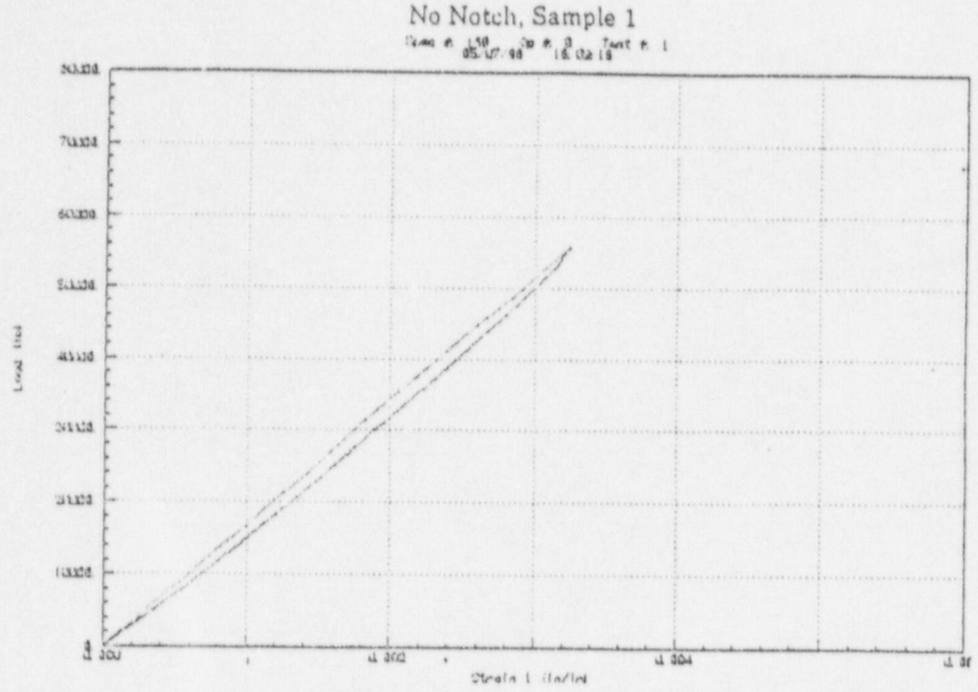

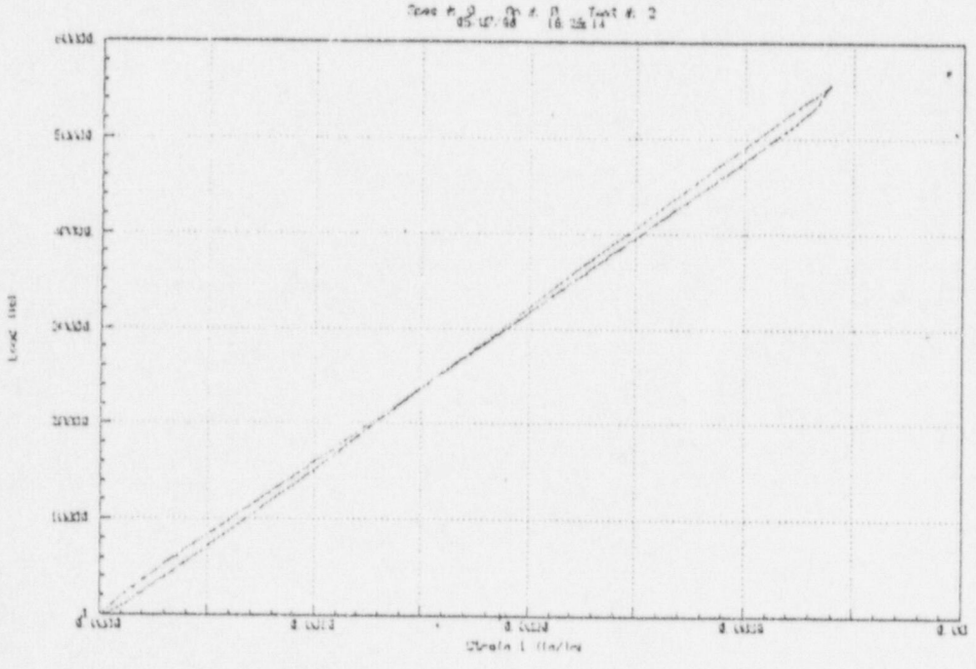

Figure 1: Load-Strain Trace for Un-notched Procured Bolts in the as-received Condition.

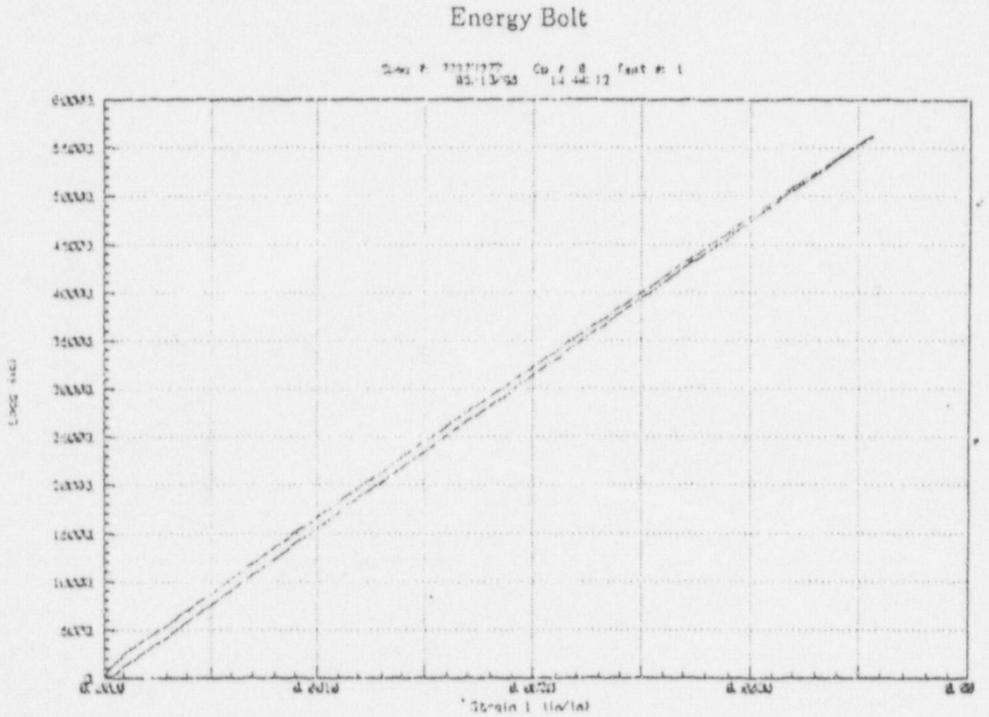

Figure 2: Load-Strain Trace for GGNS Un-notched CRD Capscrew removed from Service

0.100" Notch, Sample 1

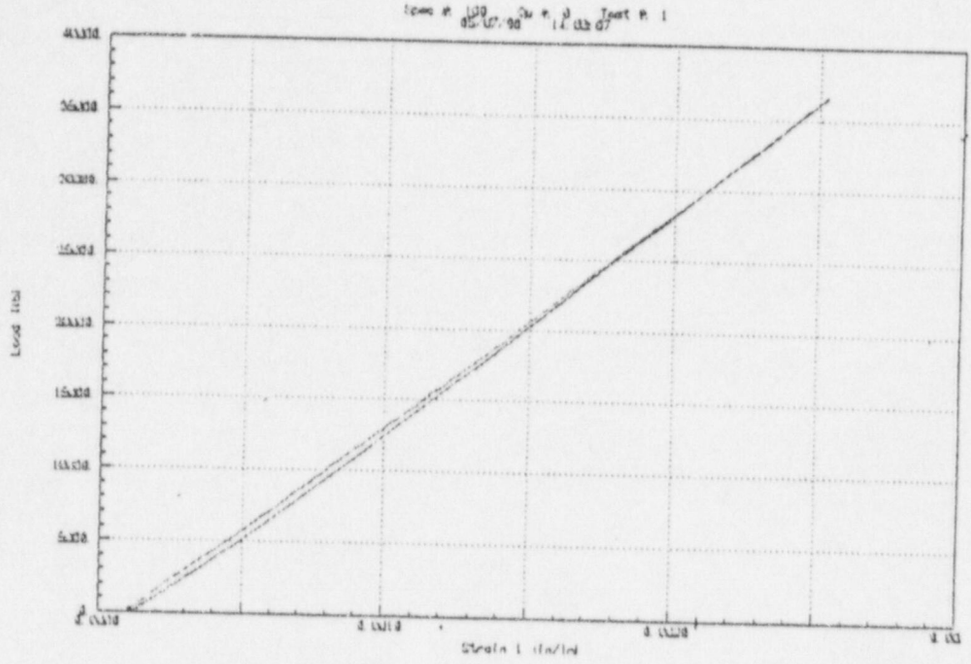

0.100" Notch, Sample 2

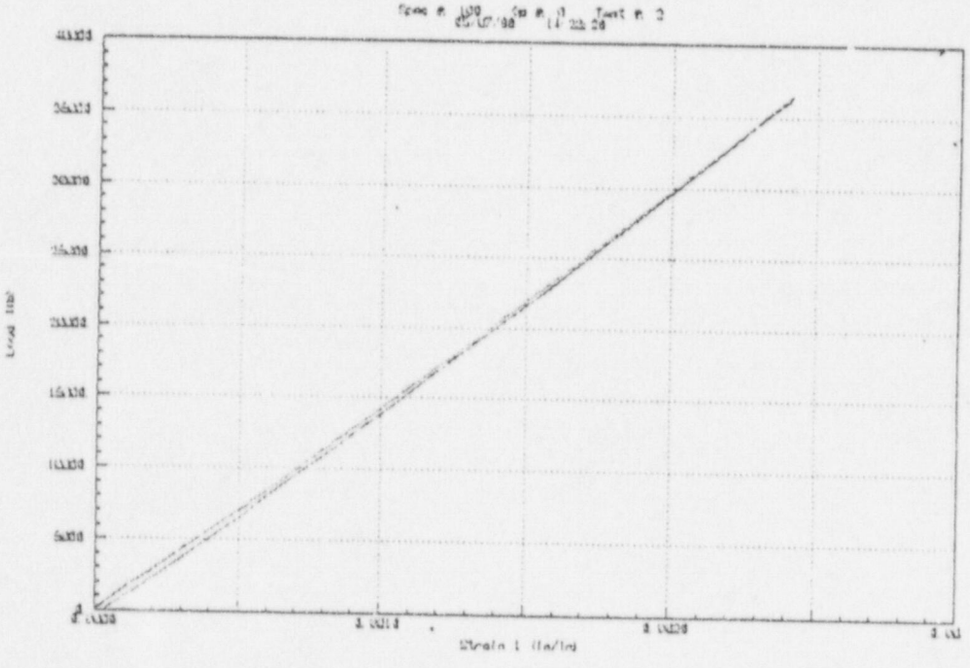

Figure 3: Load-Strain Trace for Notched Bolt: Notch Depth of 100 mils.

0.125" Notch, Sample 1

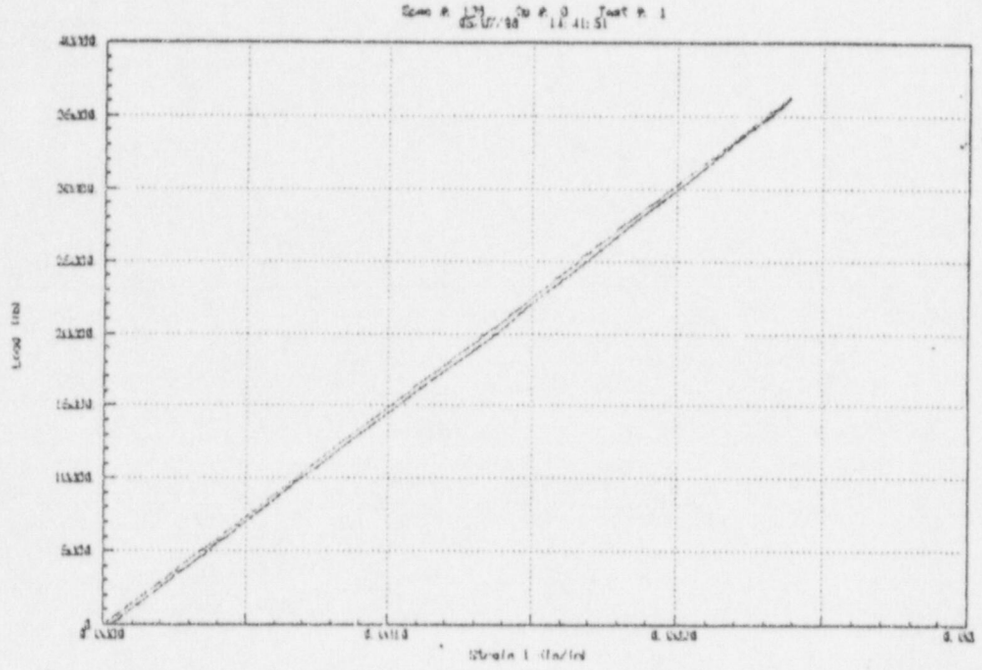

0.125" Notch, Sample 2

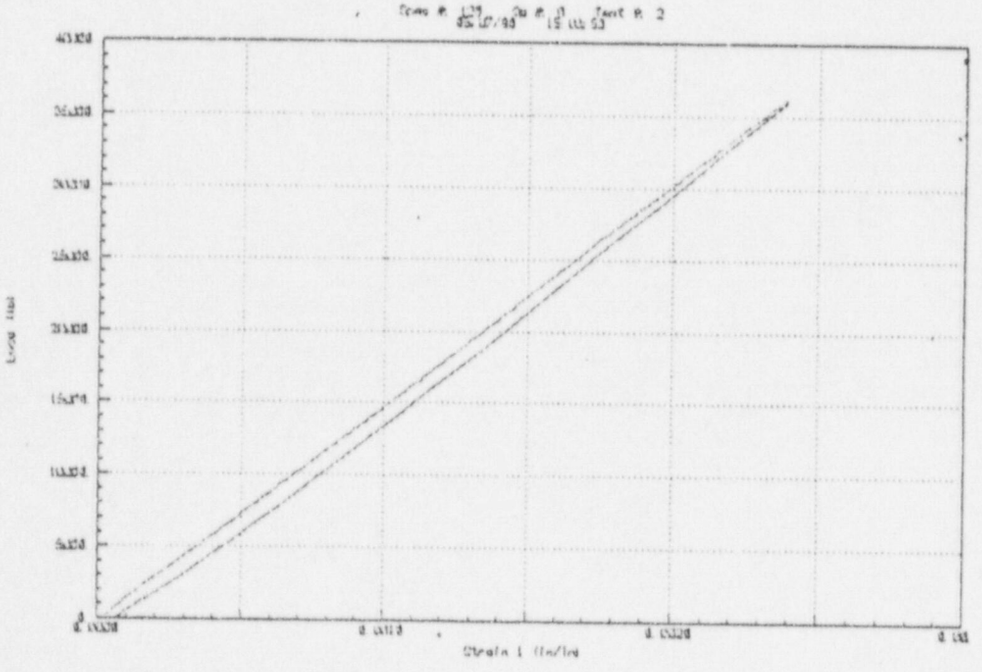

Figure 4: Load-Strain Trace for Notched Bolt: Notch Depth of 125 mils.

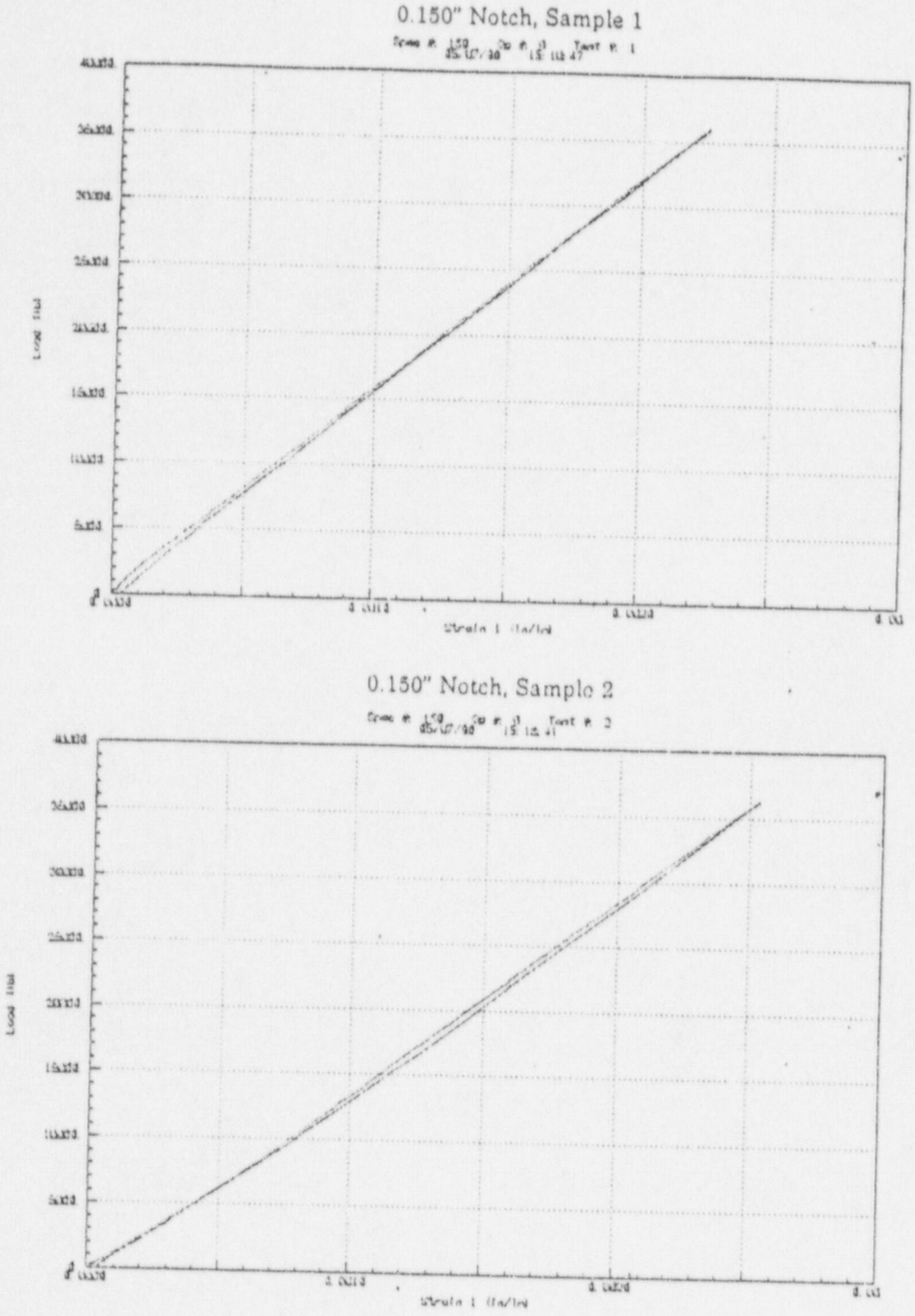

Figure 5: Load-Strain Trace for Notched Bolt: Notch Depth of 150 mils.

0.150" Notch, Max Load=58,380lbs

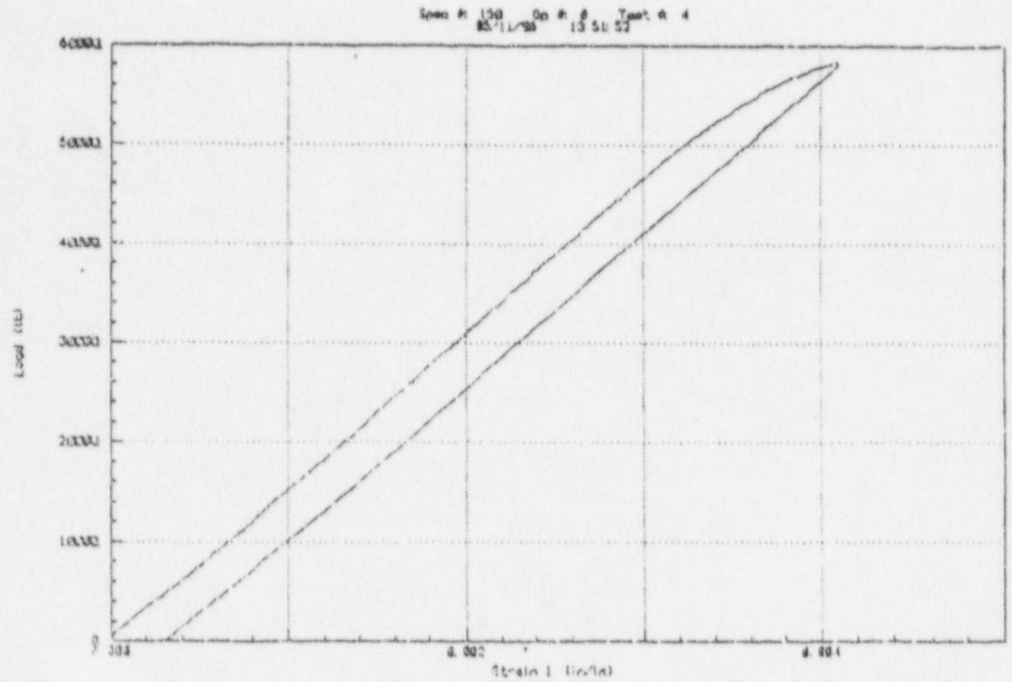

0.150" Notch, Max Load=58,380lbs

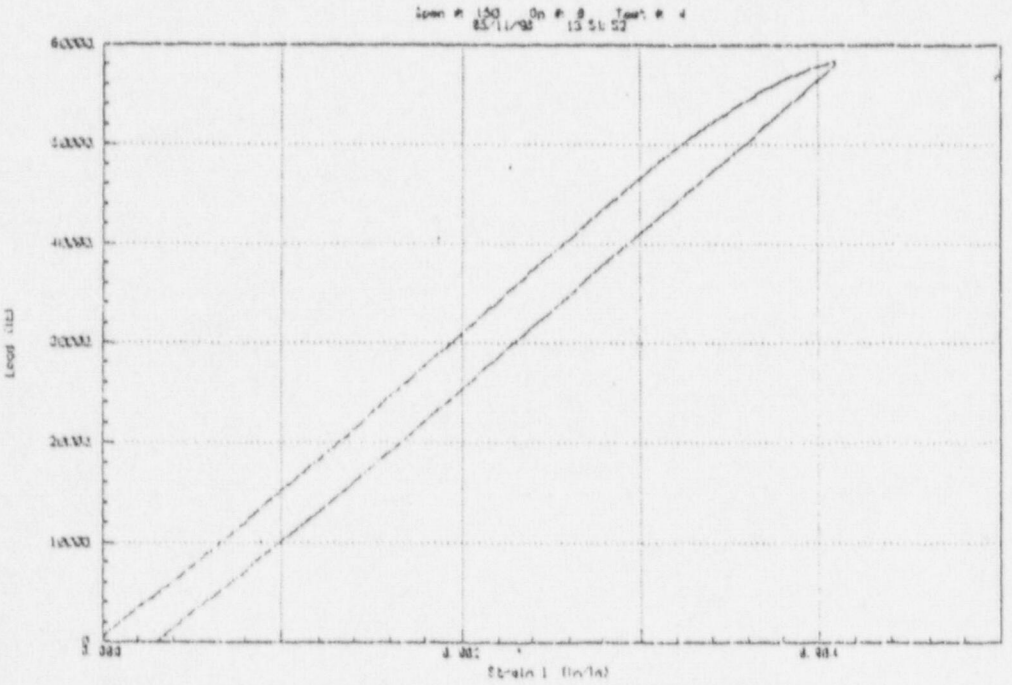

Figure 6: Load-Strain Trace for Notched Bolt Loaded Beyond Yield: Notch Depth 150 mils.

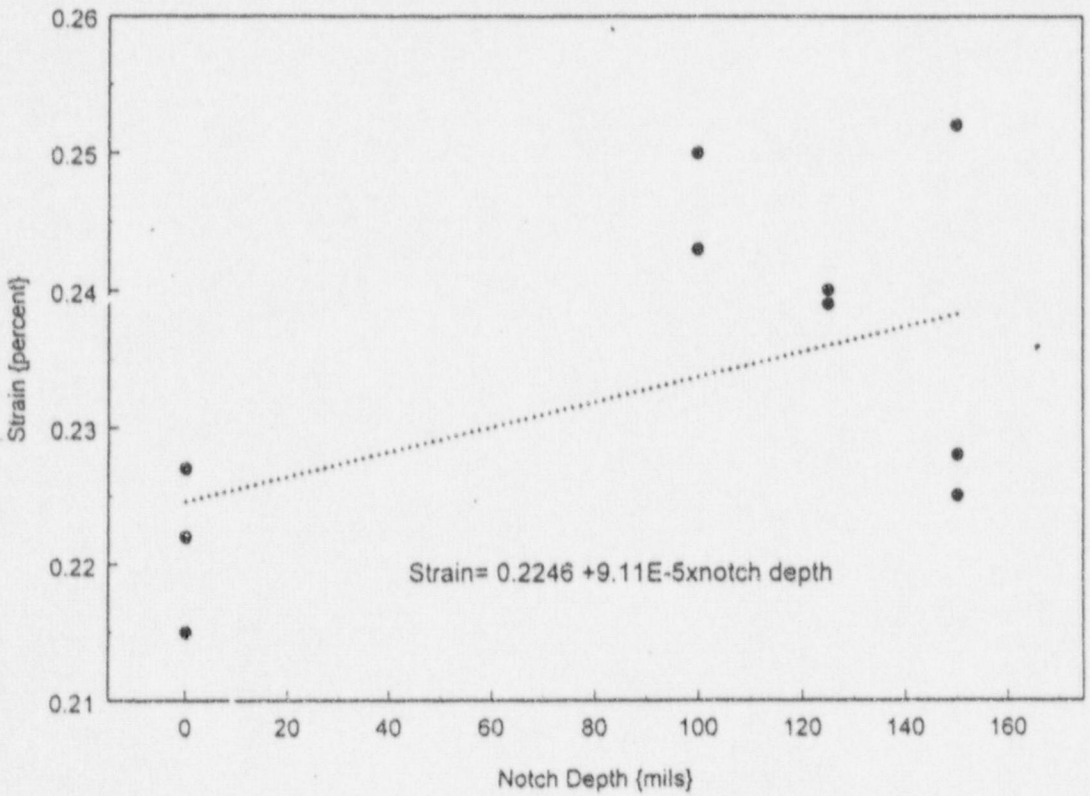

Figure 7: Nominal (measured) Strain as a function of Notch Depth. The linear regression line is also plotted. The small value for the slope indicates that nominal specimen strain is not affected by notch depth

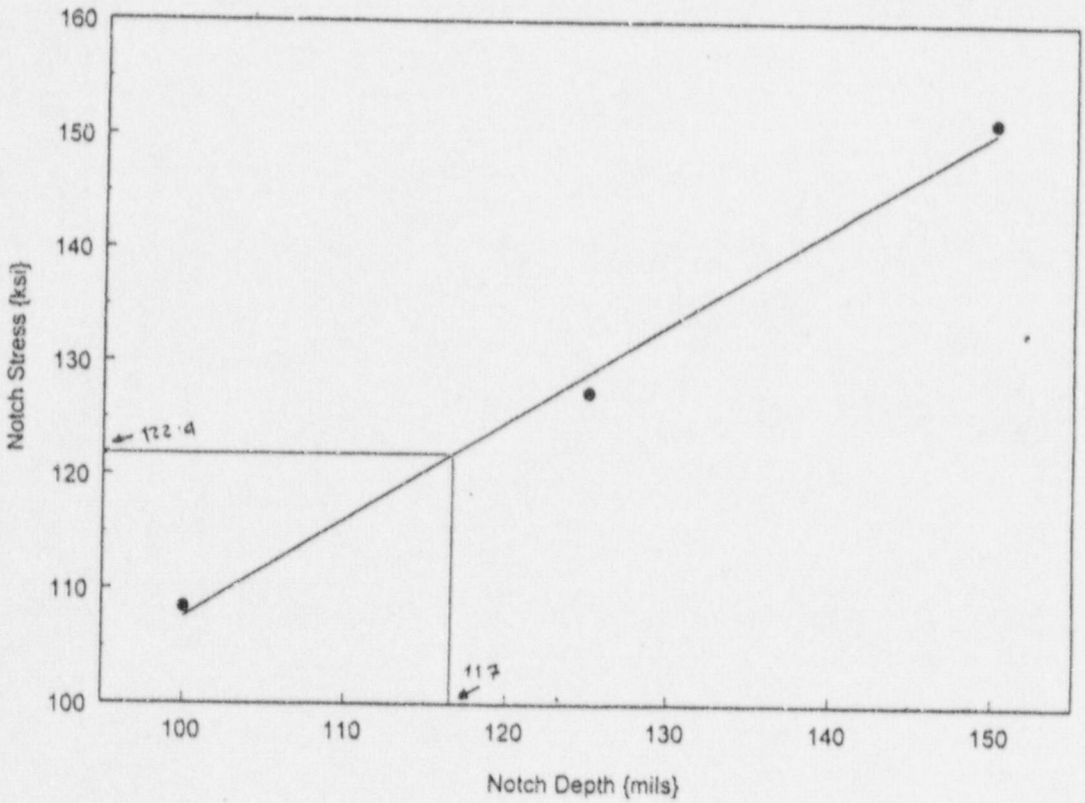

Figure 8: Notch Stress as a function of Notch Depth.
The notch stress is calculated using net cross-section area.
material yield strength is reached at a notch depth of 117 mils.

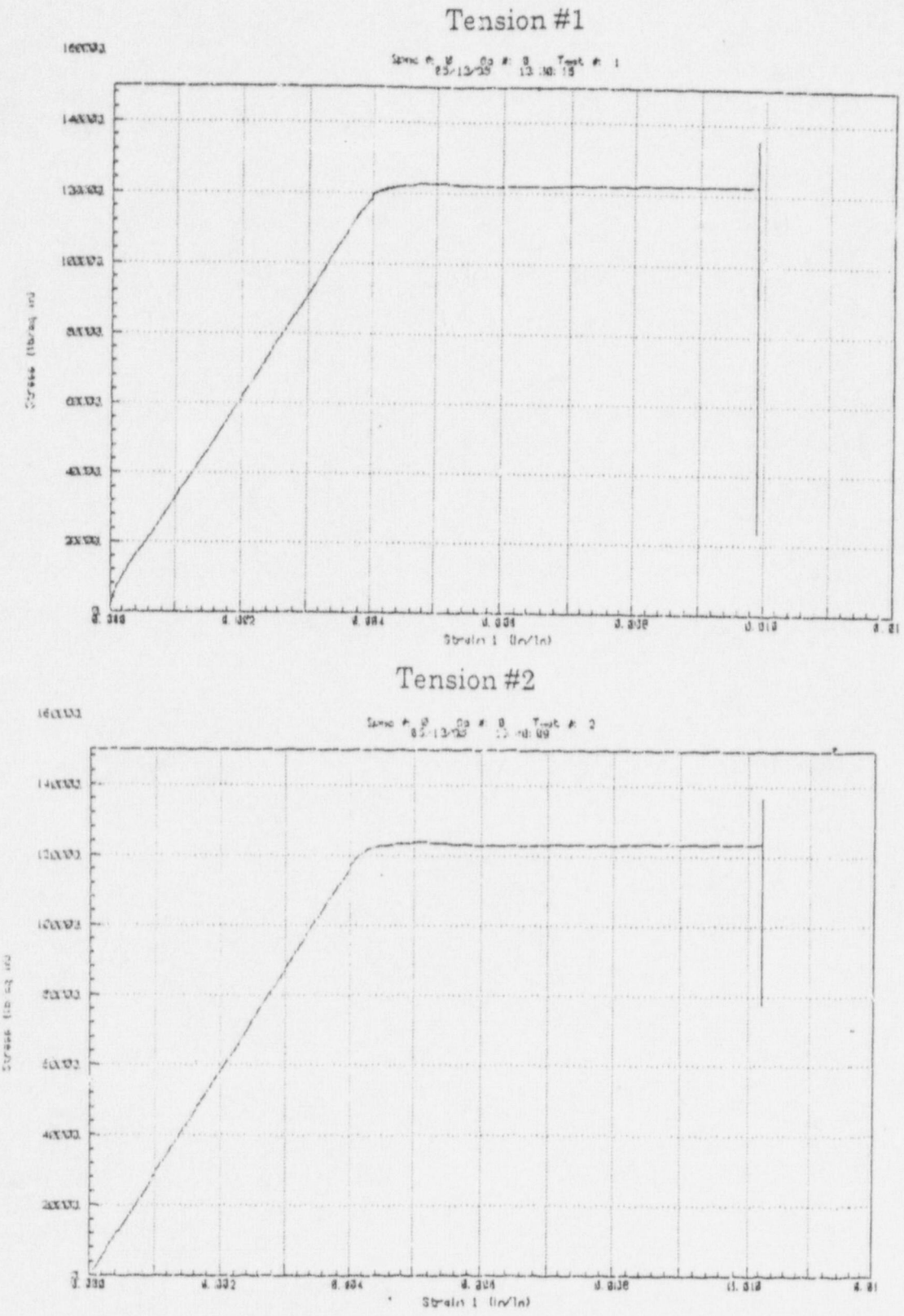

Figure 9: Stress-Strain Curves from Tension Test of Procured Bolts.

ATTACHMENT 1 to APPENDIX 4
{Notch Analysis of CRD Capscrews}

$d := 0.875$ Bolt Shank Diameter (in)

$k_{tn} := 4.9$ From Petersons chart 2.19 @ r/D=0.012 & d/D between .647 and .765

$E := 29.7 \cdot 10^3$

$H := 250.41$ Ramberg-Osgood fit to Tension Data

$n := 0.131$ Ramberg-Osgood fit to Tension Data

Calculations

$\sigma_0 := 0.0$ $\sigma_{inc} := 4.0$

$i := 1 .. 50$

$\sigma_i := \sigma_{i-1} + \sigma_{inc}$

$$S_i := \frac{\sqrt{(\sigma_i)^2 + \sigma_i \cdot E \cdot \left(\frac{\sigma_i}{H}\right)^{\frac{1}{n}}}}{k_{tn}}$$

$LD_i := S_i \cdot \pi \cdot \left(\frac{d}{2}\right)^2$

$$\varepsilon_i := \frac{\sigma_i}{E} + \left(\frac{\sigma_i}{H}\right)^{\frac{1}{n}}$$

$C_i := \sigma_i \cdot \varepsilon_i$ $\varepsilon_{pct_i} := \varepsilon_i \cdot 100$

Graphical Output

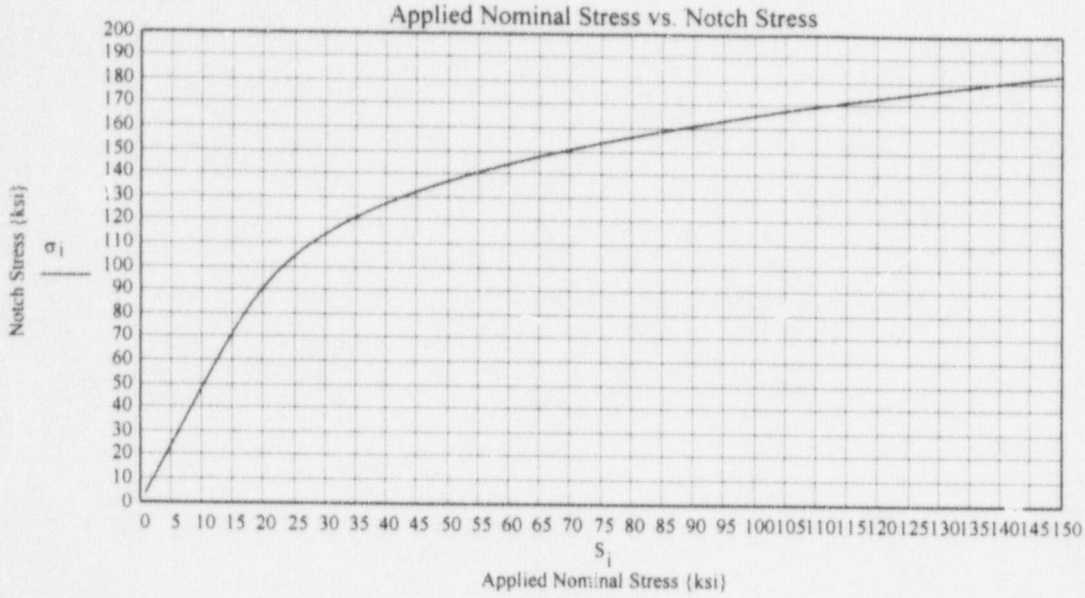

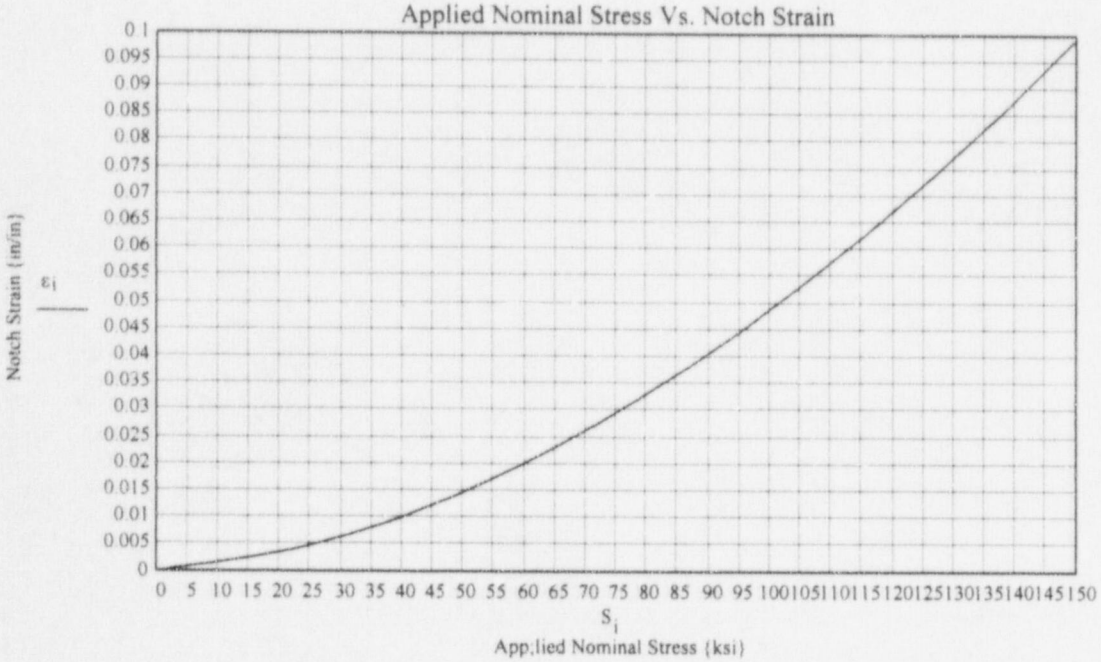

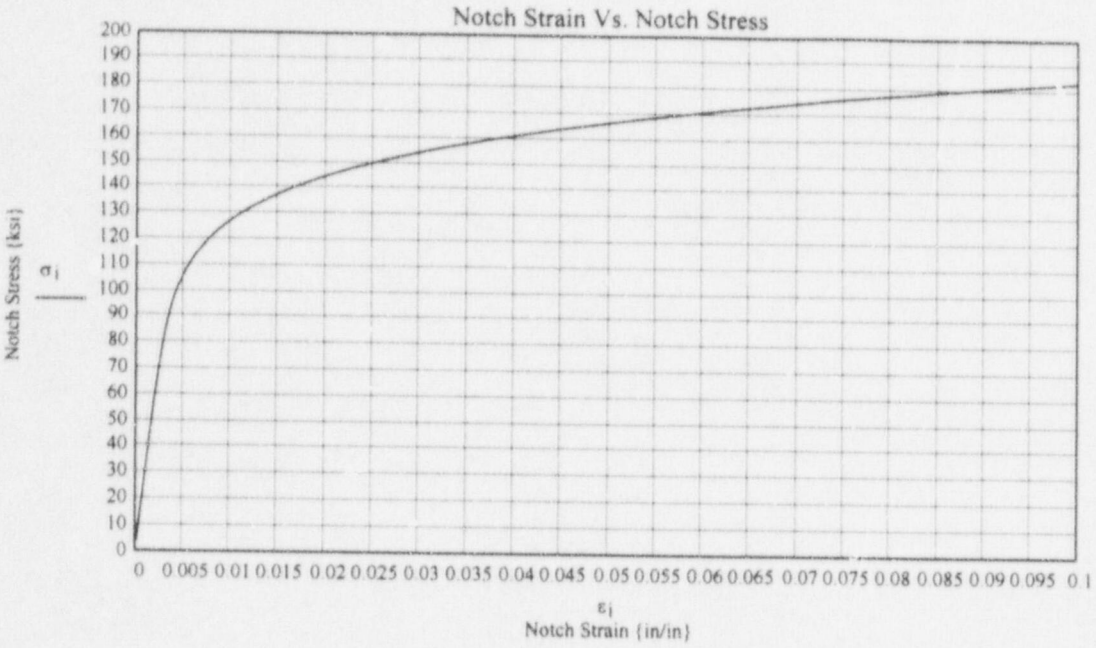
Notch Strain Vs. Notch Stress
Notch Stress {ksi}
σ_i
200 190 180 170 160 150 140 130 120 110 100 90 80 70 60 50 40 30 20 10 0
0 0.005 0.01 0.015 0.02 0.025 0.03 0.035 0.04 0.045 0.05 0.055 0.06 0.065 0.07 0.075 0.08 0.085 0.09 0.095 0.1
ε_i
Notch Strain {in/in}

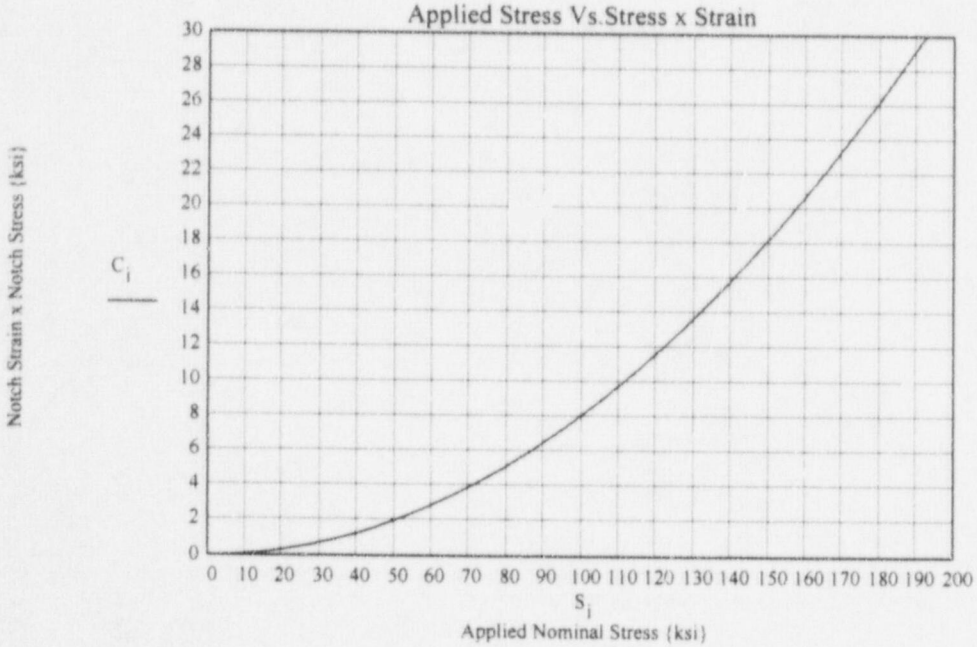
Applied Stress Vs.Stress x Strain
Notch Strain x Notch Stress {ksi}
C_i
30 28 26 24 22 20 18 16 14 12 10 8 6 4 2 0
0 10 20 30 40 50 60 70 80 90 100 110 120 130 140 150 160 170 180 190 200
S_i
Applied Nominal Stress {ksi}

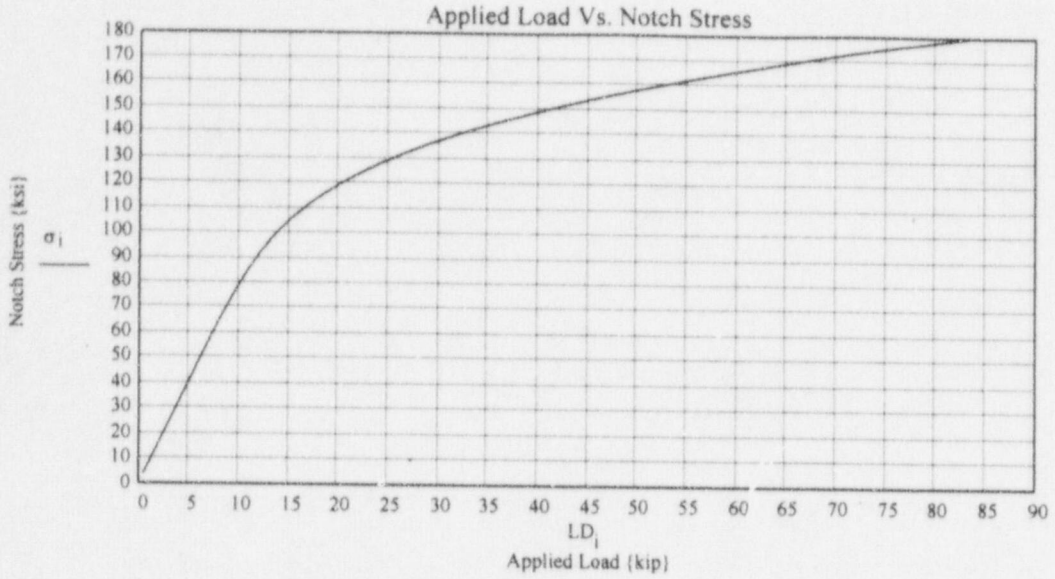

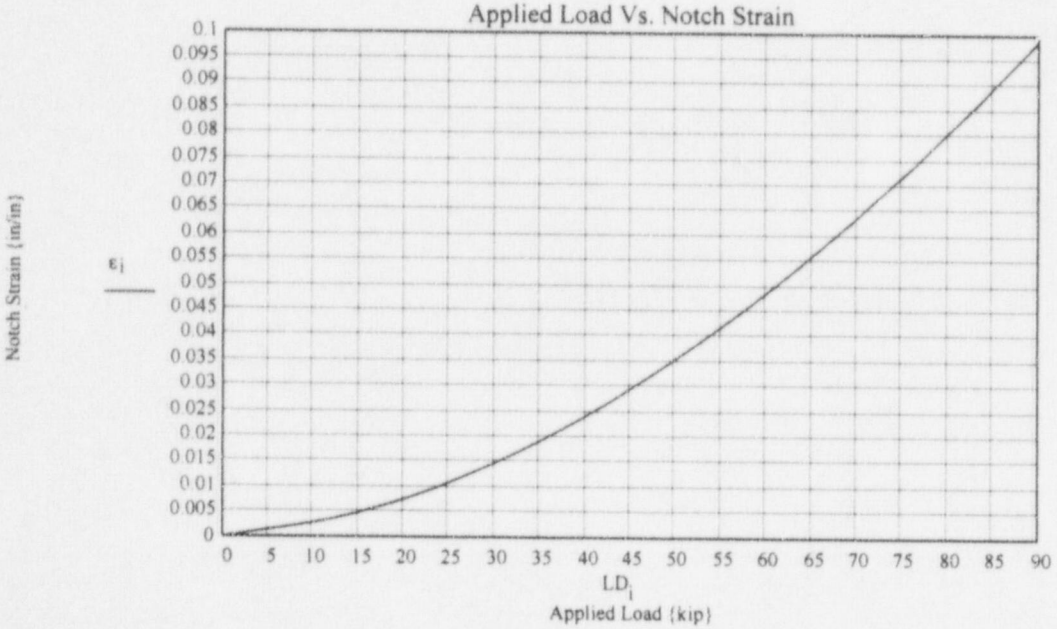

Load (kip)	Strain (in/in)
36	0.020161
43.04	0.027248
47.426	0.032236

Tabular Output

$i := 1 .. 40$

S_i	σ_i	$\varepsilon\ pct_i$	C_i
0.816	4	0.013	$5.387 \cdot 10^{-4}$
1.633	8	0.027	$2.155 \cdot 10^{-3}$
2.449	12	0.04	$4.848 \cdot 10^{-3}$
3.265	16	0.054	$8.62 \cdot 10^{-3}$
4.082	20	0.067	0.013
4.898	24	0.081	0.019
5.714	28	0.094	0.026
6.531	32	0.108	0.034
7.348	36	0.121	0.044
8.166	40	0.135	0.054
8.985	44	0.148	0.065
9.806	48	0.162	0.078
10.631	52	0.176	0.091
11.461	56	0.19	0.106
12.3	60	0.204	0.122
13.152	64	0.218	0.14
14.021	68	0.234	0.159
14.916	72	0.25	0.18
15.844	76	0.267	0.203
16.819	80	0.286	0.229
17.853	84	0.307	0.258
18.965	88	0.33	0.291
20.175	92	0.358	0.329
21.508	96	0.39	0.374
22.989	100	0.427	0.427
24.65	104	0.472	0.491
26.523	108	0.527	0.569
28.643	112	0.592	0.663
31.046	116	0.672	0.779
33.768	120	0.768	0.922
36.849	124	0.885	1.098
40.325	128	1.027	1.315
44.233	132	1.198	1.582
48.611	136	1.405	1.91
53.497	140	1.653	2.314
58.928	144	1.949	2.807
64.942	148	2.304	3.409
71.576	152	2.725	4.142
78.87	156	3.224	5.029
86.863	160	3.812	6.1

ENTERGY

Brian — Attached is copy of report after Erwin's comments resolved. — Jim

Technical Review Comments

Document Number	EP-98-003-01	Rev. 1	Subject/Title:	The Evaluation of BWR Control Rod Drive Mounting Flange Cap Screw

Document Type: Engineering Report (by Echelon)

Special Notes or Instructions:

Comment Number	Page or Section	Comment	Response/Resolution	Accept Initials
1.	overall	This is an impressive piece of work!		
2.	p. 5	Inset below 1st paragraph -- references for RBS do not appear to match those listed in the reference section. Should be references 16 & 17, I assume.	Changed - accept	BCG
3.	p. 9	1st para., 3rd sentence -- Seems like "produce" should be "increase" in "undoubtedly produce average stresses". 1st sentence, lower para. -- The wording "A total reduction factor of 0.632" suggests preload reduced by 63.2% but rather it is reduced to 63.2% of its initial value. However, I think it's okay; the factors are called "reduction factors" and one can determine correct meaning from the context and calculation.	changed "produce" to increase — No - reduction factor is appropriate.	BCG BCG
4.	p. 13	Immediately below middle of page -- Change "form" to "from".	changed - ok	BCG
5.	p. 14	1st sentence is worded awkwardly. 3rd paragraph, middle of page -- It seems that an implicit assumption is that the flaw is not present or does not develop during this 1000-hour period. If true, maybe the assumption should be stated.	What does your imply? - the 1000 hrs is for preload relaxation!	BCG BCG
6.	p. 15	1st complete para., item 2) -- Should "shank length" be "shank width"?	changed	BCG
7.	p. 17	2nd para., 1st sentence -- Change "subscript" to "subscripted".	Changed	BCG
8.	p. 18	Equations (1) & (3) -- Correct position of "x" in exponential term. Delete extraneous header in middle of page.	deleted extra header. — no change ~~[illegible]~~ changed "x" (meant to look like subscript)	BCG BCG
9.	p. 21	last para., 2nd last sentence -- Change "foe" to "for".		

Reviewed By:	Erwin Zoch	Date	7/23/98	Resolved By:	Brian C. Gray
Department:	Site Engineering	Ext.	8-558-4810	Date:	7/27/98

ENTERGY

ENGINEERING REPORT REVIEW COMMENTS

Document Number	Rev.	Document Title	Safety Related?
EP-~~98~~-003	01	**The Evaluation of BWR Control Rod Drive Mounting Flange Cap Screw**	YES [X] NO [ ]

Document Type: [ ] Administrative Guide [ ] Standard [ ] Instructional Guide [ ] Procedure [ ] Design Guide [ ] Appendix

Special Instruction or Notes: **Please return comments to Brian Gray at Echelon by Wednesday, July 22, 1998.**

Comment No.	Page or Section	Comment	Response/Resolution	Accept Initials
		No Comment		BCG

Post-it™ brand fax transmittal memo 7671 | # of pages ▸ 1

To BRIAN GRAY	From S C LEWIS
Co.	Co.
Dept.	Phone # 6154
Fax # 5394	Fax #

Reviewed By: JAMES A. SMITH — Date 7-22-98
Print
Signature

Department: NP&I/M&CH Ext.: 6265

Resolved By: Brian C. Gray Date: 7/27/98

ENTERGY

RECOMMENDATION FOR APPROVAL

Engineering Report No.: **EP-98-003-01**

Reviews Completed: Brian C. Gray — Preparer — Date: 7-29-98

Concurrence: N/A — Responsible Manager, ANO — Date:

Concurrence: [signature] — Responsible Manager, GGNS — Date: 8/18/98

Concurrence: N/A — Responsible Manager, W3 — Date:

Concurrence: _____ — Responsible Manager, RBS — Date:

ENTERGY

RECOMMENDATION FOR APPROVAL

Engineering Report No.: **EP-98-003-01**

Reviews Completed: Brian C. Gray — Preparer — Date: 7-29-98

Concurrence: N/A — Responsible Manager, ANO — Date: _____

Concurrence: _____ — Responsible Manager, GGNS — Date: _____

Concurrence: N/A — Responsible Manager, W3 — Date: _____

Concurrence: W. Brian — Responsible Manager, RBS — Date: 8/18/98